Theses and Dissertations

2016

The Role of Epidermal Stem/Progenitor-Like Cells In HPV-Mediated Pre-Neoplastic Transformation

Yvon L. Woappi
University of South Carolina

THE ROLE OF EPIDERMAL STEM/PROGENITOR-LIKE CELLS IN HPV-MEDIATED
PRE-NEOPLASTIC TRANSFORMATION

by

Yvon L. Woappi

Bachelor of Science
University of Pittsburgh, 2011

Submitted in Partial Fulfillment of the Requirements

For the Degree of Doctor of Philosophy in

Biomedical Science

School of Medicine

University of South Carolina

2016

Accepted by:

Lucia A. Pirisi, Major Professor

Chandrashekhar Patel, Chairman, Examining Committee

Kim Creek, Committee Member

Daping Fan, Committee Member

Phillip Buckhaults, Committee Member

Cheryl L. Addy, Vice Provost and Dean of the Graduate School

DEDICATION

To my God, the Almighty. To my father's memory, Christ Woappi. To my mother, Annie-Laure Woappi; my brother Loic Stephane Woappi; my sisters Elise-Christelle Woappi and Anne-Elise. To my beloved friends and lifelong mentors for always supporting me and standing by me.

ACKNOWLEDGEMENTS

It is a pleasure to thank the many people who made this thesis possible. I fall short on words to express my gratitude towards my mentors Dr. Lucia Pirisi-Creek and Dr. Kim Creek. Dr. Pirisi-Creek has truly made my time in her laboratory a memorable and integral part of my life. Recalling our research motto, "scientific precision and detail", is exactly what I have aimed to continually develop during my training. Even though there were low phases, I've always felt motivated to overcome each obstacle and to rise above them like a soaring phoenix, and this is only because of the endless patience, encouragement, and faith that Lucia had in me. Working in her lab these past four years has felt like a retreat of sorts, a place of discovery, where ideas are continually generated and explored. I thank her for sharing her expertise and research insight with me, for being a friend, and a strong support system in times of need.

My sincere thanks to all my committee members, for their valuable advice and discussions which helped me grow as a scientist, and ultimately as a person. I also wish to thank my colleagues, Dr. Swati Tomar, Dr. Elena Mourateva, Maria Hosseinipour, Christian Graves, Dr. Junfeng Wang and so many others for allowing me the opportunity to learn from them. Very special thanks to Dr. Richard Hunt, Dr. Bert Ely, Dr. Wayne Carver and Dr. Eddie Goldsmith for selecting me for this elite program and for giving me the opportunity to fulfill my dream of pursuing biomedical research. My sincere thanks to Dr. Ashok Chauhan and Dr. Wanden Ai; not forgetting the administrative and custodial staff.

ABSTRACT

The role of epidermal basal stem cells in dysplasia is a matter of great interest in the human papillomavirus (HPV)-driven cancers. To assess the relationship between "stemness" and HPV-mediated transformation, we made use of 3-D suspension culture and fluorescence activated cell sorting (FACS) to purify stem/progenitor-like cells from primary normal human keratinocyte (NHKc) cultures. We found that NHKc cells derived from multicellular keratinocyte spheroids were enriched for a basal subpopulation of epidermal stem-like cells, that could be maintained for prolonged time in culture and used to conduct transfection experiments with full-length HPV16 DNA. Thus, by using these stem cell enrichment methods, we set out to investigate in detail the effects of increased and decreased basal stem cell density on keratinocytes' immortalization and transformation efficiencies. We hypothesized that stem cell properties of NHKc cultures established from neonatal genital skin would positively influence susceptibility to transformation by HPV16 DNA. Our findings reveal that epidermal stem cells (EpSCs) are more effectively immortalized and transformed by oncogenic HPV16 DNA, while terminally differentiated keratinocyte populations fail to successfully immortalize in culture. Tissue stem cell density may prove useful in predicting individual susceptibility to HPV16-mediated transformation in persons with persistent HPV infections, improving on current triage and follow-up measures.

PREFACE

All the work presented henceforth was conducted by Yvon L. Woappi and

colleagues while in the laboratory of Lucia. A. Pirisi-Creek at the University of South

Carolina, Columbia, SC. All projects involving human specimens and associated methods

were reviewed by the Institutional Review Board at the University of South Carolina and

Palmetto Health, which confirmed our assessment that the use of de-identified skin

specimens, as described in this thesis, does not constitute human subjects research.

TABLE OF CONTENTS

LIST OF FIGURES

x

LIST OF TABLES

LIST OF SYMBOLS

*   P values $\leq$ 0.05

**   P values $\leq$ 0.01

***   P values $\leq$ 0.001

LIST OF ABBREVIATIONS

APOBEC 3B .... APOBEC 3B: Apolipoprotein B mRNA editing enzyme 3B

BSA .... Bovine serum albumin

CP ....Committee progenitors

CSC ....Cancer stem cell

DR media ....Differentiation resistant media

EGFR ....Epidermal Growth Factor Receptor

EpSCs.. Epidermal Stem Cells

FGF ....Fibroblast growth factor

FITC...Fluorescein isothiocyanate

GAPDH...Glyceraldehyde 3-phosphate dehydrogenase

GFP .... Green fluorescence protein

HKc/HPV16...................................... Human keratinocytes transfected with HPV16 DNA

HKc/HPV16^{im} ....Human keratinocytes successfully immortalized by HPV16 DNA

HKc/DR .... HPV16 immortalized human keratinocytes grown in DR media

HKc/DR-Six1....................... HKc/DR line exogenously expressing Six Homeobox 1 gene

HKc/DR^{tr}......................................HKc/DR line successfully transformed by HPV16 DNA

HPV...Human papilloma virus

HPV16..Human papillomavirus type 16

FITC...Fluorescein isothiocyanate

INTα6..Integrin alpha 6

KSC..Keratinocyte stem cells

CHAPTER 1

INTRODUCTION

Human papillomavirus (HPV) infection is the most common viral infection of the reproductive tract and is the cause of many squamous cell carcinomas, principally cancer of the cervix. Cervical cancer remains the leading type of cancer in women and the second leading cause of cancer death in women worldwide (Clifford, Smith, Plummer, Muñoz, & Franceschi, 2003). Although infection by high-risk HPV types is relatively common, cervical cancer is comparatively rare. This is in large part attributed to the 90% clearance of all HPV infections within two years of onset (Clifford et al., 2003; Pinto & Crum, 2000). Consequently, approximately 10% of women infected by oncogenic HPV will develop persistent infections, with a fraction of these infections progressing into cancer. In addition to HPV persistence, host-cell specific factors greatly contribute to cervical cancer risk. As of today, the target cell of HPV infection remains unknown, but infection requires that virus particles gain access to the epidermal basal layer and enter dividing basal cells that constitute the proliferative compartment of the epidermis. Therefore, most cervical cancers are believed to arise within the cervical transformation zone where tissue stem cells are presumed to reside (Longworth & Laimins, 2004); thus keratinocyte stem cells are speculated to be the main target cells of HPV infection. In recent years, it has been demonstrated that keratinocyte stem cells have sphere formation ability and express putative epidermal stem cell markers such as low levels of EGF

receptor (EGFR) and elevated levels of adhesion protein Integrin alpha 6 (INTα6), which

is expressed primarily on the basal membrane of the epidermis and has been postulated as

the main receptor of cell entry for HPV type 16 (HPV16) (Yoon, Kim, Park, & Cheong,

2001a). In contrast, keratinocytes with high levels of EGFR or low levels of integrin

alpha 6 (INTα6) acquire a more differentiated phenotype and have poorer growth

potential in culture(Le Roy et al., 2010a) (La Fleur, Johansson, & Roberg, 2012a). Most

recently, studies have proposed that the expression of HPV oncogenes in keratinocytes

stem cells *in vivo* promotes abnormal mobilization of these cells and contributes to cancer

initiation. These epidermal stem cells are also speculated to provide a reservoir of latently

infected cells that can persist for long periods of time (Michael, Lambert, & Strati,

2013a). The question then arises as to the relationship between the presence of basal stem

cells in an epithelium and susceptibility of that epithelium to HPV-mediated

transformation. We hypothesized that stem cell properties of the cervical epithelium or

the genital skin could influence susceptibility to transformation by HPV. Thus, this

project explores the relationship between the stem cell properties of normal human

epidermal skin cells in culture and these cells' susceptibility to transformation By HPV,

the etiological agent of approximately 5% of all known human cancers[1].

Through the use of 3-D suspension culture and fluorescence activated cell sorting

(FACS), we have successfully purified epidermal stem/progenitor cells from neonatal

foreskin tissue. We conducted extensive immortalization experiments with these enriched

populations and found that theses cell populations are several-fold more susceptible to

transformation by HPV16 DNA than mass cultured cells from the same individual

donors. Together, our findings provide experimental evidence that HPV16 DNA may

preferentially transform basal stem cell-like keratinocytes. The results of these studies

could help identify among the many people who present with persistent HPV infections,

the relatively few that are truly at risk for developing cancer.

CHAPTER 2

SPHEROID-DERIVED CULTURES OF PRIMARY HUMAN KERATINOCYTES ARE ENRICHED FOR BASAL STEM/PROGENITOR-LIKE CELLS

The epidermis of the skin is a stratified multilayer tissue maintained by constant renewal of suprabasal keratinocytes. During the process of epidermal renewal, regeneration is governed by a putative population of epidermal stem cells (EpSCs) found in the basal layer, the regenerative compartment of the skin interfollicular epidermis (IFE) (Blanpain & Fuchs, 2006). In the basal layer, EpSCs remain small in size, stain positive for basal cytokeratins, and express high levels of integrin alpha 6 (ITGα6) which mediates their attachment to the basement membrane (Barrandon & Green, 1987; Coulombe, Kopan, & Fuchs, 1989; Jones & Watt, 1993; Tani, Morris, & Kaur, 2000; Watt, Jordan, & O'Neill, 1988). During IFE renewal, basal EpSCs are primed for activation by environmental cues and divide to generate rapidly proliferating transit-amplifying cells (TAC). The proliferating TAC subsequently leave the basal surface and initiate a stepwise squamous differentiation program which replenishes lost suprabasal layers (Blanpain & Fuchs, 2006). The activation of basal EpSCs is characterized by the co-expression of basal cytokeratin 14 and the proliferative transcription factor P63, while EpSCs' upward movement to suprabasal layers is associated with a loss of the basal cytokeratins and a gradual decrease in P63 protein levels. During commitment to suprabasal differentiation, epidermal keratinocytes increase in size and amplify cellular

4

EGF signaling through the induction of the EGF receptor (EGFR) (Miettinen et al., 1995; Nanney, Magid, Stoscheck, & King, 1984; Rheinwald & Green, 1975; Takeuchi et al., 2001). During later stages of differentiation keratinocytes completely lose P63 expression and begin to express high levels of involucrin, K10, and several other genes involved in the formation of the cornified envelope (Hsu, Li, & Fuchs, 2014; Parsa, Yang, McKeon, & Green, 1999; Pellegrini et al., 2001).

In most studies, epidermal renewal has been attributed to a discrete population of basal stem cells (Clayton et al., 2007; Doupe et al., 2012; Redvers, Li, & Kaur, 2006; Schneider et al., 2003), but whether the IFE is hierarchically replenished by a single cell population that can switch between quiescence and activation, or whether IFE regeneration is stochastically carried out by several groups of committed progenitors (CP) is still being debated (De Rosa & De Luca, 2012; Hsu et al., 2014; Sada et al., 2016). In normal epidermal tissue, the stepwise regeneration of the IFE is tightly regulated by cell attachment to the basement membrane. Therefore, cell-surface detachment of normal human keratinocytes (NHKc) results in terminal differentiation, quickly followed by suspension-induced cell death (anoikis) (Green, 1977; Wakita & Takigawa, 1999). This phenotypic response is also accompanied with marked induction of EGFR expression (Wakita & Takigawa, 1999). Studies by our group and others have demonstrated that dramatic increase in EGFR drive keratinocyte proliferation but are poorly tolerated by NHKc (Akerman et al., 2001a; Bheda, Creek, & Pirisi, 2008a; Le Roy et al., 2010b; Takeuchi et al., 2001; Zyzak et al., 1994). While, lower expression of cell surface EGFR by keratinocytes is associated with quiescence, spheroid formation, and has been attributed to epidermal stem/progenitor-like cells (Fortunel, 2003; La Fleur,

Johansson, & Roberg, 2012b; Le Roy et al., 2010b; Sun, Goderie, & Temple, 2005; Vollmers et al., 2012). As a result, keratinocyte stem cell (KSC) studies have employed EGFR cell surface levels and cells' spheroid-forming abilities as an assessment of keratinocyte stemness (Le Roy et al., 2010b; Shamir & Ewald, 2014; Toma, McKenzie, Bagli, & Miller, 2005; Vollmers et al., 2012; Yu et al., 2006). Despite recent reports indicating that spheroid culture can improve skin cells' potency (Borena et al., 2014; Higgins, Richardson, Ferdinando, Westgate, & Jahoda, 2010; Kang, Kwack, Kim, Kim, & Sung, 2012; Vollmers et al., 2012), the regenerative effects of spheroid culture on (NHKc) has never been thoroughly investigated.

We employed a 3-D spheroid culture model system to investigate spheroid forming ability of 59 different NHKc strains isolated from individual neonatal foreskin explants. We found that only 40% of all NHKc strains were capable of aggregating into multicellular spheroids, while 60% of strains failed to form viable spheroids when cultured in suspension. Spheroid-derived (SD) cells displayed considerable cellular heterogeneity and expressed a marked induction of stem cell reprogramming factors within 24 h in suspension culture. When transposed into 2-D monolayer culture, SD cells readily restored keratinocyte colonies that stained positive for nuclear P63, basal cytokeratin 14, and were enriched for a basal stem/progenitor subpopulation of ITGα6^{high}/EGFR^{low} cells. Furthermore, adherent spheroids expressed a transcriptome signature corresponding to ectoderm commitment and epidermis reconstitution. Our findings show NHKc spheroid cultivation as an efficient method of enriching epidermal skin stem/progenitor-like cells from neonatal skin, and provide a powerful new tool for investigating epidermal basal stem cell activation in culture.

6

2.1 MATERIALS AND METHODS

Cell culture

NHKc were isolated from neonatal foreskin as previously described (Akerman et al., 2001a) and cultured in modified keratinocyte serum-free medium (KSFM), i.e.. 20 ng/mL EGF, 10 ng/mL bFGF, 0.4% bovine serum albumin (BSA), and 4μg/mL insulin, adapted from the spheroid-forming (Lagadec et al., 2010) and the sphere-propagating media (Rybak, He, Kapoor, Cutz, & Tang, 2011) described by Rybak et al. This medium will be referred to as KSFM-stem cell medium (KSFM-scm).

Spheroid formation and subcultivation

Cultured NHKc ($2x10^4$ cells) were seeded into a 96-well round-bottom plate coated with a polymerized mixture of agarose (0.05%) and KSFM-scm. The spheroids were maintained for at least 24 h in suspension prior to harvest. Multicellular suspension spheroids were plated into 2-D monolayer culture and allowed to proliferate. These cells will be referred to as SD-NHKc. Proliferating SD-NHKc were trypsinized, tested again for spheroid formation, then newly formed spheroids were again plated transposed into 2-D monolayer culture to produce secondary SD-NHKc cultures. Cell size and morphology was using Lumenera Infinity 1 software (Lumenera Corporation, Ottawa, ON).

Clonal growth assay

Cells were plated at low density (10,000-20,000 cells/dish) into duplicate 100-mm dishes, and fed KSFM-scm every 4 days, until ~25% confluence, then fed every 2 days.

Cultures were serially passaged (1:100) in 100-mm dishes until cell proliferative capacity was exhausted. Cell numbers and viability were determined using Countess Automated Cell Counter (Invitrogen, CA). Cumulative population doublings were calculated according to the formula: population doublings = (log N / N_0) / log$_2$, where N represents the total cell number obtained at each passage and N_0 represents the number of cells plated at the beginning of the experiment(Ma et al., 2015). Duplicate dishes were stained with 10% Giemsa stain to assess colony size and morphology.

Colony-forming efficiency assay

Spheroid non-forming NHKc (NF-NHKc) and spheroid forming NHKc (SF-NHKc) cultures were plated at 10,000 cells/dish in duplicate wells of a 6-well plate and fed once with 8 mL of medium, then incubated for 10-20 days. Cells were fixed with methanol, then stained with 10% Giemsa. Colony forming efficiencies (C.F.E) were calculated as colony number per dish divided by the original number of cells seeded. For 2D-attached spheroid culture, C.F.E was determined by obtaining the ratio of colonies generated from each seeded spheroid to the original number of cells contained within the spheroid.

Real Time PCR

Total RNA was isolated from cells using the All Prep DNA/RNA Mini Kit (Qiagen,CA) according to manufacturer's protocol. Reverse transcription was carried out with 1μg of total RNA using the iScript cDNA Synthesis Kit (Bio-Rad, Hercules, CA). Real-time PCR was performed using iQ SYBR Green Supermix (Bio-Rad) following the

manufacturer's instructions. Amplicon products were validated by agarose gel electrophoresis (2% v/v). GAPDH was used as an internal control. All samples were assayed in triplicate. The primer sequences used for real-time PCR are shown in Supplementary Table 1.

Immunohistochemistry

Cells were grown on coverslips coated with poly-lysine until 75% confluent. The cells were then washed twice in ice-cold phosphate buffered saline (PBS), fixed with 4% paraformaldehyde for 20 min at room temperature, permeabilized with 0.5% Triton in 1% glycine and then blocked using 0.5% BSA and 5% goat serum for 30 min at room temperature. Samples were next incubated with antibodies against P63 (Thermo Scientific, 1:200 dilution), and cytokeratin 14 (Santa Cruz Biotechnology, 1:200 dilution) in blocking solution overnight at 4°C. Samples were then washed three times with (PBS) containing Tween 20 (PBST), followed by incubation with FITC-and Alexa 568-conjugated secondary antibodies (at 1:1000 dilution, Invitrogen). Nuclei were stained with 1:5000 dilution of 4', 6-diamidino-2-phenylindole (DAPI) (Invitrogen) before cells were mounted. Cells were observed using a Nikon Eclipse E600 microscope and a Zeiss confocal laser-scanning microscope.

In vitro cell lineage tracing assay

2-D monolayer cultures were transfected with the pMSCV-IRES-EGFP plasmid vector carrying enhanced green fluorescent protein (eGFP) gene. Cells were trypsinized and seeded ($2x10^4$ cells) as 3-D spheroid suspension cultures. After 24 h eGFP-

expressing spheroids were plated into monolayer 2-D cell culture. Cells were tracked

with a Zeiss Axionvert 135 fluorescence microscope using Axiovision Rel. 4.5 software.

The number of eGFP-expressing cells was determined by quantifying a calibrated pixel-

by-pixel ratio between the green fluorescent image channel and the phase contrast image

using ImageJ software.

Fluorescent activated cell sorting

Cells 2-4 x 10^6 cells/ml were stained with FITC-conjugated anti-integrinα6

(Abcam, Cambridge, MA) and PE-conjugated anti-EGFR (BD Pharmingen San Jose,

CA). Flow cytometry analysis was performed using a BD FACSAria II flow cytometer

(BD Biosciences, San Jose, CA).

Microarray and gene expression analysis

Total RNA was isolated from mass cultures of a NHKc strain and the respective

spheroid rings, in triplicates, using the Qiagen RNeasy Plus Micro Kit according to the

manufacturer's protocol. RNA quality was assessed using an Agilent 2100 Bioanalyzer

and RNA Integrity Numbers ranged from 9.0 to 9.1. Microarray experiments were

performed using the Affymetrix's platform. Total RNA samples were amplified and

biotinylated using GeneChip WT PLUS Reagent Kit (Affymetrix, Santa Clara,

CA). Briefly, 100 ng of total RNA per sample was reverse transcribed into ds-cDNA

using NNN random primers containing a T7 RNA polymerase promoter sequence. T7

RNA polymerase was then added to cDNA samples to amplify RNA, and then RNA was

copied to ss-cDNA and degraded using RNase H. ss-cDNA molecules were then

fragmented and labelled with biotin. Amplified and labeled samples were hybridized to GeneChip HuGene 2.0 ST Arrays (Affymetrix, Santa Clara, CA) for 16 h at 45°C using a GeneChip Hybridization Oven 640 and a GeneChip Hybridization, Wash, and Stain Kit (Affymetrix, Santa Clara, CA). Hybridized arrays were washed and stained using GeneChip Fluidics Stations 450 (Affymetrix, Santa Clara, CA). Arrays were scanned using a GeneChip Scanner 3000 7G system and computer workstation equipped with GeneChip Command Console 4.0 software (Affymetrix, Santa Clara, CA). Following completion of array scans, probe cell intensity (CEL) files were imported into Expression Console Software (Affymetrix, Santa Clara, CA) and processed at the gene-level using Affymetrix's HuGene-2_0-st library file and Robust Multichip Analysis (RMA) algorithm to generate CHP files. After confirming data quality within Expression Console, CHP files containing log2 expression signals for each probe were then imported into Transcriptome Analysis Console Software version 3.0.0.466 (Affymetrix, Santa Clara, CA) to analyze cell type specific transcriptional responses using one-way between-subject analysis of variance.

Statistical analysis

Data were expressed as the mean ± standard deviation (SD). Differences between mean values were analyzed using Student's *t*-test. $P < 0.05$, $P < 0.01$ or $P < 0.001$ were considered statistically significant and indicated in the figures by *, ** or *** respectively.

2.2 RESULTS

Normal HKc strains derived from different individuals display varied behaviors in suspension culture. To investigate the anchorage-independent growth potential of normal human keratinocyte strains (NHKc) derived from skin explants of different donors, cells were plated at a density of 2×10^4 cells/well in KSFM-scm in 96-well round-bottomed plates coated with a semi-solid polymerized mixture of agarose and KSFM-scm (Figure 2.1). Under these conditions, cells grow as self-aggregating non-adherent three-dimensional spheroids of reproducible sizes (Figure 2.2B). We found that suspension cultures from some strains displayed an innate ability to aggregate into multicellular spheroids, while others consistently failed to self-assemble into spheroids throughout their time in suspension culture. To assess the status of cellular differentiation occurring in suspension cultures, we measured mRNA levels of the late-differentiation gene involucrin (IVL), as well as EGF receptor (EGFR), in spheroid-forming NHKc strains (SF-NHKc) and spheroid non-forming NHKc (NF-NHKc) strains cultivated in suspension for 72h, compared to the respective monolayer cultures. We found that suspension cultures from NF-NHKc presented a 35-fold upregulation of IVL mRNA compared to a 20.6-fold increase in SF-NHKc, relative to adherent monolayer mass cultures from the same strains (Figure 2.2C). This marked surge in IVL mRNA expression indicate that suspension culture conditions considerably stimulated terminal differentiation in keratinocytes from both strain groups. Yet, when assessing EGFR mRNA levels, we found a 45-fold greater increase in NF-NHKc suspensions compared to SF-NHKc suspensions, relative to levels found in monolayer cultures (Figure 2.2C). These data indicate that suspension cultures from SF-NHKc are more resistant to

suspension-induced differentiation than suspension cultures from NF-NHKc. We thus

chose to determine the ratio of cell viability in NF-NHK and SF-NHKc suspension

cultures by trypan blue dye exclusion staining and found that suspension cultures from

SF-NHKc maintained significantly greater cell viabilities as compared to NF-NHKc

(Figure 2.2D). These data indicate that cells from certain NHKc strains are better

resistant to terminal differentiation and suspension-induced cell death (anoikis).

NHKc spheroids produce functionally viable colonies. To further explore the

anoikis resistance observed in spheroid suspensions, we decided to test the functional

viability of suspension cultures from SF-NHKc and NF-NHKc strains by plating them

back into 2-D polystyrene cell culture dishes (Figure 2.3A). We found that cell

suspensions from SF-NHKc readily attached to the cell culture dish and gave rise to

proliferating cells that formed several holoclonal colonies, while NF-NHKc from

suspension culture gave rise to late differentiated cells that produced abortive colonies

(Figure 2.3B-C). Next, we examined the colony forming efficiency (CFE) of the re-plated

cell suspensions by quantifying the ratio of Giemsa-stained colonies to the number of

cells seeded. We found that cells derived from SF-NHKc spheroid suspensions (SD-

NHKc) were 74.5 times more efficient at generating colonies than suspensions from NF-

NHKc (Figure 2.4E-F). Functional analysis of individual NHKc strains isolated from 59

different human neonatal foreskin specimens revealed that most individual NHKc strains

(60%) were incapable of self-aggregating into multicellular spheroids, while a smaller

fraction of strains (40%) formed spheroids that generated viable colonies when plated in

13

monolayer culture (Figure 2.4G). These observations prompted us to concentrate our efforts on characterizing spheroid-derived cell populations.

Spheroid-derived NHKc are P63/K14 double-positive cells that maintain sub-apoptotic EGFR levels in culture. To gain further insight into the growth potential of spheroid-derived NHKc (SD-NHKc) in adherent 2-D monolayer culture, we performed extensive clonal analysis using cells derived from a single transplanted SF-NHKc spheroid and their corresponding monolayer mass cultures. We observed that small-sized cells proliferated from the spheroid to form a continuous monolayer of cells (Figure 2.5A, A1). After several rounds of subcultivation in monolayer culture, SD-NHKc progenies better resisted terminal differentiation (Figure 2.5B), whereas clones generated from mass cultures readily acquired an elongated phenotype after 15 population doublings (PD) in culture (Figure 2.5C). To determine the basal epidermal status of SD-NHKc progenies, we assessed their nuclear expression of P63 and cytoplasmic expression of basal cytokeratin 14 (K14) by immunohistochemistry. We found that over 60% of SD-NHKc clones expressed nuclear P63 or basal K14, whereas less than 20% of clones generated from corresponding mass cultured cells expressed K14, and only 10% expressed nuclear P63. SD-NHKc cultures also contained 26-times more K14/P63 co-expressing cells, suggesting that SD cultures were enriched for a population of stem/progenitor-like basal keratinocytes (Figure 2.5E). Next, we measured the levels of mRNAs encoding pan-P63, cytokeratin 14, and EGFR, and found a 4.6-fold increase in P63 mRNA levels and a 2.1-fold increase in K14 mRNA levels in SD-NHKc compared to their corresponding mass cultures. Interestingly, SD-NHKc expressed non-significant

14

differences in EGFR mRNA levels compared to mass cultures (Figure 2.6F). We then

investigated cell surface levels of EGFR in monolayer cultures using fluorescence

activated cell sorting analysis (FACS). Cell surface EGFR expression increased over 100-

fold in mass cultures after several rounds of subcloning, while EGFR levels in secondary

cultures of SD-NHKc remained at much lower levels (Figure 2.6G). The intensity of cell

surface EGFR staining seen in mass cultures also corresponded with a loss of spheroid

formation, elongated cell morphologies, and cell senescence (Figure 2.6C, H). Whereas,

secondary SD-NHKc cultures retained their spheroid forming abilities, accumulated more

population doublings (PD), and displayed small-sized cells that could be subcultivated for

over 10 weeks as monolayers (Figure 2.6H-K). These observations mirror previous

studies describing low levels of cell surface EGFR in NHKc as a feature of stem-like

keratinocytes, and intense upregulation of cell surface EGFR as a precursor of terminal

differentiation (LeRoy et al, 2010; Wakita and Takigawa, 1999). Taken together, these

data indicate that SD-NHKc are a proliferating population of basal keratinocytes, with

characteristics of stem and transit-amplifying cells (TAC) of the skin epidermis.

Spheroid-derived keratinocytes contain an increased number of

EGFR^{lo}/ITGα6^{hi} expressing cells. Given that SD-NHKc intensely expressed basal

epidermal markers, we suspected that their prolonged growth potential was primarily

sustained by a distinct fraction of KSC. To explore this possibility, we employed FACS

to purify populations of cells expressing high or low levels of EGFR and the basal

epidermal stem cell marker integrin alpha 6 (ITGα6). Interestingly, we found that about

20% of the cells in SD-NHKc cultures had low levels of EGFR and high levels of

Integrin α6 (EGFR^{lo}/ITGα6^{hi}). In contrast, EGFR^{lo}/ITGα6^{hi} cells made up only 3% of the

cells derived from mass cultured populations (Figure 2.7A, B). To determine the growth

potential of the other cell populations represented in these cultures, we cultivated the

EGFR^{lo}/ITGα6^{hi}, EGFR^{hi}/ITGα6^{hi}, and EGFR^{hi}/ITGα6^{lo} fractions from SF-NHKc mass

cultures, and carried them as monolayers. We found that EGFR^{hi}/ITGα6^{lo} cells

accumulated the fewest number of PD in culture (~3) and generated dividing colonies for

only 18 days in culture (Figure 2.7C). EGFR^{hi}/ITGα6^{hi} cells accumulated a total of 11.3

PD in culture and continued to generate dividing colonies for ~ 30 days (Figure 2.7C).

Interestingly, EGFR^{lo}/ITGα6^{hi} cells were slow-cycling during the first 15 days in culture,

then proliferated at a rate exceeding that of the other isolated cell fractions. Furthermore,

EGFR^{lo}/ITGα6^{hi} cells displayed the greatest growth potential of all FACS-isolated cells,

and generated dividing colonies for over 50 days in culture (Figure 2.7C). Moreover,

EGFR^{lo}/ITGα6^{hi} cells appeared small in size and produced large holoclonal (Barrandon &

Green, 1987) colonies with several cells that co-expressed nuclear P63 and cytokeratin 14

(Figure 2.8D-F4). Conversely, progenies from EGFR^{hi}/ITGα6^{lo} populations produced

large elongated cells that gave rise to abortive colonies and expressed undetectable levels

of P63 and cytokeratin 14 (Figure 2.9G-I4). To validate the expression of basal cell

markers detected by immunostaining, we performed real time RT-PCR analysis of pan-

P63 and K14 in both EGFR^{lo}/ITGα6^{hi} and EGFR^{hi}/ITGα6^{lo} cell fractions. PCR results

revealed a 3.4-fold upregulation of mRNA encoding P63 and a 1.7-fold upregulation of

mRNA encoding K14 in EGFR^{lo}/ITGα6^{hi} progenies compared to the unsorted cell

fraction. Conversely, EGFR^{hi}/ITGα6^{lo} populations expressed undetectable levels of P63

and K14 mRNA (Figure 2.10J).

To examine the spheroid-forming ability of different FACS-purified populations isolated from SD-NHKc, we seeded $2x10^4$ cells from each sorted population on 3-D soft agar cushions and found that EGFR^{lo}/ITGα6^{hi} cells retained spheroid-forming ability (Figure 2.10L), while EGFR^{hi}/ITGα6^{lo} cells failed to form spheroids in suspension culture (Figure 2.10K). Furthermore, when investigating the spheroid-forming abilities of EGFR^{lo}/ITGα6^{hi} cells purified from NF-NHKc strains, we found that they were better able to self-aggregate into multicellular spheroids as compared to the corresponding unsorted cell fractions (Figure 2.11M-O). Finally, we quantified the baseline proportions of EGFR^{lo}/ITGα6^{hi}, EGFR^{hi}/ITGα6^{hi}, EGFR^{hi}/ITGα6^{lo} cells between SF-NHK and NF-NHKc strains, but found no significant difference between the two groups (Figure 2.11P). Taken together these data suggest that the presence of basal stem-like cells is a major contributing factor of spheroid-forming ability in neonatal keratinocyte cultures, but is unlikely to be the sole factor mediating this phenotype from strain to strain.

NHKc spheroids express a gene signature depicting a mosaic of cell differentiation lineages. To assess the differentiation fates of NHKc during their growth in suspension, we measured mRNA levels of basal and suprabasal epidermal genes in spheroid suspensions and their corresponding SD cultures, relative to respective primary monolayer cultures. Real time RT-PCR analysis revealed a 6.3-fold upregulation in mRNAs encoding K15 in spheroid cells, while SD cultures exhibited a 3.5-fold increase in K15 expression. Spheroid cells exhibited a 6.4-fold increase in mRNAs encoding K5, while SD cultures expressed 3.0-fold more K5 mRNA than controls. Moreover, spheroid cells exhibited a 2.1-fold increase in mRNAs encoding K14, while SD cultures exhibited

17

a 4.0-fold increase (Figure 2.12A). Remarkably, spheroid suspensions equally expressed

significantly higher levels of the suprabasal epithelial markers filaggrin, K10, and

involucrin as compared to mass cultures and SD-NHKc (Figure 2.12A), suggesting that

keratinocytes within multicellular spheroids undertake a variety of differentiation

commitments, with some cells remaining basal and others undergoing terminal

differentiation. Moreover, the marked reduction in suprabasal markers seen in SD cells

suggest that cells capable of proliferating from spheroids after their culture in suspension

are better able to escape the terminal differentiation cues and are likely responsible for

the intense expression of suprabasal genes detected in multicellular spheroid suspension

cultures. To explore how 3-D spheroid culture affected epidermal proliferation programs,

we measured the mRNA expression levels of pan-P63, delta NP63, and Ki-67 in cells

collected during each stage of the spheroid re-plating assay. We found that SD-NHKc

expressed a 5.0-fold increase in mRNA encoding pan-P63, a 2.4-fold increase in mRNA

encoding delta NP63, and a 1.84-fold increase in mRNA encoding Ki-67 compared to

corresponding mass cultures (Figure 2.12B). Conversely, spheroid suspensions expressed

a mere 1.7-fold increase in pan-P63, a 0.3-fold downregulation of delta NP63, and

undetectable levels of Ki-67 (Figure 2.12B). These data indicate that cell proliferation is

substantially diminished in NHKc suspension cultures, which led us to question whether

the reduced gene expression of proliferation markers in spheroid cultures was a mere

indication of the presence of postmitotic cells or was perhaps suggestive of the presence

of slow-cycling self-renewing cells. To explore this possibility, we measured the relative

mRNA expression levels of genes encoding transcription factors involved in cell self-

renewal and found that spheroid cultures expressed a 4.9-fold increase in Nanog, a 20.5

18

fold increase in OCT-4, a 10.1-fold increase in SOX2, and a 17.1-fold increase in KLF4, whereas these levels dramatically decreased in SD-NHKc cultivated on monolayer plastic culture (Figure 2.12A-C). Given that epidermal self-renewal is mediated by basal cells, we decided to investigate the cytoplasmic intensities of basal K14 in NHKc during all three stages of the spheroid formation assay, i.e. mass culture, spheroid suspension culture, and SD culture. We found that primary keratinocyte colonies isolated from fresh skin explants stained intensely for K14 (Figure 2.13D1, D2). K14 expression was also detected during 3-D spheroid culture, particularly in cells found along the edge of the suspension spheroid (Figure 2.13D3, D4). Furthermore, when plated into 2-D monolayer plastic culture, proliferating SD-NHKc located along the spheroid's edge also expressed high levels of cytokeratin 14 (Figure 2.13D, D6). These data show that despite the induction of suprabasal markers seen in spheroid suspensions, a fraction of basal K14-positive keratinocytes are continuously maintained throughout the spheroid formation assay. To corroborate these findings, we performed serial subcultivations of SD-NHKc in 2-D and 3-D culture in order to test their ability to continually regenerate and survive through the spheroid assay selection (Figure 2.13E). We found that SD-NHKc sustained prolonged spheroid-forming abilities, but eventually lost this ability after the 3rd cycle of 2-D to 3-D subcultivation, with a progressive loss of K14-expressing cells with each consecutive cycle (Figure 5 F). Notably, the EGFR^{lo}/ITGα6^{hi} cell fraction virtually disappeared after the 4th cycle of subcultivation, while EGFR^{hi}/ITGα6^{lo} cell populations increased 3-fold (Figure 2.13G-H). Taken together, these findings reaffirm that spheroid formation is largely influenced by basal stem-like cell density in culture. Furthermore, our results indicate that besides inducing keratinocyte differentiation, spheroid culture

19

may also encourage some cells to enter a quiescent state, and express programs associated with self-renewal. The seeding of cells in 2-D monolayer culture likely reduces this self-renewal capacity, stimulating cell proliferation and commitment to terminal differentiation.

Plating multicellular spheroids on monolayer plastic triggers keratinocyte colony renewal and the formation of a cornified-like cell structure. Given the varied cell behaviors displayed by spheroid cultures, we aimed to determine the clonal fates of suspension cells in culture. Therefore, mass-cultured SF-NHKc were transfected with a plasmid transiently expressing enhanced green fluorescent protein (eGFP) and cells were seeded in 3-D agar suspension (Figure 2.14A-A2). We observed that eGFP-positive cells progressively aligned along the spheroid edge, then gradually traveled out from the spheroid (Figure 2.14B, C). By tracking the movement of eGFP-expressing spheroid cells, we quantified the proportion of cells present in different regions of the aggregated spheroid throughout its time in suspension culture. Interestingly, the fraction of cells located in the center region of the spheroid decreased considerably with time, in part due to necrosis, while the quantity of cells located outside of the spheroid increased ~ 10-fold. By day 15, over 59% of all eGFP-labelled spheroid cells were found outside of the spheroid while fractions remaining within the spheroid structure formed a dense hollow ring of cells (Figure 2.14E). When immunostained for P63 and K14, we found that cells within the floating spheroid ring expressed undetectable levels of these basal markers (Figure 2.14E1). Conversely, we detected a 27.1-fold increase in transcripts encoding IVL mRNA in cells within the spheroid ring, while cells present outside the ring

expressed considerably reduced levels of IVL (Figure 2.15F). These results suggest that the dense spheroid rings are largely composed of cells committed to terminal diferentiation, while cells that traveled outside of the spheroid are more resistant to differentiation. To gain further insight into the clonal fate of cells that traveled outside the spheroid, we plated individual eGFP-expressing spheroids into individual uncoated 2-D polystyrene cell culture dishes and tracked the movement of adherent eGFP-labeled SD cells (SD^{GFP}). Strikingly, similar to behavior observed during suspension culture, we found that SD^{GFP} migrated outwardly into the empty spaces of the dish and generated monolayer sheets along their paths (Figure 2.16G-K). Notably, within 12 days in culture, SD^{GFP} were systematically aligned along the edge of cell sheets, on the side most distal to the adherent spheroid, and progressively expanded the colony's surface area (Figure 2.16J, K). Dual immunostaining of cells found along the edge of cell sheets revealed an intense expression of K14 and nuclear P63 (Figure 2.16L-L3). When tracking a single SD^{GFP} in culture, we found that it could regenerate a dividing K14-positive colony (Figure 2.16M-N). Given that SD progenies played such a direct role in colony renewal, we aimed to further study their colony restoration patterns during spheroid seeding in 2-D monolayer culture. Giemsa staining analysis revealed that SD cells migrated in a centrifugal configuration to form colonies throughout the empty territories distal to the spheroid central point (Figure 2.16O-O1). Remarkably, the configuration of multicellular spheroids after their attachment in 2-D monolayer culture was reminiscent of the organization of a stratified epidermis, with the spheroid central point recapitulating features of a cornified envelope and the propagating cell sheets behaving as the basal layers.

21

Surface-attached spheroids express genes involved in epidermis development.

We used microarrays to determine the gene expression profile of the cornified-like spheroid rings formed from surface-attached multicellular spheroids. Hierarchical clustering analysis found that the expression of 575 genes changed within the 2-D spheroids compared to their corresponding mass cultures, with 380 genes upregulated and 185 genes downregulated (Figure 2.17A, B). The spheroid rings expressed a great number of genes involved in cornification and skin envelope formation, such as the marked induction of sciellin (SCEL) and SPINK5 (Figure 2.17C). Furthermore, we found a significant induction in upstream regulators of epidermal stratification, notably EGFR (Z-score=2.2) and P63 (Z-score=1.5). Moreover, induction of DSG1 and upstream activation of NFkB were detected, suggesting considerable mechanically-induced cellular stress reported to be expressed by keratinocyte cultures during epidermal recovery(Fitsialos et al., 2007; Johnson et al., 2014). Markedly, Gene Ontology analysis identified several distinct epidermal developmental processes activated in 2-D spheroids, notably ectoderm commitment, proliferation of skin cells, and keratinocyte differentiation (Figure 2.17E). Taken together, these findings indicate that attachment of spheroids onto a plain polystyrene cell culture dish primes keratinocytes for epidermal reconstruction, and outlines a rage of differentiation fates occurring within 2-D spheroid cultures.

2.3 FIGURES
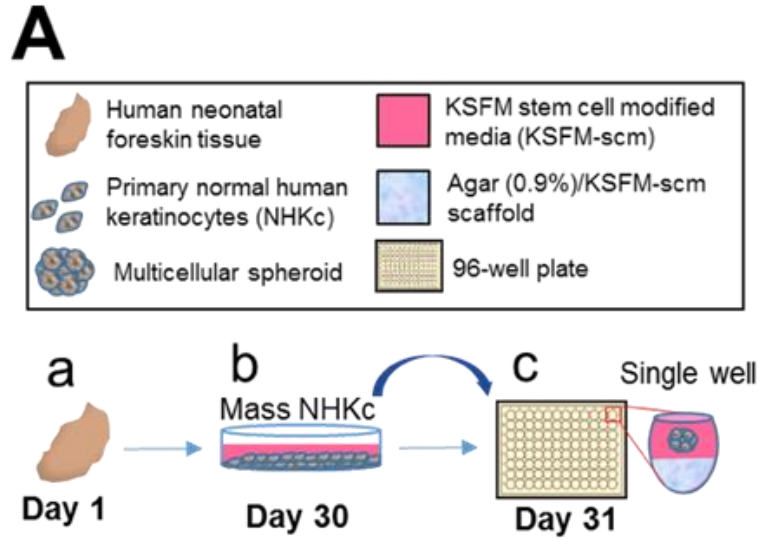
Figure 2.1 Spheroid formation assay. (A) Schematic illustrating (a) a suspension spheroid being plated back into (b) an empty uncoated 2-D polystyrene cell culture dish. After 15-20 days the adherent culture gives rise to (c) a monolayer of spheroid-derived cells which are cultivated and maintained in 2-D culture.
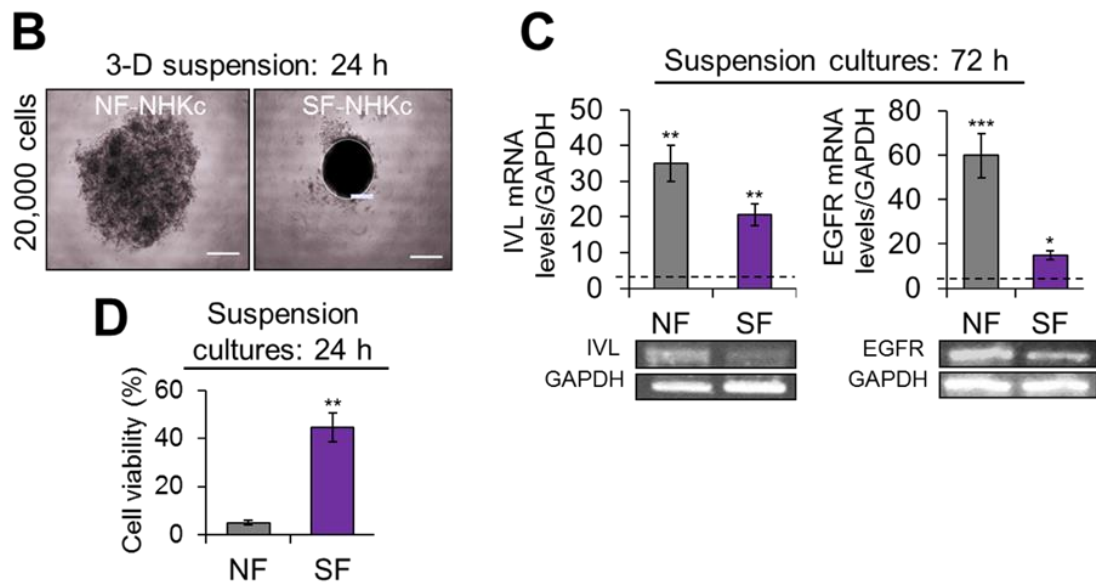
Figure 2.2 Multicellular spheroids retain cell viability in suspension culture. (B) 2×10^4 cells cultured in stem cell media were seeded onto soft agarose cushions coating individual wells of a 96-well plate. The ability for spheroid formation was assessed over the course of 144 h. Aggregation of NHKc suspensions from spheroid non-forming (NF-NHKc) and spheroid-forming (SF-NHKc) strains was observed on a Nikon TMS phase microscope using Infinity 1 Analyze Software. (C) Expression levels of involucrin (IVL) and EGF receptor (EGFR) mRNA, in NF-NHKc and SF-NHKc cells after 72 h in suspension culture as determined by reverse transcriptase real-time PCR relative to monolayer mass cultures. Dotted lines represent mRNA expression levels in monolayer mass cultures. (Bottom) amplicon products of each real time PCR reaction were ran on a 2% agarose gel and observed by ethidium bromide staining. Data were normalized to GAPDH expression. Bars indicate standard deviation, and *, **, and *** indicate statistically significant differences, with P values $\leq$ 0.05, 0.01 and 0.001, respectively. (D) Cell viability in NF-NHKc and SF-NHKc suspensions after 72 hours of 3-D suspension culture as determined by trypan blue staining.
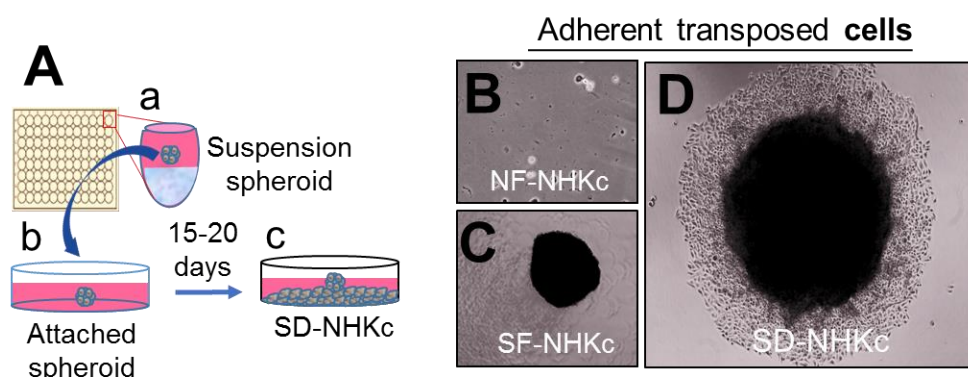
Figure 2.3 Spheroid re-plating assay. (A) Schematic illustrating (a) a suspension spheroid being plated back into (b) an empty uncoated 2-D polystyrene cell culture dish. After 15-20 days the adherent culture gives rise to (c) a monolayer of spheroid-derived cells which are cultivated and maintained in 2-D culture. (B) 2-D plated cell suspensions from NF-NHKc and (C) SF-NHKc strains into an empty well of a 6-well plate. (D) Monolayer-attached spheroid giving rise to dividing cells in 2-D culture 24 h after plating.
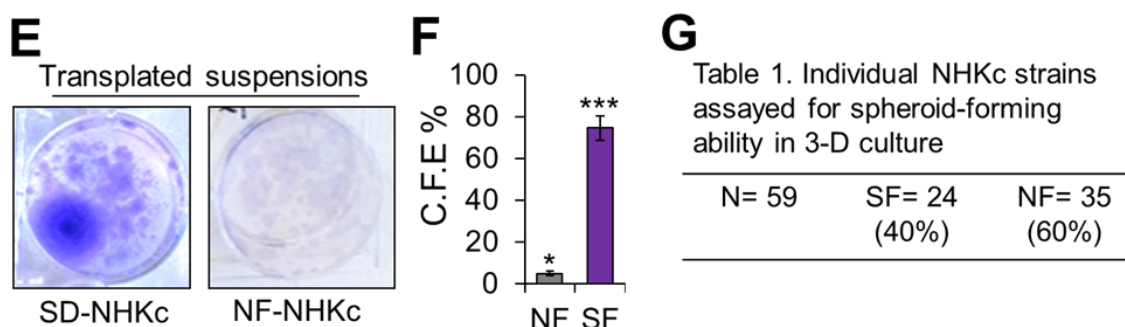
Figure 2.4 Multicellular spheroids produce functionally viable colonies when re-plated in monolayer culture. (E) Giemsa-stained re-plated suspension cultures from NF-NHKc and SF-NHKc. (F) Colony forming efficiencies (C.F.E) of re-plated cell suspensions. Bars indicate standard deviation, and *, **, and *** indicate statistically significant differences, with P values ≤ 0.05, 0.01 and 0.001, respectively. (G) Number of individual NHKc strains utilized in spheroid formation assay. Spheroid-formation growth capacity was determined in 59 individual NHKc strains derived from different neonatal subjects.
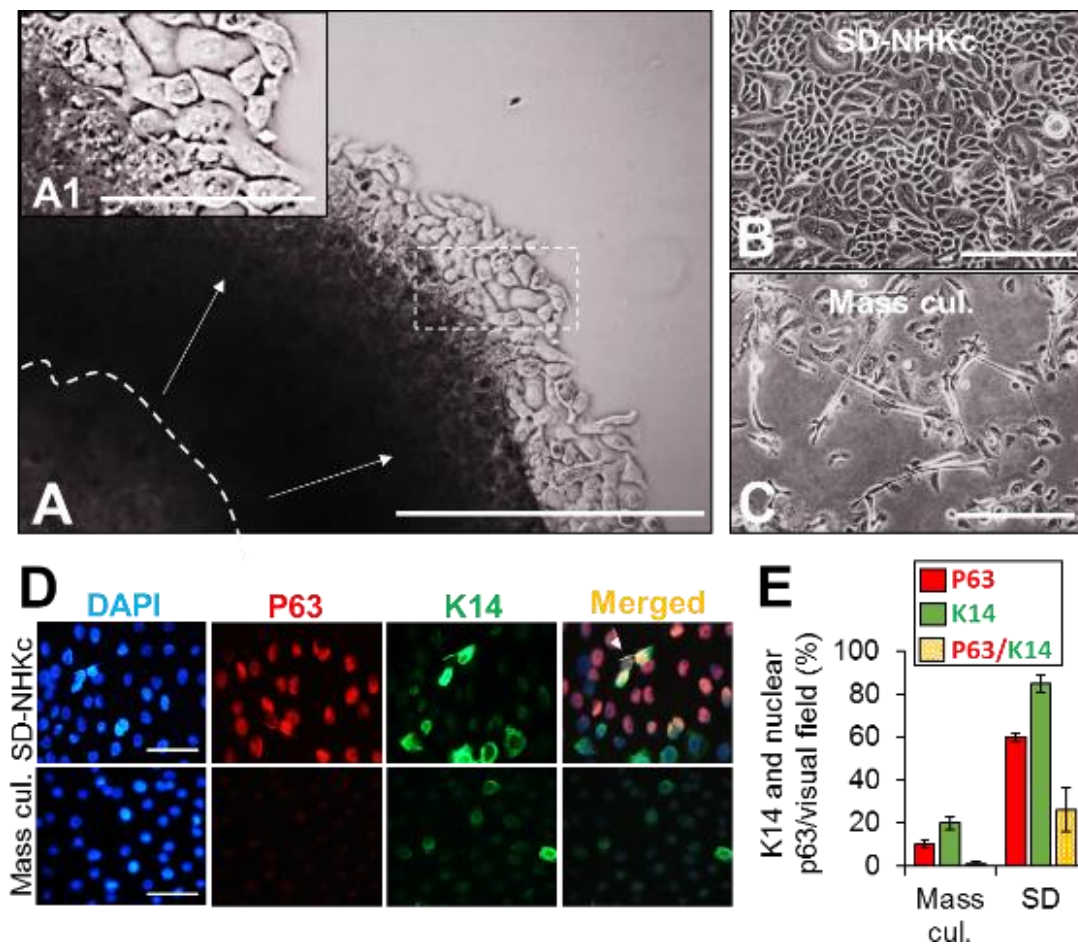
Figure 2.5 Primary spheroid-derived keratinocytes display basal epidermal cell features. (A) A single multicellular spheroid was transplanted back into a plain uncoated 2-D polystyrene cell culture dish and allowed to regenerate cells. White contour lines delineate the necrotic core from the proliferative compartment of the spheroid. Arrows depict direction of cell outflow. (A1) Magnified image of SD-NHKc actively proliferating out of the spheroid. Scale bar=20 μM. (B) Adherent SD-NHKc and (C) their corresponding mass cultured cells after 15 cumulative population doublings in monolayer culture. Scale bar=50 μM. (D) SD-NHKc and their corresponding mass cultures immunostained with antibodies against basal cytokeratin 14 (K14, green) and pan-tumor protein 63 targeting all TP63 isoforms (P63, red). Scale bar=50 μM. (E) The ratio of P63, K14, and P63/K14 co-expressing cells was quantified by measure of stained cell density per visual field.
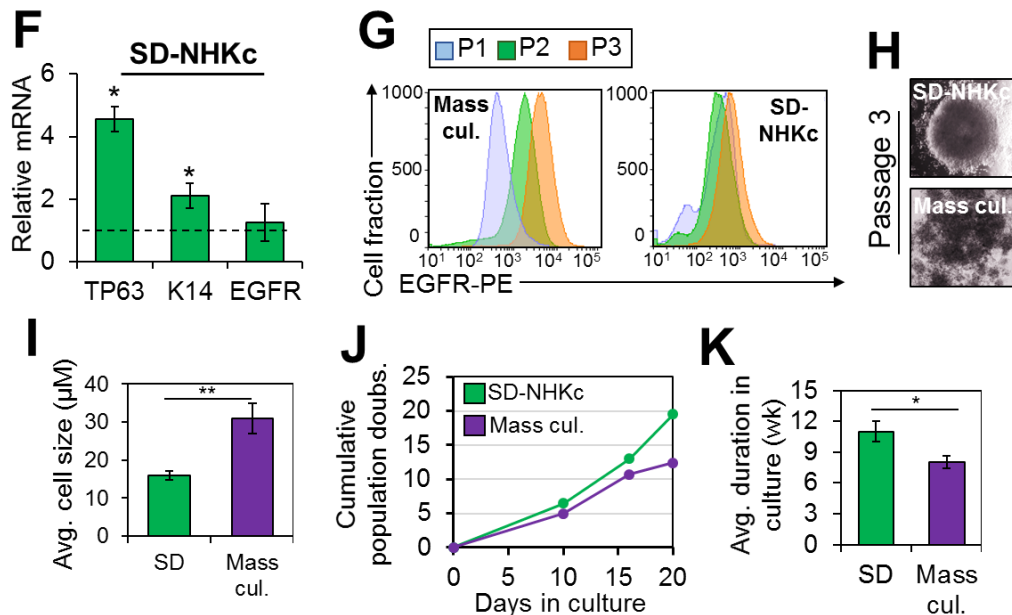
Figure 2.6 Spheroid-derived cells exhibit EpSC phenotypes. (F) The expression of mRNAs encoding pan-TP63 targeting all P63 isoforms, cytokeratin 14, and EGFR in initial generations of SD-NHKc (passage 1) relative to corresponding mass cultures (passage 0) as determined by Real-time RT-PCR. Dotted line indicates mRNA expression levels in monolayer mass cultures. Data were normalized to GAPDH expression and reported as mean +/- standard deviation of triplicate experiments using three different keratinocyte strains. (G) Cell surface expression of EGF receptor measured by fluorescent activated cell sorting (FACS) in SD-NHKc and their corresponding mass cultures after the initial passage (P1), passage 2 (P2), and passage 3 (P3) in adherent monolayer culture. (H) Spheroid-forming ability in SF-NHKc mass cultures and their corresponding SD-NHKc progenies after 3 passages in monolayer culture. (I) Mean cell size of SD-NHKc (P3) and their mass cultured counterparts (P3) was quantified by a Nikon TMS phase microscope using Infinity 1 Analyze Software. (J) Clonal growth assay assessing the cumulative population doublings of adherent SD-NHKc and their monolayer mass cultures over the course of 20 days. (K)
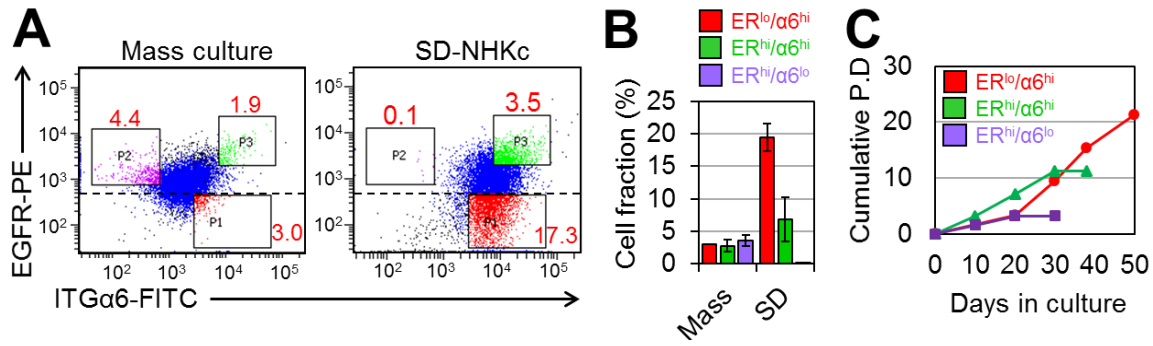
Figure 2.7 Spheroid-derived NHKc are enriched for a basal subpopulation of EGFR^{lo}/ITGα6^{hi} expressing cells. A) Representative flow cytometry data illustrating the use of epidermal cell markers integrin alpha 6 (ITGα6) and EGFR to purify desired cell populations within SD-NHKc and their corresponding mass cultures. (B) Fraction of EGFR^{lo}/ITGα6^{hi}, EGFR^{hi}/ITGα6^{hi}, and EGFR^{hi}/ITGα6^{lo} cells detected in mass cultures and their corresponding SD cultures. (C) Cumulative population doublings observed in EGFR^{lo}/ITGα6^{hi} cells, EGFR^{hi}/ITGα6^{hi}, and EGFR^{hi}/ITGα6^{lo} cells over the course of 50 days in monolayer culture.
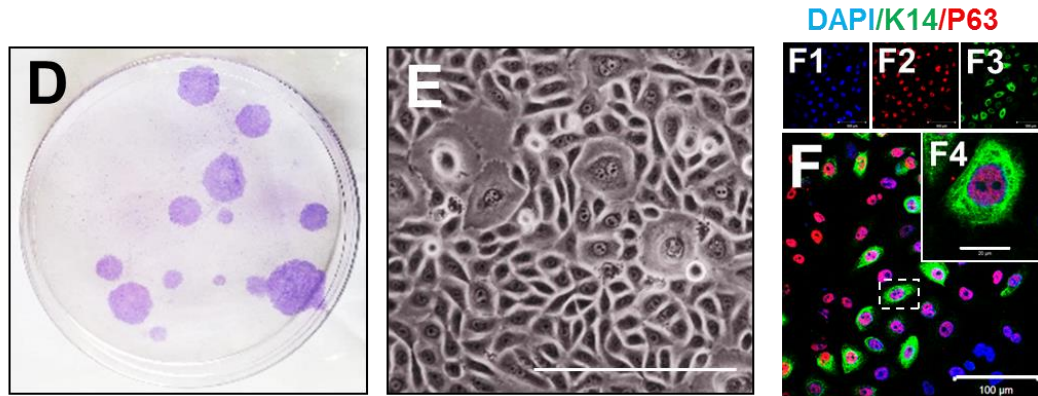
EGFR^{lo}/ITGα6^{hi}

Figure 2.8 EGFR^{lo}/ITGα6^{hi} cells are basal stem-like cells. (D) FACS-sorted EGFRlo/ITGα6hi cells were plated into a 6-well plate at a density of 10,000 cells/well and cultured until approximately 80% confluent. Colony density was assessed by Giemsa staining. (E) Phase contrast image of proliferating EGFR^{lo}/ITGα6^{hi} cell progenies in adherent culture. (F) EGFR^{lo}/ITGα6^{hi} cell progenies immunostained with antibodies against pan-tumor protein 63 targeting all TP63 isoforms (P63, red), and basal cytokeratin 14 (K14, green). Scale bar=100 µM. (F1) Cells stained with the nuclear stain DAPI and for (F2) nuclear P63 and (F3) cytoplasmic keratin 14. (F4) 40 x magnification image of a single EGFR^{lo}/ITGα6^{hi} cell progeny immunostained for nuclear P63 (red) and cytoplasmic K14 (green). Scale bar=20 µM.
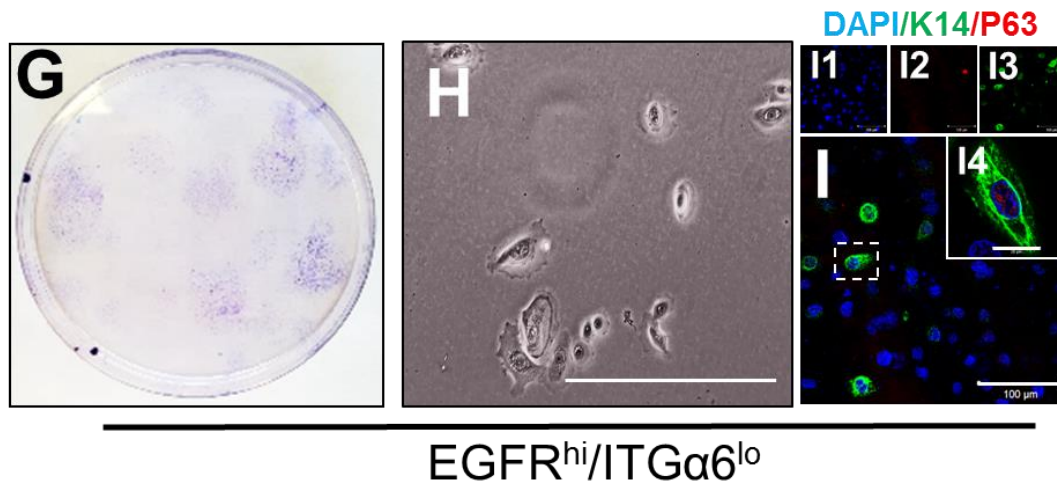
Figure 2.9 EGFR^{hi}/ITGα6^{lo} cells are terminally differentiated cells. (G) EGFR^{hi}/ITGα6^{lo} colonies stained with Giemsa. (H) Phase contrast images of EGFRhi/ITGα6lo cell progenies in adherent culture. (I) EGFR^{hi}/ITGα6^{lo} cells immunostained with antibodies against pan-tumor protein 63 targeting all TP63 isoforms (P63, red), and basal cytokeratin 14 (K14, green). Scale bar=100 μM. (I1) Cells stained with the nuclear stain DAPI, (I2) and for nuclear P63, and (I3) cytokeratin 14. (I4) 40 x magnification image of a single EGFR^{hi}/ITGα6^{lo} cell progeny immunostained for nuclear P63 (red) and cytoplasmic K14 (green). Scale bar=20 μM.
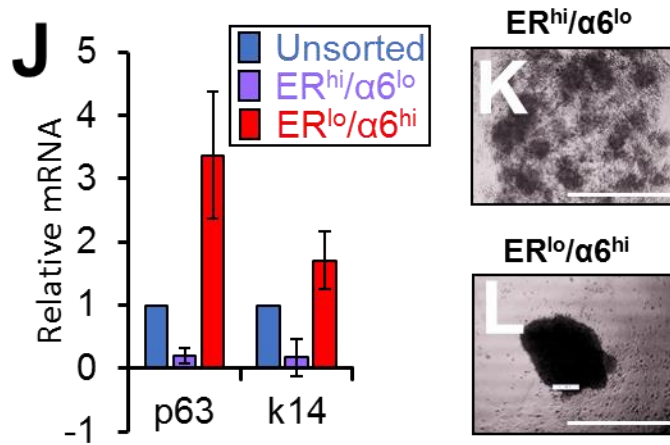
Figure 2.10 EGFR^{lo}/ITGα6^{hi} are spheroid-forming cells. (J) The expression of mRNAs encoding TP63 (all isoforms) and cytokeratin 14 in EGFR^{hi}/ITGα6^{lo} and EGFR^{lo}/ITGα6^{hi} cells relative to unsorted population as determined by Real-time RT-PCR. Data were normalized to GAPDH expression and reported as mean +/- standard deviation. (K) Phase contrast images of suspension cultures from EGFR^{hi}/ITGα6^{lo} and (L) EGFR^{lo}/ITGα6^{hi} cells isolated from a SF-NHKc strain. Scale bar=100 μM.
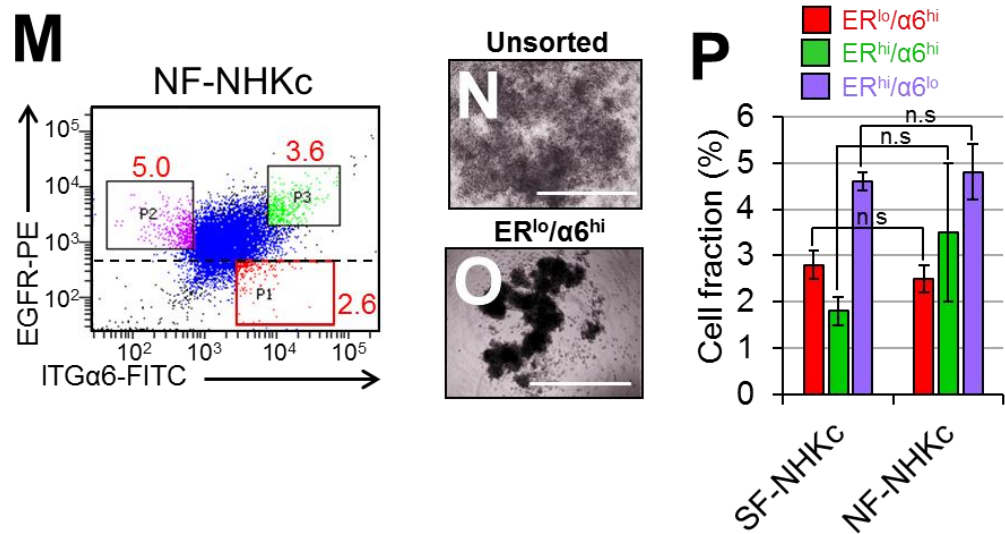
Figure 2.11 EGFR^{lo}/ITGα6^{hi} cells from NF-NHKc exhibit better cell self-aggregation in suspension culture. (M) Representative flow cytometry data illustrating the gating of EGFR^{lo}/ITGα6^{hi} cells in a NF-NHK strain. (N) Phase contrast images of suspension cultures from unsorted populations and (O) EGFR^{lo}/ITGα6^{hi} cells isolated from a corresponding SF-NHKc strain. Scale bar=100 μM. (P) Quantification of sorted cell fractions between SF-NHKc and NF-NHKc strains.
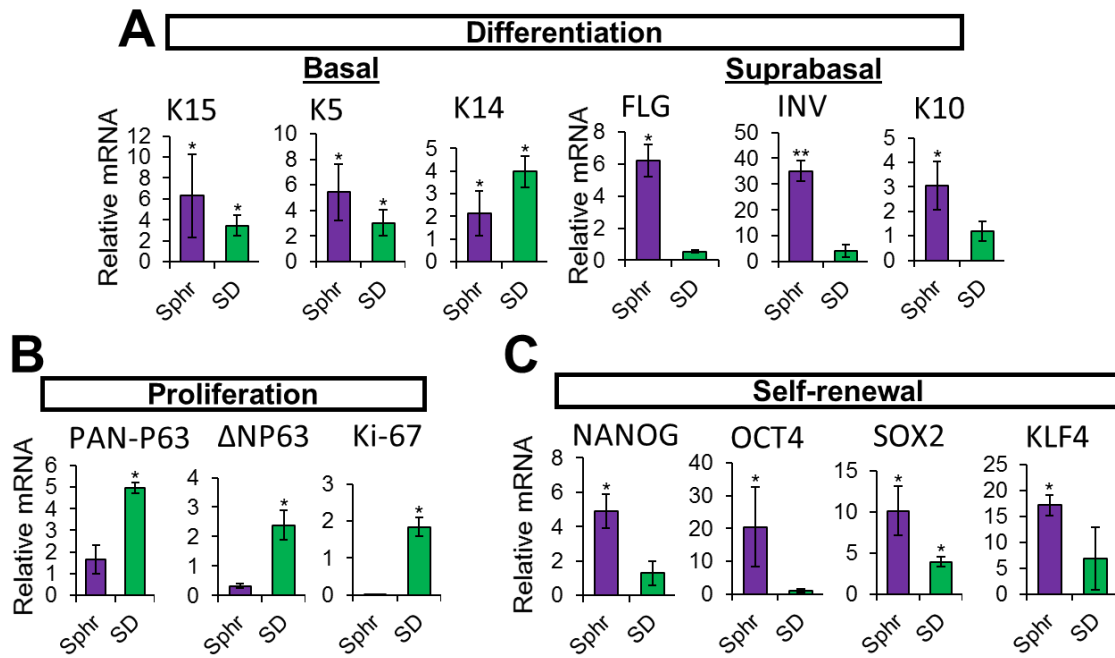
Figure 2.12 NHKc spheroid cultures exhibit gene expression profiles indicating cellular heterogeneity. (A) The expression of mRNAs encoding epidermal basal genes: K15, K5, K14; suprabasal differentiation genes: filaggrin, involucrin, K10; (B) Epidermal proliferation genes: pan-P63, delta Np63, Ki-67; (C) reprogramming genes: Nanog, Oct4, Sox2, Klf4 in suspension spheroids and SD cultures, relative to corresponding monolayer mass cultures.
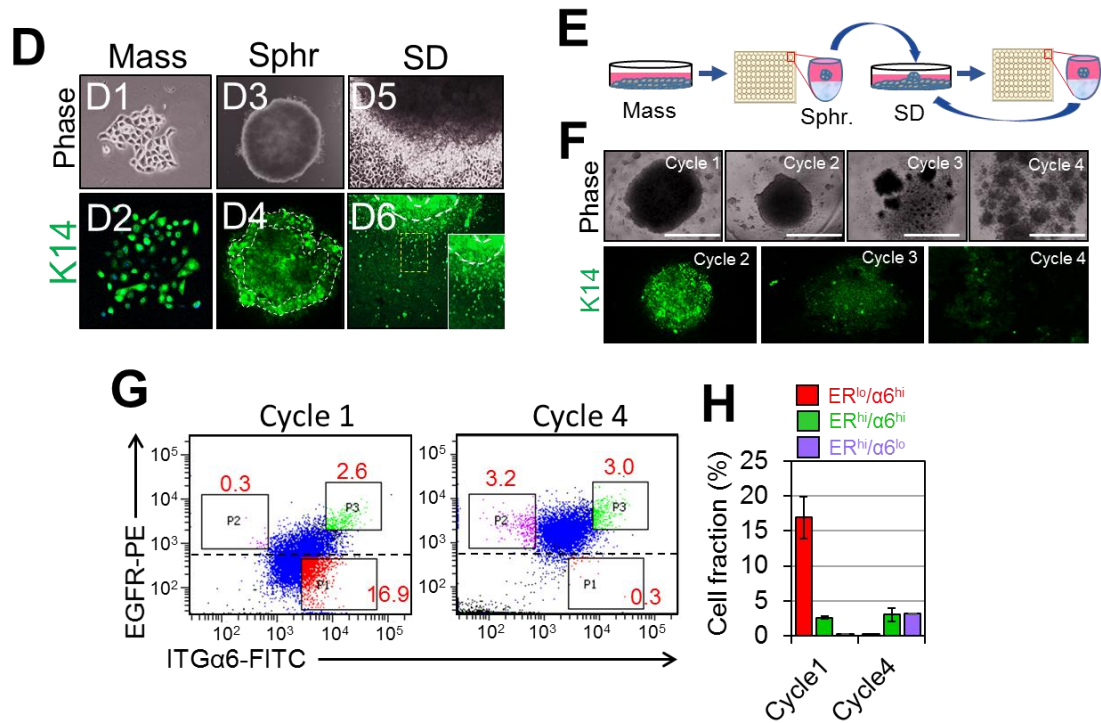
Figure 2.13 Basal stem-like cell depletion halts spheroid formation. (D) Phase contrast images of a (D1) mass cultured NHKc colony newly derived from a skin explant, (D3) its corresponding suspension spheroid, (D5) and the subsequent spheroid-derived cultures (D2, D4, D6) immunostained against keratin 14, respectively. White contour lines indicate spheroid edge. (E) Schematic depicting the spheroid subcultivation assay. (F) NHKc spheroid cultures and respective K14 expressions after 4 generation cycles of spheroid subcultivation. Scale bar=100 μM. (G) Representative flow cytometry data illustrating gated fractions of EGFR^{lo}/ITGα6^{hi}, EGFR^{hi}/ITGα6^{hi}, and EGFR^{hi}/ITGα6^{lo} cells detected in SD-NHKc after 1 and 4 generational cycles of spheroid subcultivation. (H) Quantification of sorted cell fractions in SD-NHKc after 1 and 4 generational cycles.
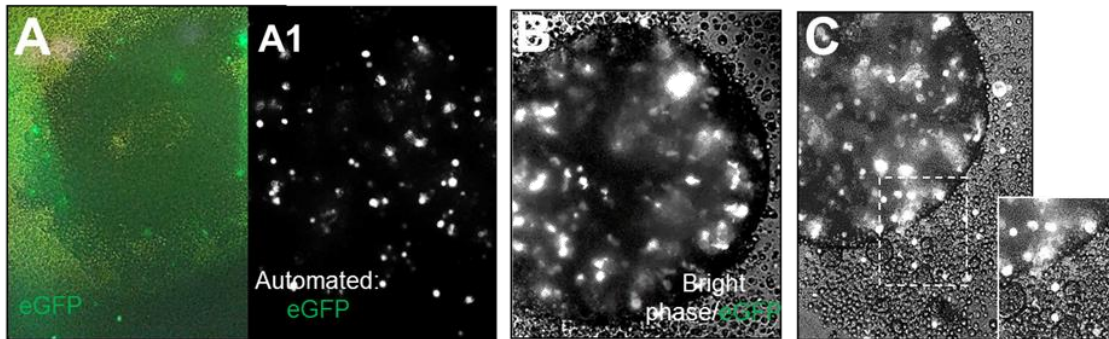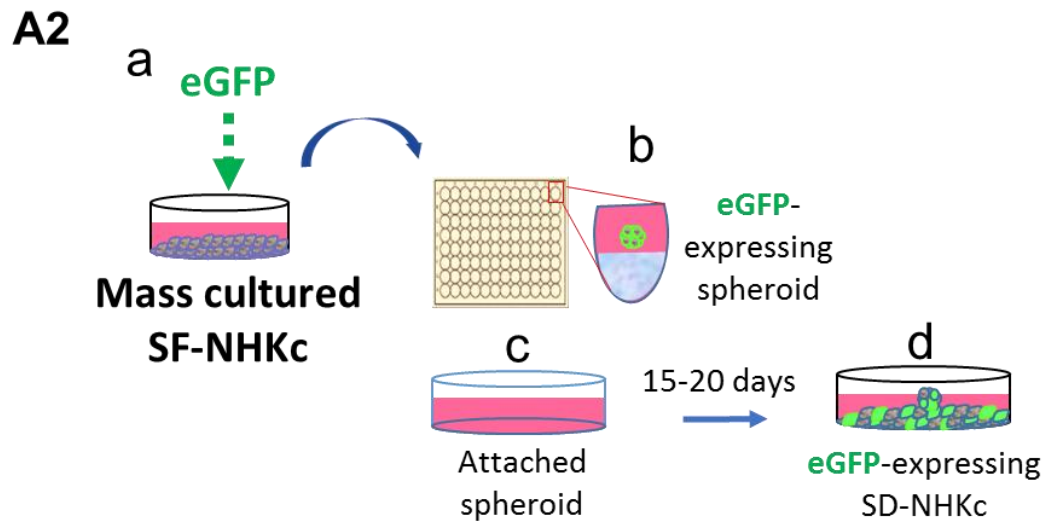
Figure 2.14 Spheroid-forming cells are mobile in 3-D suspension. (A) Manual image of eGFP-expressing SF-NHKc after 6 h in 3-D suspension culture. (A1) Automated image of eGFP-tagged progenies (white dots) at 6 h. (A2) Developing of SD^{GFP} cell cultures. (a) Mass cultured SF-NHKc were transfected with the pMSCV-IRES-EGFP plasmid vector carrying enhanced green fluorescent protein (eGFP) gene. (b) SD^{GFP} cells are then seeded on 2-D plastic culture. (c) SD^{GFP} propagating from an adherent multicellular spheroid. (B) Bright phase image of eGFP-expressing keratinocytes within a multicellular spheroid after 24 h in 3-D suspension culture. (C) eGFP-labeled cells are seen travelling out of a spheroid after 36 h in suspension culture.

D Proportion of eGFP+ cells (%)

■ Center   ▨ Edge   ■ Outside

Day 1: 2.3, 18.7, 79

Day 5: 20.8, 43.2, 36

Day 15: 5, 59.6, 35.4

E / **E1** DAPI P63 K14 — 50 µm

F Day 15 — IVL mRNA levels/β-actin *** Edge, Outside
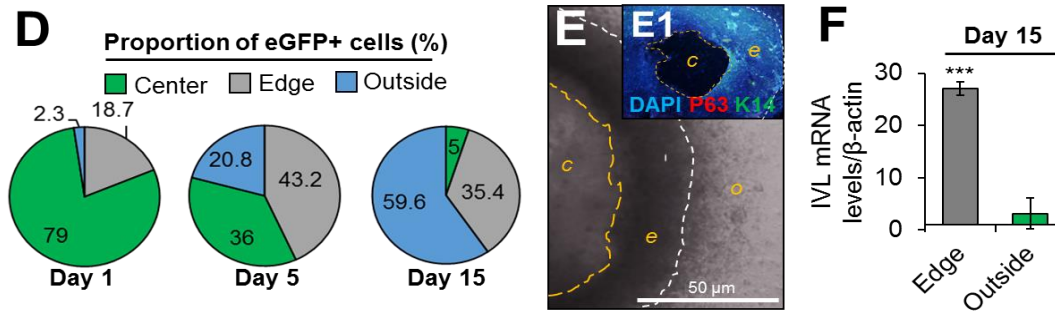
Figure 2.15 Spheroid-derived cells are resistant to differentiation in suspension culture. (D) Fluorescent tracking of eGFP-labelled cells after 15 days in suspension culture. The proportion of eGFP-expressing cells in each spheroid compartment (i.e. center, edge, or outside) was quantified at each time point by ImageJ analysis. (E) Dense ring of cells generated from a single spheroid after 15 days in suspension. White contour lines delineate the outer edge of the spheroid (o); orange contour lines delineate the spheroid's center (c) from the spheroid's inner edge (e). (E1) Dense ring of cells immunostained with DAPI, antibodies against pan-tumor protein 63 targeting all TP63 isoforms (P63, red), and basal cytokeratin 14 (K14, green). Scale bar=50 µM. (F) Expression levels of mRNAs encoding involucrin in cells within the dense floating
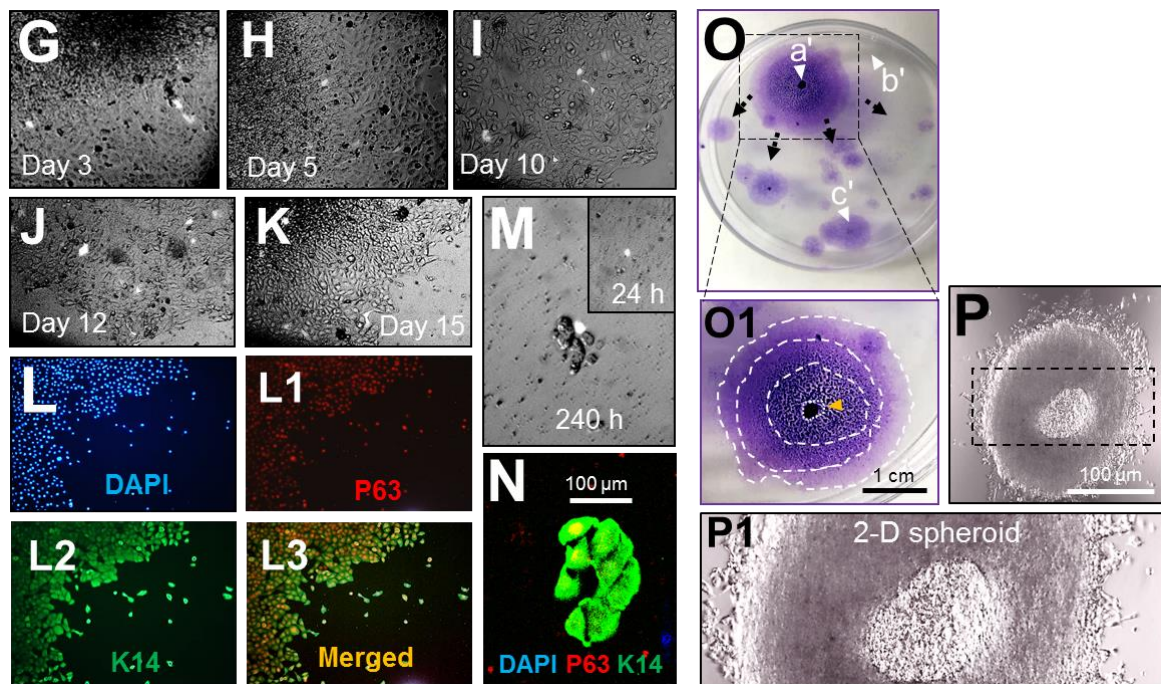
Figure 2.16 Spheroid-derived cells mobilize to regenerate basal colonies. (G-I) Monitoring eGFP-labelled SD cells (SD^{GFP}) traveling from a transposed spheroid over the course of 10 days in monolayer 2-D culture. (J-K) SD^{GFP} cells positioned at day 15 along the edge of monolayer sheets formed through the fusing of colonies. (L) Spheroid-derived cells located at the edge of monolayer sheets were immunostained against DAPI (blue) and antibodies against (L1) P63 (red), and (L2) K14 (green). (M) A single SD^{GFP} cell is seen forming a dividing colony after 10 days in 2D adherent culture. (N) Immunostaining of the generated colony with antibodies against K14 (green), P63 isoforms, and DAPI (blue). (O) Colony renewal visible by Giemsa staining 20 days after a single spheroid is attached in 2-D monolayer culture. Black arrows depict the radial migratory patterns of SD cells as they travel from (a') the adherent spheroid to (b'-c') distant spaces throughout the dish. (O) Configuration mapping of progressively expanding epidermal sheets from the attached spheroid. Contour lines delineate each new sheet layer. Orange arrow indicates the position of the spheroid's central point as it forms a ring of cornified cells. (P) Bright-field microscopic image of an adherent spheroid 15 hours after attachment in 2-D culture. (P1) Magnified image of SD cell sheets forming underneath a 2-D spheroid.
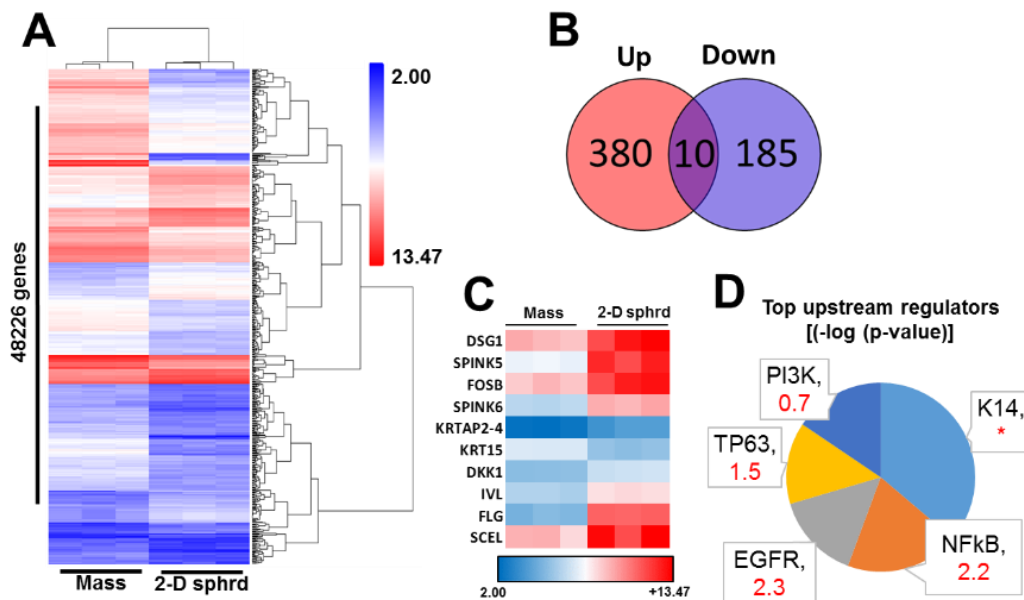
Figure 2.17 2-D spheroids express genes involved in skin epidermal development. (A) Unsupervised hierarchical clustering of log-transformed mean-centered mRNA expression levels for all transcripts deregulated twofold within the 2-D spheroid compared to monolayer mass cultures. (B) Venn diagram depicting down-regulated and upregulated mRNAs expressed by freshly attached spheroids. (C) Heatmap depicting select genes relevant to skin cornified envelope formation. (D) Illustration of upstream regulators targeted for activation in 2-D attached spheroids. Pie chart segments are proportional to the -log of the overlap p-value. Activation z-scores are indicated in red; * = undetermined activation pattern. (E) Downstream functional effects of gene transcripts upregulated and downregulated in 2-D spheroids (twofold change FDR <0.05). Gene Ontology analysis indicates activation of pathways related to cell proliferation and epidermis formation.

E
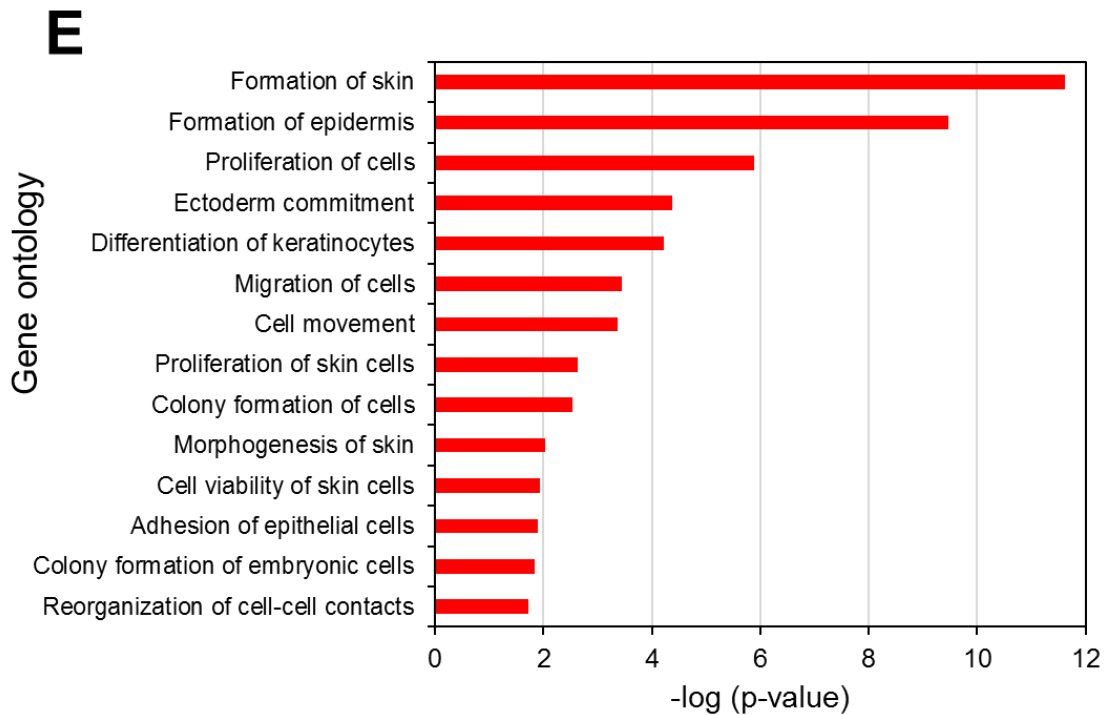
Figure 2.18 2-D spheroid cells are activated for skin reconstruction. (E) Downstream functional effects of gene transcripts upregulated and downregulated in 2-D spheroids (twofold change FDR <0.05). Gene Ontology analysis indicates activation of pathways related to cell proliferation and epidermis formation.

2.4 DISCUSSION

In this study, we demonstrate that certain strains of neonatal human keratinocyte cultures exhibit many functional properties of EpSCs and are intrinsically resistant to suspension-induced cell death (anoikis) when cultivated as 3-D spheroid suspensions. What makes newborn skin specimens unique for epidermis stem cell studies is their inherently greater reserves of EpSCs and the virtual absence of genomic insults that frequently accumulate in adult tissue (Gago et al., 2009; Pirisi, Creek, Doniger, & DiPaolo, 1988; Van Der Schueren, Cassiman, & Van Den Berghe, 1980). These

attributes allow for more precise investigations of factors driving epidermal cell activation in normal human skin tissue. In this study we found that certain NHKc strains consistently formed spheroids in suspension, while others were consistently incapable of aggregating into spheroids. Although we did not find major differences in colony forming efficiencies between freshly-isolated primary cultures from spheroid forming (SF) and spheroid non-forming (NF) NHKc strains, we observed that spheroid-forming ability was generally greater in primary cultures that expressed less cell surface EGFR. These observations strengthen earlier reports by our group describing interindividual variabilities in epidermal NHKc EGFR levels (Akerman et al., 2001a) and corroborate several findings describing EGFR[low] expressing NHKc as spheroid-forming basal KSC(Fortunel, 2003; Le Roy et al., 2010b).

When re-plated in monolayer 2-D culture, we observed that surface-adherent spheroids generated small-sized cells that traveled to produced holoclonal colonies. Colonies then fused to form epidermal sheets that stained intensely for the proliferative marker P63 and basal maker K14, indicative of TAC cells primed for epidermal regeneration (Fitsialos et al., 2007; Patel, Wilson, Harding, Finlay, & Bowden, 2006). By probing SD-NHKc with a plasmid transiently expressing eGFP, we monitored colony reconstitution patterns of SD[GFP] cells and found that a single SD progeny could form a fully dividing K14[+] colony. It is likely that the attachment of spheroids onto a plain 2-D polystyrene cell culture dish is interpreted as a 'loss of local confluence'(Guo & Jahoda, 2009; Roshan et al., 2016) by keratinocytes, thus triggering colony initiation and epidermal restoration. When conducting RT-PCR analysis on spheroids in suspension, we detected reduced mRNA levels of keratinocyte proliferation markers KI-67 and ΔNP63,

but these levels were markedly increased in SD monolayer cultures. Ingenuity Pathway Analysis (IPA) distinguished the presence of several skin cell proliferation processes activated during 2-D spheroid culture. These data support earlier studies by Guo and Jahoda, demonstrating that attachment of keratinocytes onto a plain cell culture surface stimulates skin progenitor cell activation and wound-repair (Guo & Jahoda, 2009).

We expected that secondary cultures from SD-NHKc would ubiquitously express high cell surface levels of EGFR, but we found that SD progenies maintained reduced cell surface EGFR levels and were significantly enriched for a slow-cycling $EGFR^{lo}/ITG\alpha6^{hi}$ cell subpopulation. Surprisingly, we found no significant differences in the relative proportions of $EGFR^{lo}/ITG\alpha6^{hi}$ cells between primary mass cultures from SF-NHKc and those of NF-NHKc, suggesting that an elevated number of basal keratinocytes is not the sole contributor of spheroid-forming ability in primary NHKc cultures. Incidentally, we found that spheroid suspensions expressed both basal and suprabasal markers, yet concomitantly preserved elevated expressions of mRNAs encoding pluripotent reprogramming factors Nanog, Oct-4, Sox2, and Klf4. Gene Ontology analysis revealed ectodermal commitment as a pathway significantly activated in surface-attached spheroids, indicative of the presence of a primitive cell population extant within neonatal spheroid cultures. Although it would be experimentally challenging to define the commitment lineage of all cell populations present within NHKc spheroids, the broad array of gene signatures they express reflects a mosaic of differentiation commitments (Mo et al., 2013; Pastrana, Silva-Vargas, & Doetsch, 2011; Rybak et al., 2011).

Our results point to two distinct cell lineages within multicellular NHKc spheroids: a population of basal stem/progenitor-like cells that maintain high levels of

K14 and produce holoclonal colonies in adherent culture, and a post-mitotic involucrin-expressing cell population that makes up the bulk of spheroid cultures and eventually forms a cornified-like spheroid ring of terminally differentiated cells. It is possible that uncommitted basal stem/progenitor populations present within primary NHKc cultures are signaled to remain in, or revert to, a less differentiated state during suspension culture, while CP are precipitated into terminal differentiation. A precise ratio between EpSCs, early TAC, and CP may therefore be critical in calibrating spheroids' regenerative potency and differentiation programs in culture. Additional study would be needed to further explore the molecular factors underpinning these behaviors, and to further characterize the differentiation fates undertaken by each of these cell populations. Our data are in line with increasing evidence indicating that progenitor cells can switch between quiescence and activation depending on microenvironmental signals and tissue regenerative needs (Clayton et al., 2007; Doupe et al., 2012; Horsley, Aliprantis, Polak, Glimcher, & Fuchs, 2008; Roshan et al., 2016; Tumbar et al., 2004), and corroborate reports that 3-D cultivation of mammalian cells acts as a reprogramming tool capable of reverting differentiated cells to a more primitive stem state (Borena et al., 2014; Liu et al., 2009; Rybak et al., 2011; Shamir & Ewald, 2014).

Taken together, our observations have many implications. First, the complex behaviors exhibited by primary NHKc during suspension culture provide new insight into elements that influence basal cell homeostasis, and outlines the broad array of cell plasticity stimulated during keratinocyte spheroid culture. Moreover, the fact that most EpSC investigations have been conducted in mice with a single genetic background makes human newborn skin studies better representative of the genetic diversity found

41

across human specimens. Such distinctions may have a more significant impact on mammalian epidermal studies than previously appreciated. For instance, the stark differences seen in spheroid-forming abilities between NHKc strains isolated from different individuals could be evidence of intrinsic, potentially congenital, traits influencing person-to-person propensities for basal stem/progenitor cell activation. Further study would be required to better understand the genetic and signaling networks regulating these behaviors, and how they might influence pathologies driven by aberrant basal stem/progenitor cell activation.

2.5 REFERENCES

Akerman, G. S., Tolleson, W. H., Brown, K. L., Zyzak, L. L., Mourateva, E., Engin, T. S., … Pirisi, L. (2001). Human papillomavirus type 16 E6 and E7 cooperate to increase epidermal growth factor receptor (EGFR) mRNA levels, overcoming mechanisms by which excessive EGFR signaling shortens the life span of normal human keratinocytes. *Cancer Research*, *61*(9), 3837–3843.

Akerman, G. S., Tolleson, W. H., Brown, K. L., Zyzak, L. L., Mourateva, E., Engin, T. S., … Pirisi, L. (2001). Human papillomavirus type 16 E6 and E7 cooperate to increase epidermal growth factor receptor (EGFR) mRNA levels, overcoming mechanisms by which excessive EGFR signaling shortens the life span of normal human keratinocytes. *Cancer Research*, *61*(9), 3837–3843.

Akerman, G. S., Tolleson, W. H., Brown, K. L., Zyzak, L. L., Mourateva, E., Engin, T. S., … Pirisi, L. (2001). Human papillomavirus type 16 E6 and E7 cooperate to increase epidermal growth factor receptor (EGFR) mRNA levels, overcoming

mechanisms by which excessive EGFR signaling shortens the life span of normal human keratinocytes. *Cancer Research*, *61*(9), 3837–3843.

Altomare, D., Velidandla, R., Pirisi, L., & Creek, K. E. (2013). Partial loss of Smad signaling during in vitro progression of HPV16-immortalized human keratinocytes. *BMC Cancer*, *13*(1), 424. https://doi.org/10.1186/1471-2407-13-424

Barrandon, Y., & Green, H. (1987). Three clonal types of keratinocyte with different capacities for multiplication. *Proceedings of the National Academy of Sciences*, *84*(8), 2302–2306.

Bheda, A., Creek, K. E., & Pirisi, L. (2008a). Loss of p53 induces epidermal growth factor receptor promoter activity in normal human keratinocytes. *Oncogene*, *27*(31), 4315–4323. https://doi.org/10.1038/onc.2008.65

Bheda, A., Creek, K. E., & Pirisi, L. (2008b). Loss of p53 induces epidermal growth factor receptor promoter activity in normal human keratinocytes. *Oncogene*, *27*(31), 4315–4323. https://doi.org/10.1038/onc.2008.65

Blanpain, C. (2013). Tracing the cellular origin of cancer. *Nature Cell Biology*, *15*(2), 126–134. https://doi.org/10.1038/ncb2657

Blanpain, C., & Fuchs, E. (2006). Epidermal stem cells of the skin. *Annual Review of Cell and Developmental Biology*, *22*, 339–373. https://doi.org/10.1146/annurev.cellbio.22.010305.104357

Bodily, J., & Laimins, L. A. (2011). Persistence of human papillomavirus infection: keys to malignant progression. *Trends in Microbiology*, *19*(1), 33–39. https://doi.org/10.1016/j.tim.2010.10.002

Borena, B. M., Meyer, E., Chiers, K., Martens, A., Demeyere, K., Broeckx, S. Y., … Spaas, J. H. (2014). Sphere-Forming Capacity as an Enrichment Strategy for Epithelial-Like Stem Cells from Equine Skin. *Cellular Physiology and Biochemistry*, *34*(4), 1291–1303. https://doi.org/10.1159/000366338

Chen, Y., Pirisi, L., & Creek, K. E. (2013). Ski protein levels increase during in vitro progression of HPV16-immortalized human keratinocytes and in cervical cancer. *Virology*, *444*(1–2), 100–108. https://doi.org/10.1016/j.virol.2013.05.039

Chow, L. T., Broker, T. R., & Steinberg, B. M. (2010). The natural history of human papillomavirus infections of the mucosal epithelia: NATURAL HISTORY OF HPV INFECTIONS AND PATHOLOGY. *APMIS*, *118*(6–7), 422–449. https://doi.org/10.1111/j.1600-0463.2010.02625.x

Clayton, E., Doupé, D. P., Klein, A. M., Winton, D. J., Simons, B. D., & Jones, P. H. (2007). A single type of progenitor cell maintains normal epidermis. *Nature*, *446*(7132), 185–189. https://doi.org/10.1038/nature05574

Clifford, G. M., Smith, J. S., Plummer, M., Muñoz, N., & Franceschi, S. (2003). Human papillomavirus types in invasive cervical cancer worldwide: a meta-analysis. *British Journal of Cancer*, *88*(1), 63–73. https://doi.org/10.1038/sj.bjc.6600688

Coulombe, P. A., Kopan, R., & Fuchs, E. (1989). Expression of keratin K14 in the epidermis and hair follicle: insights into complex programs of differentiation. *The Journal of Cell Biology*, *109*(5), 2295–2312.

De Rosa, L., & De Luca, M. (2012). Cell biology: Dormant and restless skin stem cells. *Nature*, *489*(7415), 215–217. https://doi.org/10.1038/489215a

Doupe, D. P., Alcolea, M. P., Roshan, A., Zhang, G., Klein, A. M., Simons, B. D., &

    Jones, P. H. (2012). A Single Progenitor Population Switches Behavior to

    Maintain and Repair Esophageal Epithelium. *Science*, *337*(6098), 1091–1093.

    https://doi.org/10.1126/science.1218835

Doupé, D. P., & Jones, P. H. (2012). Interfollicular epidermal homeostasis: dicing with

    differentiation. *Experimental Dermatology*, *21*(4), 249–253.

    https://doi.org/10.1111/j.1600-0625.2012.01447.x

Evander, M., Frazer, I. H., Payne, E., Qi, Y. M., Hengst, K., & McMillan, N. A. (1997).

    Identification of the alpha6 integrin as a candidate receptor for papillomaviruses.

    Journal of Virology, *71*(3), 2449–2456.

Fakhry, C. (2006). Clinical Implications of Human Papillomavirus in Head and Neck

    Cancers. *Journal of Clinical Oncology*, *24*(17), 2606–2611.

    https://doi.org/10.1200/JCO.2006.06.1291

Fitsialos, G., Chassot, A.-A., Turchi, L., Dayem, M. A., LeBrigand, K., Moreilhon, C., …

    Ponzio, G. (2007). Transcriptional signature of epidermal keratinocytes subjected

    to in vitro scratch wounding reveals selective roles for ERK1/2, p38, and

    phosphatidylinositol 3-kinase signaling pathways. *The Journal of Biological

    Chemistry*, *282*(20), 15090–15102. https://doi.org/10.1074/jbc.M606094200

Flesken-Nikitin, A., Hwang, C.-I., Cheng, C.-Y., Michurina, T. V., Enikolopov, G., &

    Nikitin, A. Y. (2013). Ovarian surface epithelium at the junction area contains a

    cancer-prone stem cell niche. *Nature*, *495*(7440), 241–245.

    https://doi.org/10.1038/nature11979

Fortunel, N. O. (2003). Long-term expansion of human functional epidermal precursor

cells: promotion of extensive amplification by low TGF- 1 concentrations.

Journal of Cell Science, *116*(19), 4043–4052. https://doi.org/10.1242/jcs.00702

Fuchs, E. (2012). The Impact of Cell Culture on Stem Cell Research. *Cell Stem Cell*,

10(6), 640–641. https://doi.org/10.1016/j.stem.2012.03.010

Gago, N., Pérez-López, V., Sanz-Jaka, J. P., Cormenzana, P., Eizaguirre, I., Bernad, A.,

& Izeta, A. (2009). Age-Dependent Depletion of Human Skin-Derived Progenitor

Cells: Age-Dependent Depletion of Human SKPs. *STEM CELLS*, *27*(5), 1164–

1172. https://doi.org/10.1002/stem.27

Green, H. (1977). Terminal differentiation of cultured human epidermal cells. *Cell*, *11*(2),

405–416.

Guo, A., & Jahoda, C. A. B. (2009). An improved method of human keratinocyte culture

from skin explants: cell expansion is linked to markers of activated progenitor

cells. *Experimental Dermatology*, *18*(8), 720–726. https://doi.org/10.1111/j.1600-

0625.2009.00900.x

Henderson, S., Chakravarthy, A., Su, X., Boshoff, C., & Fenton, T. R. (2014). APOBEC-

Mediated Cytosine Deamination Links PIK3CA Helical Domain Mutations to

Human Papillomavirus-Driven Tumor Development. *Cell Reports*, *7*(6), 1833–

1841. https://doi.org/10.1016/j.celrep.2014.05.012

Herfs, M., Yamamoto, Y., Laury, A., Wang, X., Nucci, M. R., McLaughlin-Drubin, M.

E., … Crum, C. P. (2012). A discrete population of squamocolumnar junction

cells implicated in the pathogenesis of cervical cancer. *Proceedings of the*

National Academy of Sciences, *109*(26), 10516–10521.

https://doi.org/10.1073/pnas.1202684109

Higgins, C. A., Richardson, G. D., Ferdinando, D., Westgate, G. E., & Jahoda, C. A. B.

(2010). Modelling the hair follicle dermal papilla using spheroid cell cultures:

Letter to the Editor. *Experimental Dermatology*, *19*(6), 546–548.

https://doi.org/10.1111/j.1600-0625.2009.01007.x

Horsley, V., Aliprantis, A. O., Polak, L., Glimcher, L. H., & Fuchs, E. (2008). NFATc1

Balances Quiescence and Proliferation of Skin Stem Cells. *Cell*, *132*(2), 299–310.

https://doi.org/10.1016/j.cell.2007.11.047

Hossein Neamatzadeh, Reza Soleimanizad, Masoud Zare-Shehneh, Saba Gharibi,

Abolfazl Shekari, & Amir Bahman Rahimzadeh. (1996). Association between p53

Codon 72 (Arg72Pro) Polymorphism and Primary Open-Angle Glaucoma in

Iranian Patients. https://doi.org/10.6091/ibj.1379.2014

Hsu, Y.-C., Li, L., & Fuchs, E. (2014). Emerging interactions between skin stem cells

and their niches. *Nature Medicine*, *20*(8), 847–856.

https://doi.org/10.1038/nm.3643

Hufbauer, M., Biddle, A., Borgogna, C., Gariglio, M., Doorbar, J., Storey, A., … Akgul,

B. (2013). Expression of Betapapillomavirus Oncogenes Increases the Number of

Keratinocytes with Stem Cell-Like Properties. *Journal of Virology*, *87*(22),

12158–12165. https://doi.org/10.1128/JVI.01510-13

Johnson, J. L., Koetsier, J. L., Sirico, A., Agidi, A. T., Antonini, D., Missero, C., &

Green, K. J. (2014). The Desmosomal Protein Desmoglein 1 Aids Recovery of

Epidermal Differentiation after Acute UV Light Exposure. *Journal of*

Investigative Dermatology, *134*(8), 2154–2162.

https://doi.org/10.1038/jid.2014.124

Jones, P. H., & Watt, F. M. (1993). Separation of human epidermal stem cells from transit amplifying cells on the basis of differences in integrin function and expression. *Cell*, *73*(4), 713–724.

Kang, B. M., Kwack, M. H., Kim, M. K., Kim, J. C., & Sung, Y. K. (2012). Sphere Formation Increases the Ability of Cultured Human Dermal Papilla Cells to Induce Hair Follicles from Mouse Epidermal Cells in a Reconstitution Assay. *Journal of Investigative Dermatology*, *132*(1), 237–239. https://doi.org/10.1038/jid.2011.250

Kines, R. C., Thompson, C. D., Lowy, D. R., Schiller, J. T., & Day, P. M. (2009). The initial steps leading to papillomavirus infection occur on the basement membrane prior to cell surface binding. *Proceedings of the National Academy of Sciences*, *106*(48), 20458–20463. https://doi.org/10.1073/pnas.0908502106

Kowli, S., Velidandla, R., Creek, K. E., & Pirisi, L. (2013). TGF-β regulation of gene expression at early and late stages of HPV16-mediated transformation of human keratinocytes. *Virology*, *447*(1–2), 63–73.

https://doi.org/10.1016/j.virol.2013.08.034

La Fleur, L., Johansson, A.-C., & Roberg, K. (2012a). A CD44high/EGFRlow Subpopulation within Head and Neck Cancer Cell Lines Shows an Epithelial-Mesenchymal Transition Phenotype and Resistance to Treatment. *PLoS ONE*, *7*(9), e44071. https://doi.org/10.1371/journal.pone.0044071

La Fleur, L., Johansson, A.-C., & Roberg, K. (2012b). A CD44high/EGFRlow Subpopulation within Head and Neck Cancer Cell Lines Shows an Epithelial-Mesenchymal Transition Phenotype and Resistance to Treatment. *PLoS ONE*, *7*(9), e44071. https://doi.org/10.1371/journal.pone.0044071

Lagadec, C., Vlashi, E., Della Donna, L., Meng, Y., Dekmezian, C., Kim, K., & Pajonk, F. (2010). Survival and self-renewing capacity of breast cancer initiating cells during fractionated radiation treatment. *Breast Cancer Research*, *12*(1), R13. https://doi.org/10.1186/bcr2479

Lawson, D. A., Bhakta, N. R., Kessenbrock, K., Prummel, K. D., Yu, Y., Takai, K., … Werb, Z. (2015). Single-cell analysis reveals a stem-cell program in human metastatic breast cancer cells. *Nature*, *526*(7571), 131–135. https://doi.org/10.1038/nature15260

Le Roy, H., Zuliani, T., Wolowczuk, I., Faivre, N., Jouy, N., Masselot, B., … Polakowska, R. (2010a). Asymmetric Distribution of Epidermal Growth Factor Receptor Directs the Fate of Normal and Cancer Keratinocytes In Vitro. *Stem Cells and Development*, *19*(2), 209–220. https://doi.org/10.1089/scd.2009.0150

Le Roy, H., Zuliani, T., Wolowczuk, I., Faivre, N., Jouy, N., Masselot, B., … Polakowska, R. (2010b). Asymmetric Distribution of Epidermal Growth Factor Receptor Directs the Fate of Normal and Cancer Keratinocytes In Vitro. *Stem Cells and Development*, *19*(2), 209–220. https://doi.org/10.1089/scd.2009.0150

Letian, T., & Tianyu, Z. (2010). Cellular receptor binding and entry of human papillomavirus. *Virology Journal*, *7*(1), 2. https://doi.org/10.1186/1743-422X-7-2

Liu, Y., Clem, B., Zuba-Surma, E. K., El-Naggar, S., Telang, S., Jenson, A. B., … Dean, D. C. (2009). Mouse Fibroblasts Lacking RB1 Function Form Spheres and Undergo Reprogramming to a Cancer Stem Cell Phenotype. *Cell Stem Cell*, *4*(4), 336–347. https://doi.org/10.1016/j.stem.2009.02.015

Longworth, M. S., & Laimins, L. A. (2004). Pathogenesis of Human Papillomaviruses in Differentiating Epithelia. *Microbiology and Molecular Biology Reviews*, *68*(2), 362–372. https://doi.org/10.1128/MMBR.68.2.362-372.2004

Ma, D., Chua, A. W. C., Yang, E., Teo, P., Ting, Y., Song, C., … Lee, S. T. (2015). Breast cancer resistance protein identifies clonogenic keratinocytes in human interfollicular epidermis. *Stem Cell Research & Therapy*, *6*(1). https://doi.org/10.1186/s13287-015-0032-2

Maglennon, G. A., McIntosh, P., & Doorbar, J. (2011). Persistence of viral DNA in the epithelial basal layer suggests a model for papillomavirus latency following immune regression. *Virology*, *414*(2), 153–163. https://doi.org/10.1016/j.virol.2011.03.019

Michael, S., Lambert, P. F., & Strati, K. (2013a). The HPV16 oncogenes cause aberrant stem cell mobilization. *Virology*, *443*(2), 218–225. https://doi.org/10.1016/j.virol.2013.04.008

Michael, S., Lambert, P. F., & Strati, K. (2013b). The HPV16 oncogenes cause aberrant stem cell mobilization. *Virology*, *443*(2), 218–225. https://doi.org/10.1016/j.virol.2013.04.008

Miettinen, P. J., Berger, J. E., Meneses, J., Phung, Y., Pedersen, R. A., Werb, Z., & Derynck, R. (1995). Epithelial immaturity and multiorgan failure in mice lacking

epidermal growth factor receptor. *Nature*, *376*(6538), 337–341.

https://doi.org/10.1038/376337a0

Mo, J., Sun, B., Zhao, X., Gu, Q., Dong, X., Liu, Z., … Sun, R. (2013). The in-vitro

spheroid culture induces a more highly differentiated but tumorigenic population

from melanoma cell lines. *Melanoma Research*, *23*(4), 254–263.

https://doi.org/10.1097/CMR.0b013e32836314e3

Nanba, D., Toki, F., Tate, S., Imai, M., Matsushita, N., Shiraishi, K., … Barrandon, Y.

(2015). Cell motion predicts human epidermal stemness. *The Journal of Cell

Biology*, *209*(2), 305–315. https://doi.org/10.1083/jcb.201409024

Nanney, L. B., Magid, M., Stoscheck, C. M., & King, L. E. (1984). Comparison of

Epidermal Growth Factor Binding and Receptor Distribution in Normal Human

Epidermis and Epidermal Appendages. *Journal of Investigative Dermatology*,

83(5), 385–393. https://doi.org/10.1111/1523-1747.ep12264708

Oh, B. Y., Lee, W. Y., Jung, S., Hong, H. K., Nam, D.-H., Park, Y. A., … Cho, Y. B.

(2015). Correlation between tumor engraftment in patient-derived xenograft

models and clinical outcomes in colorectal cancer patients. *Oncotarget*, *6*(18),

16059–16068. https://doi.org/10.18632/oncotarget.3863

Parsa, R., Yang, A., McKeon, F., & Green, H. (1999). Association of p63 with

proliferative potential in normal and neoplastic human keratinocytes. *The Journal

of Investigative Dermatology*, *113*(6), 1099–1105. https://doi.org/10.1046/j.1523-

1747.1999.00780.x

Pastrana, E., Silva-Vargas, V., & Doetsch, F. (2011). Eyes wide open: a critical review of

    sphere-formation as an assay for stem cells. *Cell Stem Cell*, *8*(5), 486–498.

    https://doi.org/10.1016/j.stem.2011.04.007

Patel, G. K., Wilson, C. H., Harding, K. G., Finlay, A. Y., & Bowden, P. E. (2006).

    Numerous keratinocyte subtypes involved in wound re-epithelialization. *The*

    Journal of Investigative Dermatology, *126*(2), 497–502.

    https://doi.org/10.1038/sj.jid.5700101

Pellegrini, G., Dellambra, E., Golisano, O., Martinelli, E., Fantozzi, I., Bondanza, S., …

    De Luca, M. (2001). p63 identifies keratinocyte stem cells. *Proceedings of the*

    National Academy of Sciences of the United States of America, *98*(6), 3156–3161.

    https://doi.org/10.1073/pnas.061032098

Peterson, S. C., Eberl, M., Vagnozzi, A. N., Belkadi, A., Veniaminova, N. A., Verhaegen,

    M. E., … Wong, S. Y. (2015). Basal Cell Carcinoma Preferentially Arises from

    Stem Cells within Hair Follicle and Mechanosensory Niches. *Cell Stem Cell*,

    16(4), 400–412. https://doi.org/10.1016/j.stem.2015.02.006

Pignon, J.-C., Grisanzio, C., Geng, Y., Song, J., Shivdasani, R. A., & Signoretti, S.

    (2013). p63-expressing cells are the stem cells of developing prostate, bladder,

    and colorectal epithelia. *Proceedings of the National Academy of Sciences*,

    110(20), 8105–8110. https://doi.org/10.1073/pnas.1221216110

Pinto, A. P., & Crum, C. P. (2000). Natural history of cervical neoplasia: defining

    progression and its consequence. *Clinical Obstetrics and Gynecology*, *43*(2), 352–

    362.

Pirisi, L., Creek, K. E., Doniger, J., & DiPaolo, J. A. (1988). Continuous cell lines with

    altered growth and differentiation properties originate after transfection of human

    keratinocytes with human papillomavirus type 16 DNA. *Carcinogenesis*, *9*(9),

    1573–1579.

Pirisi, L., Yasumoto, S., Feller, M., Doniger, J., & DiPaolo, J. A. (1987). Transformation

    of human fibroblasts and keratinocytes with human papillomavirus type 16 DNA.

    Journal of Virology, *61*(4), 1061–1066.

Redvers, R. P., Li, A., & Kaur, P. (2006). Side population in adult murine epidermis

    exhibits phenotypic and functional characteristics of keratinocyte stem cells.

    Proceedings of the National Academy of Sciences of the United States of America,

    103(35), 13168–13173. https://doi.org/10.1073/pnas.0602579103

Rheinwald, J. G., & Green, H. (1975). Serial cultivation of strains of human epidermal

    keratinocytes: the formation of keratinizing colonies from single cells. *Cell*, *6*(3),

    331–343.

Roshan, A., Murai, K., Fowler, J., Simons, B. D., Nikolaidou-Neokosmidou, V., & Jones,

    P. H. (2016). Human keratinocytes have two interconvertible modes of

    proliferation. *Nature Cell Biology*, *18*(2), 145–156.

    https://doi.org/10.1038/ncb3282

Rybak, A. P., He, L., Kapoor, A., Cutz, J.-C., & Tang, D. (2011). Characterization of

    sphere-propagating cells with stem-like properties from DU145 prostate cancer

    cells. *Biochimica Et Biophysica Acta*, *1813*(5), 683–694.

    https://doi.org/10.1016/j.bbamcr.2011.01.018

Ryser, M. D., Myers, E. R., & Durrett, R. (2015). HPV Clearance and the Neglected Role of Stochasticity. *PLOS Computational Biology*, *11*(3), e1004113. https://doi.org/10.1371/journal.pcbi.1004113

Sada, A., Jacob, F., Leung, E., Wang, S., White, B. S., Shalloway, D., & Tumbar, T. (2016). Defining the cellular lineage hierarchy in the interfollicular epidermis of adult skin. *Nature Cell Biology*, *18*(6), 619–631. https://doi.org/10.1038/ncb3359

Schmitt, A., Rochat, A., Zeltner, R., Borenstein, L., Barrandon, Y., Wettstein, F. O., & Iftner, T. (1996). The primary target cells of the high-risk cottontail rabbit papillomavirus colocalize with hair follicle stem cells. *Journal of Virology*, *70*(3), 1912–1922.

Schneider, T. E., Barland, C., Alex, A. M., Mancianti, M. L., Lu, Y., Cleaver, J. E., … Ghadially, R. (2003). Measuring stem cell frequency in epidermis: a quantitative in vivo functional assay for long-term repopulating cells. *Proceedings of the National Academy of Sciences of the United States of America*, *100*(20), 11412–11417. https://doi.org/10.1073/pnas.2034935100

Shamir, E. R., & Ewald, A. J. (2014). Three-dimensional organotypic culture: experimental models of mammalian biology and disease. *Nature Reviews Molecular Cell Biology*, *15*(10), 647–664. https://doi.org/10.1038/nrm3873

Sherman, L., & Schlegel, R. (1996). Serum- and calcium-induced differentiation of human keratinocytes is inhibited by the E6 oncoprotein of human papillomavirus type 16. *Journal of Virology*, *70*(5), 3269–3279.

Sun, Y., Goderie, S. K., & Temple, S. (2005). Asymmetric distribution of EGFR receptor during mitosis generates diverse CNS progenitor cells. *Neuron*, *45*(6), 873–886. https://doi.org/10.1016/j.neuron.2005.01.045

Takeuchi, K., Kato, M., Suzuki, H., Akhand, A. A., Wu, J., Hossain, K., … Nakashima, I. (2001). Acrolein induces activation of the epidermal growth factor receptor of human keratinocytes for cell death. *Journal of Cellular Biochemistry*, *81*(4), 679–688.

Tani, H., Morris, R. J., & Kaur, P. (2000). Enrichment for murine keratinocyte stem cells based on cell surface phenotype. *Proceedings of the National Academy of Sciences of the United States of America*, *97*(20), 10960–10965.

Toma, J. G., McKenzie, I. A., Bagli, D., & Miller, F. D. (2005). Isolation and characterization of multipotent skin-derived precursors from human skin. *Stem Cells (Dayton, Ohio)*, *23*(6), 727–737. https://doi.org/10.1634/stemcells.2004-0134

Tomar, S., Graves, C. A., Altomare, D., Kowli, S., Kassler, S., Sutkowski, N., … Pirisi, L. (2016). Human papillomavirus status and gene expression profiles of oropharyngeal and oral cancers from European American and African American patients: Gene Expression and Racial Disparity in Oropharyngeal/Oral Cancer. *Head & Neck*, *38*(S1), E694–E704. https://doi.org/10.1002/hed.24072

Tumbar, T., Guasch, G., Greco, V., Blanpain, C., Lowry, W. E., Rendl, M., & Fuchs, E. (2004). Defining the epithelial stem cell niche in skin. *Science (New York, N.Y.)*, *303*(5656), 359–363. https://doi.org/10.1126/science.1092436

Van Der Schueren, B., Cassiman, J. J., & Van Den Berghe, H. (1980). Morphological

    characteristics of epithelial and fibroblastic cells growing out from biopsies of

    human skin. *The Journal of Investigative Dermatology*, *74*(1), 29–35.

Vollmers, A., Wallace, L., Fullard, N., Höher, T., Alexander, M. D., & Reichelt, J.

    (2012). Two- and Three-Dimensional Culture of Keratinocyte Stem and Precursor

    Cells Derived from Primary Murine Epidermal Cultures. *Stem Cell Reviews and*

    Reports, *8*(2), 402–413. https://doi.org/10.1007/s12015-011-9314-y

Wakita, H., & Takigawa, M. (1999). Activation of epidermal growth factor receptor

    promotes late terminal differentiation of cell-matrix interaction-disrupted

    keratinocytes. *The Journal of Biological Chemistry*, *274*(52), 37285–37291.

Wan, F., Miao, X., Quraishi, I., Kennedy, V., Creek, K. E., & Pirisi, L. (2008). Gene

    expression changes during HPV-mediated carcinogenesis: A comparison between

    an *in vitro* cell model and cervical cancer. *International Journal of Cancer*,

    123(1), 32–40. https://doi.org/10.1002/ijc.23463

Watt, F. M., Jordan, P. W., & O'Neill, C. H. (1988). Cell shape controls terminal

    differentiation of human epidermal keratinocytes. *Proceedings of the National*

    Academy of Sciences of the United States of America, *85*(15), 5576–5580.

Webb, A., Li, A., & Kaur, P. (2004). Location and phenotype of human adult

    keratinocyte stem cells of the skin. *Differentiation; Research in Biological*

    Diversity, *72*(8), 387–395. https://doi.org/10.1111/j.1432-0436.2004.07208005.x

Woodworth, C. D., Doniger, J., & DiPaolo, J. A. (1989). Immortalization of human

    foreskin keratinocytes by various human papillomavirus DNAs corresponds to

    their association with cervical carcinoma. *Journal of Virology*, *63*(1), 159–164.

Xu, H., Pirisi, L., & Creek, K. E. (2015). Six1 overexpression at early stages of HPV16-

    mediated transformation of human keratinocytes promotes differentiation

    resistance and EMT. *Virology*, *474*, 144–153.

    https://doi.org/10.1016/j.virol.2014.10.010

Xu, H., Zhang, Y., Altomare, D., Pena, M. M., Wan, F., Pirisi, L., & Creek, K. E. (2014).

    Six1 promotes epithelial-mesenchymal transition and malignant conversion in

    human papillomavirus type 16-immortalized human keratinocytes.

    Carcinogenesis, *35*(6), 1379–1388. https://doi.org/10.1093/carcin/bgu050

Yoon, C. S., Kim, K. D., Park, S. N., & Cheong, S. W. (2001a). alpha(6) Integrin is the

    main receptor of human papillomavirus type 16 VLP. *Biochemical and*

    Biophysical Research Communications, *283*(3), 668–673.

    https://doi.org/10.1006/bbrc.2001.4838

Yoon, C. S., Kim, K. D., Park, S. N., & Cheong, S. W. (2001b). alpha(6) Integrin is the

    main receptor of human papillomavirus type 16 VLP. *Biochemical and*

    Biophysical Research Communications, *283*(3), 668–673.

    https://doi.org/10.1006/bbrc.2001.4838

Yu, H., Fang, D., Kumar, S. M., Li, L., Nguyen, T. K., Acs, G., … Xu, X. (2006).

    Isolation of a Novel Population of Multipotent Adult Stem Cells from Human

    Hair Follicles. *The American Journal of Pathology*, *168*(6), 1879–1888.

    https://doi.org/10.2353/ajpath.2006.051170

Zyzak, L. L., MacDonald, L. M., Batova, A., Forand, R., Creek, K. E., & Pirisi, L.

    (1994). Increased levels and constitutive tyrosine phosphorylation of the

    epidermal growth factor receptor contribute to autonomous growth of human

papillomavirus type 16 immortalized human keratinocytes. *Cell Growth &*

Differentiation: The Molecular Biology Journal of the American Association for

Cancer Research, 5(5), 537–547.

CHAPTER 3

STEM CELL PROPERTIES OF NORMAL HUMAN KERATINOCYTES
INFLUENCE TRANSFORMATION RESPONSE TO HPV16 DNA

Human papilloma virus (HPV) infections are believed to arise in stratified squamous epithelia regions rich in rapidly-cycling stem-like cells, such as the squamocolumnar junction of the cervix, the lingual and palatine tonsils in the oropharynx, and the transitional zone in the anal-rectal canal (Fakhry, 2006; Pinto & Crum, 2000). The target cell of HPV infection remains unknown, but infection requires virus particles to gain access to the epidermal basal layer where they are believed to be endocytosed by dividing basal keratinocytes, thereby inducing aberrant cellular proliferation (Chow, Broker, & Steinberg, 2010; Kines, Thompson, Lowy, Schiller, & Day, 2009; Maglennon, McIntosh, & Doorbar, 2011). Since the basal layer constitutes the proliferative compartment of the epidermis and a niche for epidermal stem cells, keratinocyte stem cells (KSC) have long been postulated as the target cells of HPV infection and a reservoir of latently infected cells that can persist to initiate HPV-mediated cancers (Bodily & Laimins, 2011; Maglennon et al., 2011; Ryser, Myers, & Durrett, 2015).

One of the main challenges in studying the role of basal stem cells in HPV-driven neoplasia is the scarcity of primary normal epithelial tissue. Thus, neonatal foreskin epidermal tissue has been extensively used to study HPV-driven neoplasia (Pirisi et al., 1988; Woodworth, Doniger, & DiPaolo, 1989). Epidermal skin stem cell (EpSCs) studies

have demonstrated that basal KSC maintain intense integrin alpha 6 (INTα6) levels, reduced cell surface EGF receptor (EGFR) levels, and display spheroid-forming abilities in suspension culture, while differentiating keratinocytes express elevated EGFR levels and fail to form spheroids in suspension culture (Doupé & Jones, 2012; Le Roy et al., 2010b; Wakita & Takigawa, 1999). We have previously reported that basal levels of EGFR in normal human epidermal skin tissue varies from person to person, and demonstrated that lower EGFR levels in the basal compartment of the epidermis corresponded with exuberant keratinocyte proliferation after infection with a retrovirus encoding the HPV16 E6 and E7 oncogenes, while NHKc strains derived from epidermis expressing increased basal EGFR levels responded to infection with meager proliferation (Akerman et al., 2001b). By using *in vitro* colony formation and tumor sphere assays, studies have demonstrated that HPV E7 and E6-expressing keratinocytes show increased stem cell properties and greater sphere formation abilities, indicating that the stem cell phenotype is also selected for during immortalization by the virus oncogenes (Hufbauer et al., 2013). Lately, *in vivo* studies have demonstrated that targeted expression of HPV E6 and E7 oncogenes in epidermal KSC promote abnormal cellular mobilization and contribute to cancer initiation(Michael et al., 2013a). However, a non-basal subpopulation of TSZ cells has also been revealed to be responsible for cancer initiation in HPV-driven cancers (Herfs et al., 2012). Thus, the precise role of epidermal stem cells in HPV-driven dysplasia continues to be a matter of debate.

In our model system for HPV type 16 (HPV16)-mediated human cell carcinogenesis, monolayer cultures of normal human keratinocyte (NHKc) are immortalized by transfection with full-length HPV16 DNA (HKc/HPV16). Cells then

progress toward malignancy in a step-wise manner that includes growth factor

independence, differentiation- resistance (HKc/DR), and ultimately tumorigenicity in

nude mice (Pirisi et al., 1988; Pirisi, Yasumoto, Feller, Doniger, & DiPaolo, 1987; H. Xu

et al., 2014). In this present study, we made use of our *in vitro* model system to closely

investigate the relationship between the density of basal epidermal stem-like

keratinocytes in culture and the susceptibility of these cultures to HPV-mediated pre-

neoplastic transformation. By transfecting various progenitor/stem-like NHKc cultures

with full-length HPV16 DNA, we found that these cultures responded to transfection

with exuberant proliferation and readily acquired differentiation resistance (DR) and

EMT-like features when continually subcultured in DR conditions. Moreover, HPV16

DNA conferred epidermal stem/progenitor-like cell characteristics in all successfully

transfected lines and stimulated the expression of several genes involved in basal

progenitor cell proliferation. Conversely, NHKc cultures enriched for cells committed to

terminal differentiation (TD) were considerably resistant to immortalization by HPV16

DNA and failed to establish proliferating clones in DR growth conditions.

These data demonstrate varying immortalization susceptibilities among epidermal

keratinocyte populations and indicate that EpSCs play an inextricable role in HPV-

mediated transformation in culture. Our findings reveal that the stem/progenitor cell

status of a keratinocyte is a foremost phenotypic determinant of its susceptibility to pre-

neoplastic transformation by oncogenic HPV16 DNA.

3.1 MATERIAL AND METHODS

Cell culture and cell lines

NHKc were isolated from neonatal foreskin as previously described (Akerman et al., 2001b) and cultured in modified keratinocyte serum-free medium (KSFM), i.e.. 20 ng/mL EGF, 10 ng/mL bFGF, 0.4% bovine serum albumin (BSA), and 4μg/mL insulin, adapted from the spheroid-forming (Lagadec et al., 2010) and sphere-propagating media(Rybak et al., 2011). This medium will be referred to as KSFM-stem cell medium (KSFM-scm). NHKc were passage into individual wells of a 6-well plate (~200,000 cells/well) and immortalized by transfection with 1 μg of a plasmid containing a dimer of the full-length HPV16 DNA sequence (pMHPV16d) or with the vector control (pdMMTneo) as previously described in detail (Pirisi et al., 1988, 1987). All cells were co-transfected with the pMSCV-IRES-EGFP plasmid (3:1 w/w), transiently expressing GFP to monitor transfection efficiency. HPV16 immortalized cells lines (HKc/HPV16) were derived from 15 different foreskin donors, 10 of which were non-spheroid forming strains (NF-NHKc) and 5 of which were from spheroid-forming strains (SF-NHKc). Proliferating spheroid-derived cells (SD-NHKc) from corresponding SF-NHKc were also trypsinized, passaged into 6-well plates, and transfected to established immortalized SD/HPV16 lines. Another group of HKc/HPV16 cell lines were established form FACS-purified keratinocyte populations isolated from three individual foreskin donors. Cells $(2x10^4)$ from respective FACS-sorted populations were directly seeded into individual wells of a 6-well plate and allowed to grow until ~75% confluence. Confluent FACS-sorted cells were then transfected following the protocol above. Moreover, differentiation resistant cells (HKc/DR) were obtained from each successfully immortalized line

(HKc/HPV16^{im}) by cultivating them in KSFM supplemented with 1 mM calcium chloride and 5% FBS (Pirisi et al., 1988). All cell lines were routinely split 1:600 when confluent, medium was changed 24 h after passaging and every 48 h thereafter.

Clonal growth assay

Cells were plated in duplicate 100-mm dishes at low density (5000 cells/dish), and fed KSFM-scm every 10 days. Cultures were then serially passaged (1:600) in 100-mm dishes to determine cumulative population doubling (PD) over time. Cell viability was obtained by Countess Automated Cell Counter (Invitrogen, CA). Cumulative population doublings were calculated according to the formula: population doublings = ($\log N / N_0$) / $\log_2$, where N represents the total cell number obtained at each passage and N_0 represents the number of cells plated at the start of the experiment(Ma et al., 2015). Matching dishes were stained with 10% Giemsa stain to assess colony size and morphology.

Immortalization and transformation assay

HKc/HPV16 cultures were serially diluted to a final concentration of ~1-5 cells per 200μL and seeded into individual wells of an uncoated 96-well plate, in duplicates. Colonies were serially plated every 20 days into new wells of a 96-well plate at a 1:5 ratio until their clonogenecity potential was exhausted and stably immortalized clones established. Matching duplicate plates were fixed in absolute methanol and stained with 10% Giemsa. The ratio between clones generated and the initial number of clones that formed was taken as a measure of immortalization efficiency. Stably immortalized

63

HKc/HPV16 colonies are referred to as (HKc/HPV16^{im}). Similar *in vitro* limiting dilution analysis was performed to assess transformation efficiency, except experimentation began with stably immortalized clones from respective HKc/HPV16^{im} lines, and cells were continually maintained in DR medium.

Spheroid formation and tumoroid assay

Cultured cells ($2x10^4$) were seeded into a 96-well round-bottom plate coated with a polymerized mixture of agarose (0.05%) and KSFM-scm. The spheroids were maintained for at least 24 h in suspension until used for further experimentations. For tumoroid formation, $2x10^6$ cells from individual clonally transformed HKc/DR lines (HKc/DR^{tr}) were plated onto a 100-mm dish coated with 3mL of a polymerized mixture of agarose and DR media. Cells were allowed to aggregate overnight and tumoroid size was followed for 10 days in suspension culture. Tumoroid size and morphology was determined by Lumenera Infinity1 software analysis (Lumenera Corporation, Ottawa, ON). At day 5 and day 10, single tumoroid aggregates were isolated fixed in 2% PFA, sectioned, and counterstained with hematoxylin and eosin (H&E). Sections were imaged by Nikon Eclipse E600 microscope.

Real Time PCR

Total RNA was isolated from cells using the All Prep DNA/RNA Mini Kit (Qiagen,CA) according to manufacturer's protocol. Reverse transcription was carried out with 1μg of total RNA using iScript cDNA Synthesis Kit (Bio-Rad, Hercules, CA). Real-time PCR was performed using iQ SYBR Green Supermix (Bio-Rad) following

manufacturer's instructions. Amplicon products were validated by agarose gel electrophoresis (2% v/v). GAPDH was used as an internal control. All samples were assayed in triplicate. The primer sequences used for real-time PCR are shown in Supplementary Table 1.

Immunohistochemistry

Cells were grown on cover slips coated with poly-lysine until 75% confluent. The cells were then washed twice in ice-cold PBS, fixed with 4% paraformaldehyde for 20 min at room temperature, permeabilized with 0.5% Triton in 1% glycine and then blocked using 0.5% bovine serum albumin (BSA) and 5% goat serum for 30 min at room temperature. Samples were next incubated with antibodies against P63 (Thermo Scientific, 1:200 dilution), cytokeratin 14 (Santa Cruz Biotechnology, 1:200 dilution), Fibronectin (Santa Cruz Biotechnology, 1:200 dilution), or E-cadherin (Santa Cruz Biotechnology, 1:200 dilution) in blocking solution overnight at 4°C. Samples were then washed three times with Phosphate Buffered Saline (PBS) with Tween 20 (PBST), followed by incubation with FITC-and Alexa 568- conjugated secondary antibodies (at 1:1000 dilution, Invitrogen). Nuclei were stained with 1:5000 dilution of 4', 6-diamidino-2-phenylindole (DAPI) (Invitrogen) before cells were mounted. Samples were observed using a Zeiss confocal laser-scanning microscope.

Fluorescent activated cell sorting analysis (FACS)

Cell (2-4 x 10^6 cells/ml) were stained with FITC-conjugated anti-integrinα6 (Abcam, Cambridge, MA) and PE-conjugated anti-EGFR (BD Pharmingen San Jose,

CA). FACS-sorted populations were collected by centrifugation at 112g x 5 min, the supernatant was removed and the cell pellets resuspended in fresh KSFM-scm. Cells were seeded into individual wells of a 6-well plate for subsequent experiments. FACS analysis was performed using a BD FACSAria II flow cytometer (BD Biosciences, San Jose, CA) in conjunction with the Flowing Software (V2.5.1, Turku, Finland).

Cell migration and invasion assay

HKc/HPV16[im] and respective HKc/DR[tr] were grown at ~80% confluence on 60-mm dishes in a humidified 5% CO2 incubator at 37°C. To generate wounding, a single linear scratch was created using the edge of a 200µL micropipette tip. Wounding area restored was monitored every 6 h by Lumenera Infinity1 software analysis (Lumenera Corporation, Ottawa, ON). The invasive ability of HKc/DR-Ctrl and HKc/DR-Six1 was measured as previously described(H. Xu et al., 2014). In brief, $2x10^4$ cells were seeded onto the upper surface of a Martigel matrix, and cells that invaded through the matrix and into the lower chamber were fixed and stained with 1% crystal violet and counted in five randomly chosen areas. Each experiment was performed in triplicate wells and repeated three times.

Statistical analysis

Data were expressed as the mean ± standard deviation (SD). Differences between mean values were analyzed using Student's *t*-test. $P < 0.05$, $P < 0.01$ or $P < 0.001$ were considered statistically significant and indicated in the figures by *, ** or *** respectively.

3.2 RESULTS

Mass cultured keratinocytes display similar growth rates but varied colony patterns after transfection with HPV16 DNA. To determine growth responses of normal human keratinocyte strains (NHKc) isolated from neonatal skin explants of various donors, non-spheroid forming NHKc (NF-NHKc) and spheroid-forming NHKc (SF-NHKc) mass cultures were transfected with the pMHPV16d plasmid, containing two copies of the HPV16 genome in a head-to-tail configuration within the pdMMTneo vector, or with the pdMMTneo vector only, and co-transfected with a plasmid transiently expressing eGFP to monitor transfection efficiency (Figure 3.1-3.2, A-C). To establish successfully transfected clones, HKc/pMHPV16d and HKc/pdMMTneo were serially passaged at 1:500 critical dilutions in 100-mm dishes until HKc/pdMMTneo control cells senesced (Figure 3.2D-E). We found that HPV16-transfected NF-NHKc strains (NF/HPV16) displayed small sized colonies that respected cell-cell contract inhibition and maintained a distinguishable perimeter around each other (Figure 3.3F, a-c), while HPV16-transfected SF-NHKc strains (SF/HPV16) displayed widespread colonies that lost contact inhibition and expanded beyond their colony boundaries (Figure 3.3F, d-f). Colonies from SF-HPV16 therefore occupied more surface area within the dish (Figure 3.4G), but were less numerous than colonies from NF-HPV16 strains (Figure 3.4H). To determine the rate of cell proliferation of successfully transfected cells, we seeded $5x10^3$ cells per 100-dish and serially passaged them 1:600 over the course of several days in culture. We found no significant difference in cumulative population doublings (PD) in SF/HPV16 compared to NF/HPV16 strains.

Spheroid-derived NHKc strains respond to HPV16 transfection with exuberant cell proliferation. To assess the growth response of NHKc directly derived from NHKc spheroids, a single multicellular spheroid was plated back onto an uncoated 60-mm dish and spheroid-derived cells (SD-NHKc) were allowed to recapitulate monolayer cultures. SD-NHKc ($1x10^5$ cells) and corresponding mass cultured cells were then passaged into a 6-well plate and transfected with the pMHPV16d plasmid or pdMMTneo vector (Figure 3.5A). Strikingly, we found that SD-NHKc responded to transfection with exuberant proliferation and underwent nearly 20 population doublings (PD) within 20 days in culture, compared to the ~ 10 PD acquired by their mass-cultured HKc/HPV16 counterparts (Figure 3.6B). Furthermore, SD/HPV16 reached complete colony confluence within 10 days in culture, while HKc/HPV16 established from mass-cultures failed to achieve complete dish confluence in that time (Figure 3.6-3.7B-C). These findings indicate that enriched populations of stem/progenitor-like keratinocytes are considerably more responsive to the HPV16 transfection protocol than mass cultured cells.

Full-length HPV16 DNA abrogates suspension-induced cell death and induces basal stem cell features in mass cultured NHKc. Given that stem-like SD-NHKc cultures were markedly more responsive to transfection by HPV16 DNA, we aimed to determine the influence of HPV16 DNA on keratinocyte stem cell properties in cultures. Of the 15 HKc/HPV16 lines established from mass cultured keratinocytes, we found that all continually appeared small in size and maintained an immature basal appearance throughout their time in culture (Figure 3A). Conversely, HKc/neo controls

displayed flattening cells that readily senesced after 5 passages in cultures (Figure 3.6B).

Furthermore, HKc/HPV16 lines established from mass cultured NHKc maintained

intense expression of P63 and K14, despite undergoing multiple rounds of serial

subcultivation (Figure 3.7C), while P63 and K14 levels decreased considerably in

HKc/neo after 5 passages (Figure 3.7D). We previously demonstrated that HPV16

oncogenes could stimulate EGFR mRNA levels and overcome mechanisms by which

excessive EGFR signaling shortens NHKc life span (Akerman et al., 2001a; Bheda et al.,

2008a). To determine how transfection with full length HPV16 DNA influenced cell

surface EGFR expression in HKc/HPV16 established from various mass cultured strains,

we interrogated SF and NF HKc lines after their transfection with HPV16 DNA. FACS

analysis detected a ~10-fold increase in cell surface EGFR in both SF/HPV16 and

NF/HPV16 strains alike, relative to HKc/neo (Figure 3.8E). These findings reveal that

regardless of stem cell status or innate spheroid forming ability, transfection by HPV16

DNA always induced aberrant EGFR signaling. Given that HKc/HPV16 intensely

expressed the proliferative marker EGFR, yet continually maintained a phenotype typical

of basal keratinocytes, we decided to measure their mRNA levels of genes responsible for

epidermal basal stem/progenitor cell proliferation. We found a 17.3-fold induction of

P63, a 11.3-fold induction of Ki-67, a 9.6-fold induction of EGFR, and an 11.0-fold

induction of ALDH1 in HKc/HPV16, relative to HKc/neo controls (Figure 3.9F). This

demonstrates that HPV16 DNA stimulates aberrant activation of genes responsible for

basal stem cell proliferation, while hindering mechanisms by which cells achieve

terminal differentiation. Given the widespread colony phenotype observed in some

strains after transfection with HPV16 DNA, we aimed to determine the influence of

HPV16 on keratinocyte cell-to-cell junctions. Confocal imaging revealed that transfection of NHKc with HPV16 DNA resulted in a marked reduction in the number of intercellular desmosome junctions, enabling HKc/HPV16 to overcome cell-cell contact inhibition (Figure 3G). We therefore decided to assess the effect of HPV16 DNA on suspension spheroid formation and found that SF-NHKc retained their spheroid-forming ability after transfection with HPV16 DNA (Figure 3.10Ha, d). Strikingly, most NF-NHKc strains also acquired spheroid-forming abilities after transfection with HPV16 DNA (NF/HPV16 $^{\Delta pos}$) (Figure 3.10Hb, e), with a few strains resisting spheroid formation despite transfection with HPV16 DNA (NF/HPV16 $^{\Delta neg}$) (Figure 3.10Hc, f). In total, of the 15 established HKc/HPV16 strains, all SF strains (5/5) retained their spheroid-forming abilities after transfection with HPV16 DNA (Figure 3.10I). Among the NF strains, 80% (8/10) acquired the ability to form spheroids after transfection, with the remaining 20% (2/10) resisting spheroid-formation despite successful transfection with HPV16 DNA (Figure 3.10I).

Stem/progenitor keratinocytes are preferentially immortalized by HPV16 DNA. Given that HPV16 DNA stimulated exuberant proliferation in SD-NHKc cultures and conferred basal stem cell properties to NHKc mass cultures, we assessed the immortalization response of various FACS-purified keratinocyte populations (Figure 3.11A, B). We found that the stem-like ITGα6^{high}/EGFR^{low} cell population displayed the best growth response after transfection with HPV16 DNA, followed by the transit-amplifying ITGα6^{high}/EGFR^{high} cell population, and ITGα6^{high} cells, respectively. Unexpectedly, we observed that ITGα6^{low}/EGFR^{high} and ITGα6^{low} cells consistently

failed to proliferate beyond 25 days in culture and typically senesced after accumulating

5 PD, despite successful transfection with HPV16 DNA (Figure 3.11C, D). To challenge

these findings, we made critical dilutions (1-5 cells/well) of various HKc/HPV16 lines

established from FACS-purified populations and seeded them into individual uncoated

wells of 96-well plates. Resultant colonies were clonally subcultured and continually

assessed for colony renewal (Figure 3.12E). We found that $ITG\alpha6^{low}/EGFR^{high}$-HPV16

and $ITG\alpha6^{low}$/HPV16 populations had difficulty sustaining repeated subcloning at limited

dilutions (Figure 3.13F). Conversely, $ITG\alpha6^{high}/EGFR^{high}$-HPV16 cells gave rise to many

dividing clones even after six rounds of subcloning at limited dilutions. Notably,

$ITG\alpha6^{high}/EGFR^{low}$-HPV16 cells gave rise to the greatest number of stably immortalized

clones and sustained the subcultivation protocol with greater fitness. Next, we assessed

the immortalization responses of various HKc/HPV16 lines and found that HKc/HPV16

established from mass cultures (i.e. $NF^{\Delta neg}$/HPV16, $NF^{\Delta pos}$/HPV16, SF/HPV16) sustained

the limited dilution experiment with difficulty, while lines established from spheroid-

derived cultures gave rise to a significantly greater number of stably immortalized clones

(Figure 3.13F). When quantifying the ratio of successfully proliferating colonies

generated by each line, we found that mass cultured strains constantly achieved less than

25% immortalization efficiency. Moreover, we found no significant difference in

immortalization efficiencies between $NF/16^{\Delta neg}$ and $NF/16^{\Delta pos}$ strains. Strikingly,

SD/HPV16 cultures achieved over 2-fold greater immortalization efficiencies (57%)

compared to corresponding mass cultured SF/HPV16 (23%) (Figure 3.14G). SD/HPV16

also generated more confluent colonies that stained darker by Giemsa compared to

colonies from mass cultured HKc/HPV16 lines (Figure 3.13F), suggesting that

immortalized stem/progenitor populations are not merely more efficient at cell renewal, but also sustain greater proliferative potential throughout their time in culture. Our data also indicate that terminally differentiated cells lacking the basal marker ITGα6 are considerably more resistant to immortalization by HPV16 DNA, while transit-amplifying cells (TAC), and keratinocyte stem cells (KSC) are significantly more susceptible to immortalization by the full length HPV16 genome.

Immortalized stem/progenitor-like keratinocytes readily acquire differentiation-resistance with pre-EMT-like features. We have previously established that resistance to differentiation stimuli is a vital step in the progression to neoplastic transformation in HKc/HPV1 6(Pirisi et al., 1987). We thus chose to assess whether stably immortalized HKc/HPV16 clones (HKc/HPV16^{im}) from our various cell lines could directly transition from growth in basal medium to growth in DR medium without the prerequisite of a growth-factor independence (GFI) growth interphase, and whether their respective clones produced could sustain repeated subcloning at limited dilutions in differentiation resistant (DR) media (Figure 3.15A). Remarkably, we found that SD/HPV16 and ITGα6^{high}/EGFR^{low}-HPV16 cells gave rise to significantly more DR clones than ITGα6^{high}/EGFR^{high}-HPV16 and HKc/HPV16 lines established from keratinocyte mass cultures. Unexpectedly, we found no significant difference in the proportion of DR clones produced between ITGα6^{high}/EGFR^{high}-HPV16 and HKc/HPV16 lines established from mass cultures (Figure 3.16C), suggesting that TA NHKc and mass cultured cells had similar immortalization susceptibilities to HPV16 DNA. These findings also indicate that stem-like NHKc and KSC are particularly more susceptible to

72

HPV-mediated transformation as compared to other keratinocyte cell fractions. To further

characterize HPV16-transformed cells, we chose to expand successfully immortalized

HKc/HPV16 clones (HKc/HPV16[im]), as well as successfully transformed DR clones

(HKc/DR[tr]), in individual 100-mm dishes. We found that though HKc/HPV16[im] lines

maintained cobblestone-like morphologies typical of basal epithelial cells, HKc/DR[tr]

displayed a mesenchymal phenotype reminiscent of fibroblastic cells (Figure 3.16D, a-b).

When assessing spheroid forming abilities in HKc/DR[tr] lines, we found that they formed

considerably larger spheroids in suspension compared to their corresponding

HKc/HPV16[im] (Figure 3.16D, c-d). Next, we assessed spheroid forming abilities in

HKc/DR[tr] from various strains and found that all of our established HKc/DR[tr] could form

spheroids that were considerably larger in size and visible without the help of a

microscope (Figure 3.16D, e). Strikingly, HKc/DR[tr] lines established from NF$^{\Delta neg}$/-

HPV16 also displayed spheroid-forming abilities (Figure 3.16D, right). These data

suggest that spheroid formation is a phenotype closely associated with HPV-mediated

transformation and thus cells with an innate ability to self-assemble into spheroids have

an added advantage towards HPV-driven immortalization. Given that HKc/DR[tr] lines lost

their cobblestone-like shapes and displayed mesenchymal features, we decided to assess

the intensity and localization of genes associated with epithelial to mesenchymal

transition (EMT) in HKc/DR[tr] lines and corresponding HKc/HPV16[im]. We found that

HKc/HPV16[im] expressed reduced cytoplasmic levels of fibronectin (FN1) and intense

levels of E-cadherin on their plasma and nuclear membranes. Whereas, HKc/DR[tr]

expressed intense cytoplasmic levels of fibronectin and markedly reduced levels of E-

cadherin (Figure 3.18E). Furthermore, HKc/DR[tr] developed elongated spindles typical of

fibroblastic cells, while HKc/HPV16[im] conserved their round cobblestone-like shapes

(Figure 3.18E). We also detected a 0.8-fold induction in mRNA encoding E-cadherin in

HKc/HPV16[im] compared to a 0.5-fold induction in HKc/DR[tr]; a 1.3-fold induction of

FN1 mRNA in HKc/HPV16[im] compared to 1.8-fold induction in HKc/DR[tr]; a 0.1-fold

induction of Snail mRNA in HKc/HPV16[im] compared to 0.9-fold induction in HKc/DR[tr];

a 0.06-fold induction of Twist mRNA in HKc/HPV16[im] compared to 0.6-fold induction

in HKc/DR[tr], relative to HKc/neo control respectively. Next we assessed cell surface

levels of EGFR in HKc/HPV16[im] and HKc/DR[tr], relative to HKc/neo. Similarly to levels

seen in freshly established HKc/HPV16 (Figure 3.18E), we detected a ~10-fold induction

in cell surface EGFR intensity in HKc/HPV16[im] relative to HKc/neo (Figure 3.17G).

Strikingly however, HKc/DR[tr] presented a ~100-fold increase in cell surface EGFR,

relative to HKc/neo (Figure 3.17G). Our findings demonstrate that marked induction of

cell surface EGFR is dramatically increased during cells progression to transformation

mediated by HPV16 DNA. This marked EGFR upregulation is also closely associated

with the pre-EMT-like phenotypes observed in transformed keratinocyte cultures. Given

that HKc/DR[tr] presented such elevated cell surface EGFR levels, we chose to explore

their migratory potential in culture. By utilizing wound-scratch assays, we found that

HKc/DR[tr] readily restored over 80% of the wounded area within 24 h in culture, while

HKc/HPV16[im] restored a mere 25% of the wound. Next, we investigated HKc/DR[tr]

invasiveness by testing their migratory patterns through Matrigel. We found that

HKc/DR[tr] had difficulty invading through Matrigel compared to HKc/DR-Six1, a

previously established tumorigenic HKc/DR cell line (H. Xu et al., 2014). This data

indicate that HKc/DR[tr] are a migratory population of transformed cells are undergoing an

EMT-like transition but lack invasiveness potential, suggesting that this transformed cell

state is not sufficient for tumorigenicity. Additional events are likely required for

HKc/DR[tr] lines to achieve invasiveness in culture or tumorigenicity in mice.

Bulk suspensions of HKc/DR[tr] form tumoroid-like aggregates that

recapitulate features of squamous intraepithelial lesions. Since spheroid formation

was closely associated with HPV-mediated transformation, we chose to assess whether

prolonged spheroid growth of HKc/DR[tr] cells could further encourage pre-neoplastic

transformation of immortalized cultures. To this aim, we seeded 1.5×10^6 HKc/DR[tr] cells

on a 100-mm dish coated with a polymerized mixture of soft agarose and DR medium.

Within 5 days, we found that HKc/DR[tr] cells aggregated into tumoroid-like structures that

continually grew (Figure 3.20A-A1). We next assessed tumoroid histologies at day 5 and

found that they appeared remarkably similar to epidermal squamous carcinoma, with

several cells exhibiting characteristics of hyperchromatic basal cells (Figure 3.20B).

These tumoroid cultures continued to grow and maintained pre-neoplastic-like histologies

beyond 10 days in suspension culture (Figure 3.21C-D). Given the wide presence of

hyperchromatic cells that was observed in tumoroid cells, we chose to measure mRNA

expression levels of several genes involved in proliferation of basal stem cells. We found

that tumoroid-like suspensions expressed a 68.2-fold induction of Ki-67, a 37.3-fold

induction of survivin, a 10.1-fold induction of ALDH1, and a 31.0-fold induction of

SIX1, relative to HKc/DR[tr] cultivated as monolayers (Figure 3.21E). These data indicate

that suspension cultivation of HPV16-transformed cells further encourages neoplastic

transformation in HKc/HPV16 cultures and greatly enrich them for pre-neoplastic stem-like proliferative cells.

3.3 FIGURES
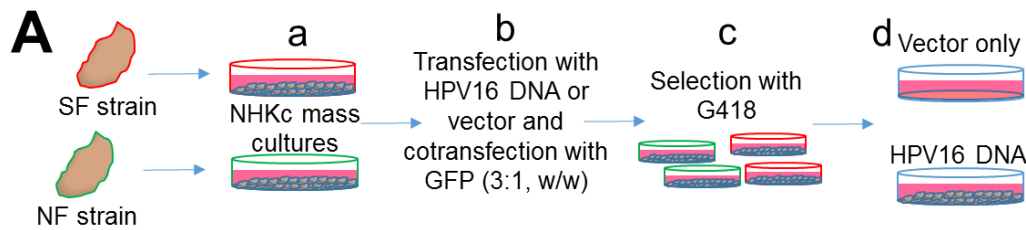
Figure 3.1 Transfection of mass cultured NHKc. (A) Schematic overview of the transfection protocol. NHKc isolated from (a) SF-NHKc strains were (b) transfected with full-length HPV16 DNA or pdMMTneo (control), then (c) selected in G418 and repeatedly subcultured until control cells senesced.
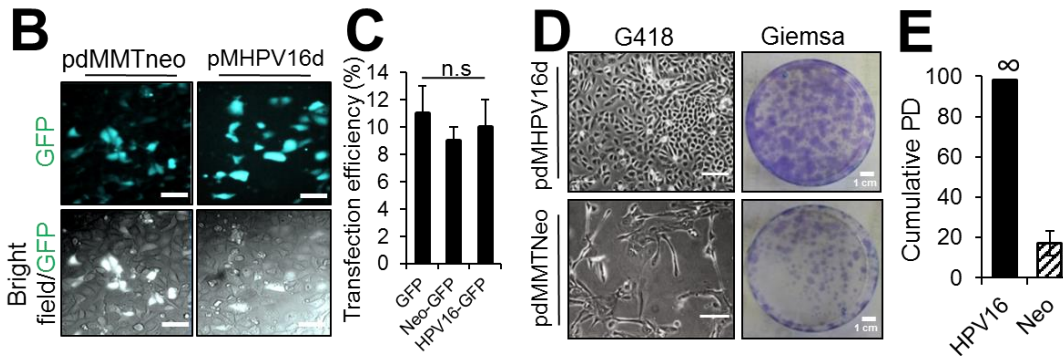
Figure 3.2 Selecting successfully transfected cells. (B) NHKcs transfected with 1 µg of pMHPV16d or pdMMTneo vector control, and co-transfected with GFP (3:1 w/w) to (C) monitor transfection efficiency. GFP expression was analyzed 48 h post-transfection and fluorescent cells were quantified by ImageJ. (D) Transfected cells were selected with G418 (100 mg/mL) for 48 h and (E) repeatedly subcultured until vector-only transfected cells senesced.
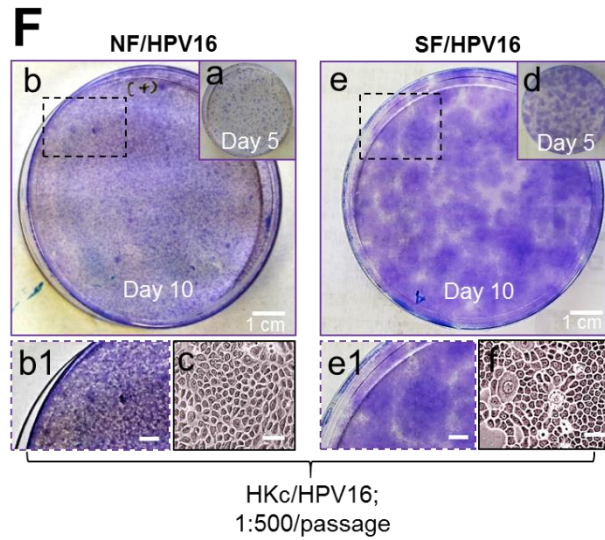
Figure 3.3 Primary NHKc strains display varied colony phenotypes after transfection with HPV16 DNA. (F) Transfection response assessed using Countess Automated Cell Counter and ImageJ to determine colony density and morphologies at day 5 and day 10 after seeding 5x103 cells per 100-mm dish. (a) Colony morphology of a successfully transfected NF-NHKc strain (NF/HPV16) at day 5 and (b-b1) day 10. (c) Phase contrast image of a NF/HPV16 colony at day 10. (d) Colony morphology of a successfully transfected SF-NHKc strain (SF/HPV16) at day 5 and (e-e1) day 10. (f) Phase contrast image of a NF/HPV16 colony at day 10.
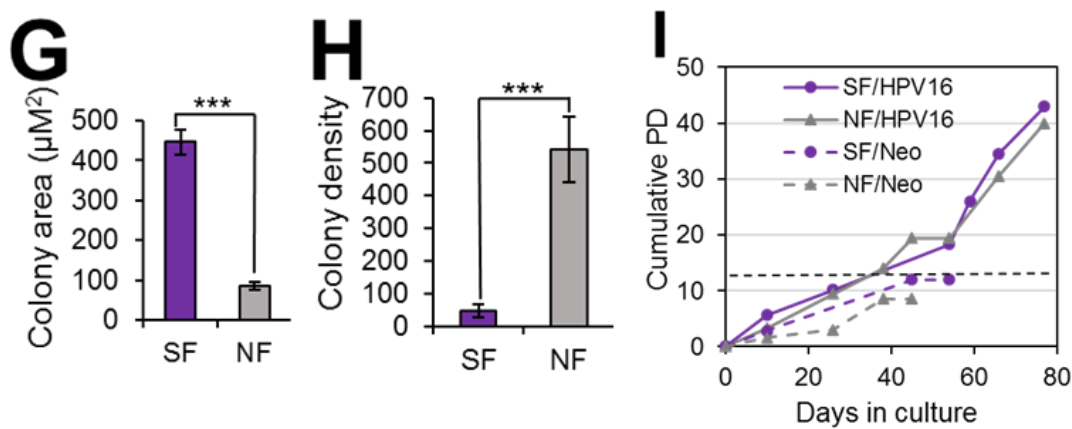
Figure 3.4 HKc/HPV16 lines established from mass cultures display similar growth responses after transfection with HPV16 DNA. (B) Cumulative population doublings of SD-HKc/HPV16 strains isolated from four different individuals, along with their corresponding mass cultured HKc/HPV16, and their respective HKc/pdMMTneo controls. Bars indicate standard deviation, and * indicate statistically significant P values ≤ 0.01, respectively.
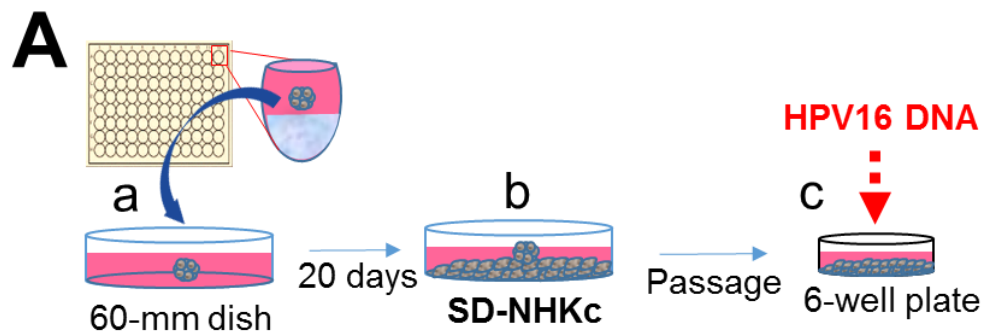
Figure 3.5 Transfecting SD-NHKc. (G) Colony size, (H) colony density, and (I) cumulative population doublings in successfully HPV16-transfected cells and pdMMTneo controls over the course of several days in culture. Bars indicate standard deviation, and *, **, and *** indicate statistically significant P values ≤ 0.05, 0.01 and 0.001, respectively.
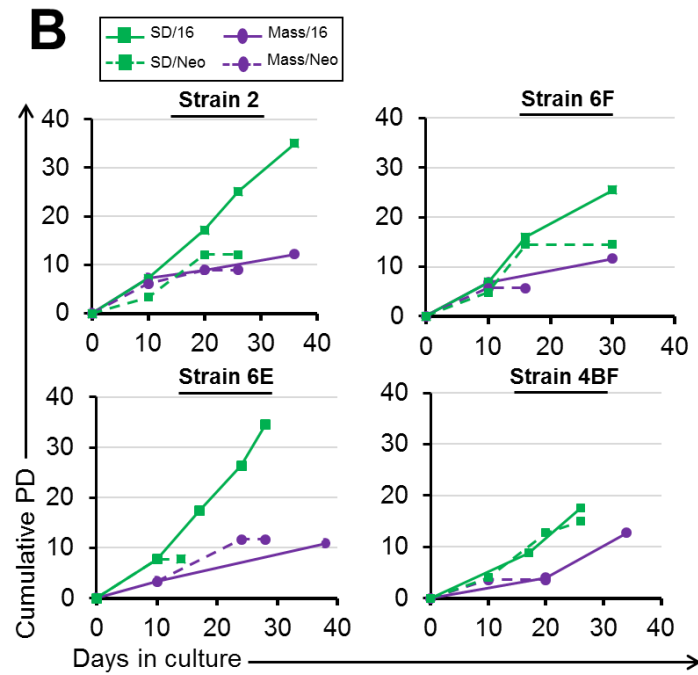
Figure 3.6 Spheroid-derived cells respond to transfection with HPV16 DNA with exuberant cell proliferation. (A) Schematic depicting a single suspension NHKc spheroid (a) transplanted back into an uncoated 60-mm dish, then (b) 1x105 of the spheroid-derived cells (SD-NHKc) are (c) passaged into single wells of a 6-well plate and transfected with the full-length HPV16 genome.
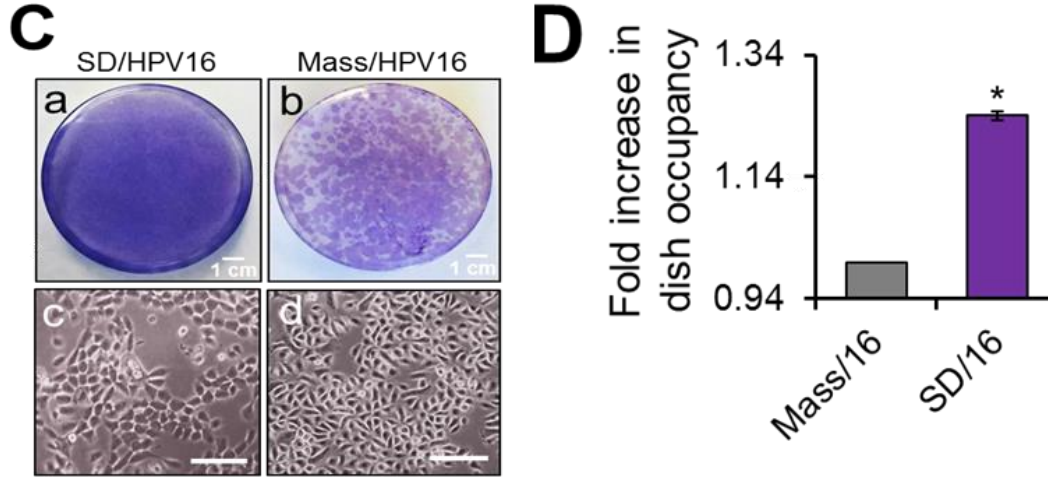
Figure 3.7 SD/HPV16 exhibit complete confluence in culture. (C) 5 x 103 cells were plated in a 100-mm dish after successful transfection and colony patterns were examined by Giemsa staining at day 10. (a) SD-HKc/HPV16 strain and (b) corresponding mass-cultured HKc/HPV16 strain after 10 days in culture. (c) Phase contrast images of SD/HPV16 colonies and (d) corresponding HKc/HPV16 mass cultured colonies. (D) Fold increase in dish occupancy was determine by quantifying the percentage of dish surface area occupied by SD-HKc/HPV16 colonies after 10 days in culture, relative to corresponding mass-cultured HKc/HPV16 strain.
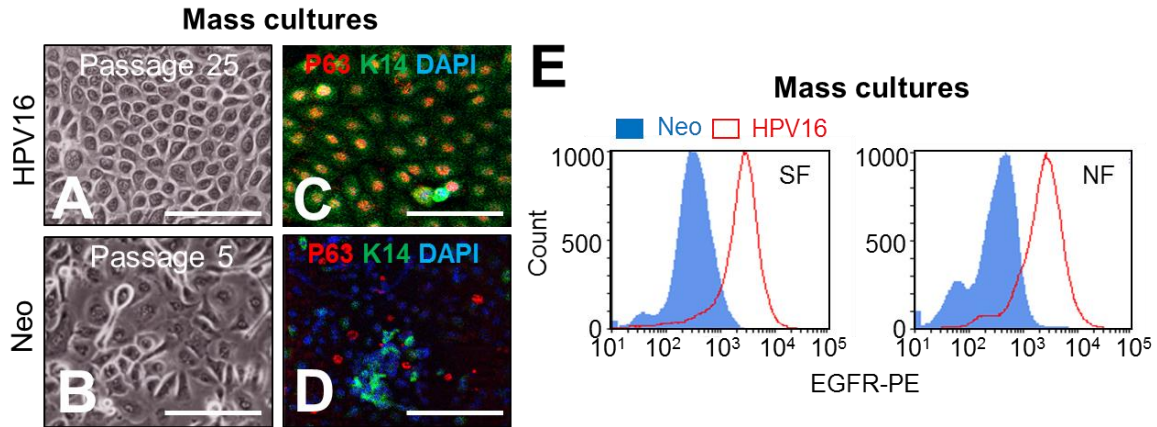
Mass cultures

Figure 3.8 Transfection with HPV16 DNA induces basal stem cell characteristics in mass cultured keratinocytes. (A) Phase contrast image of mass cultured keratinocytes 25 passages after immortalization by HPV16 (HKc/HPV16). (B) Respective HKc/neo controls after 5 passages in culture. (C-D) HKc/HPV16 and corresponding HKc/neo cells stained with DAPI, immunostained with antibodies against pan-tumor protein 63 targeting all TP63 isoforms (P63, red), and basal cytokeratin 14 (K14, green). Scale bar=100 μM. (E) Flow cytometry analysis of cell surface EGFR levels in mass cultured HKc/HPV16 and HKc/neo cells from spheroid-forming (SF)) and spheroid non-forming (NF) strains.
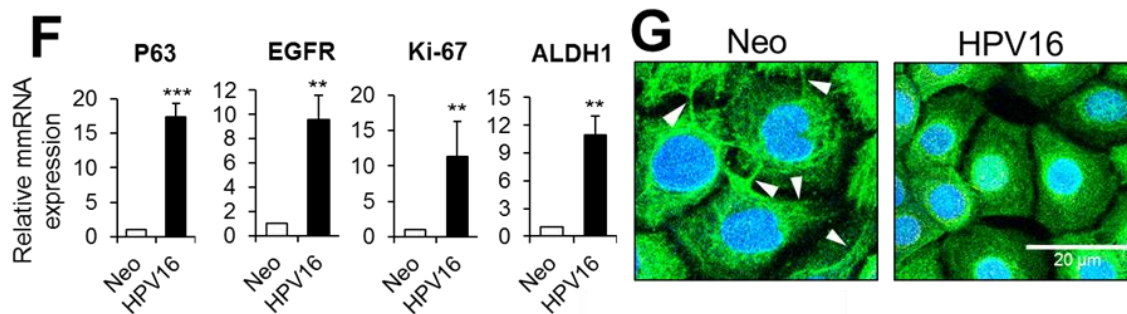
Figure 3.9 HKc/HPV16 express intense mRNA levels of epidermal proliferative genes. (F) Expression levels of mRNAs encoding pan-TP63, EGFR, Ki-67, and ALDH1 in HKc/HPV16 relative to HKc/neo cells both at passage 5, as determined by Real-time RT-PCR. Data were normalized to GAPDH expression and reported as mean +/- standard deviation. Bars indicate standard deviation, and *, **, and *** indicate statistically significant P values ≤ 0.05, 0.01 and 0.001, respectively. (G) Confocal imaging of HKc/HPV16 and HKc/neo cells at 63x magnification. Arrows depict intercellular desmonsomes present within HKc/neo controls.

81

H

	SF	NF^Δpos	NF^Δneg
NHKc	a	b	c
HPV16	d	e	f

I

Table 1. Distribution of keratinocyte strains with spheroid-forming ability before and after transfection with HPV16 DNA

		Spheroid non-forming strains (n=10)	
	SF (n=5)	NF^Δpos (n=8)	NF^Δneg (n=2)
NHKc	Yes 5/5 (100%)	No 0/8 (0%)	No 0/2 (0%)
HKc/HPV16	Yes 5/5 (100%)	Yes 8/8 (80%)	No 0/2 (20%)
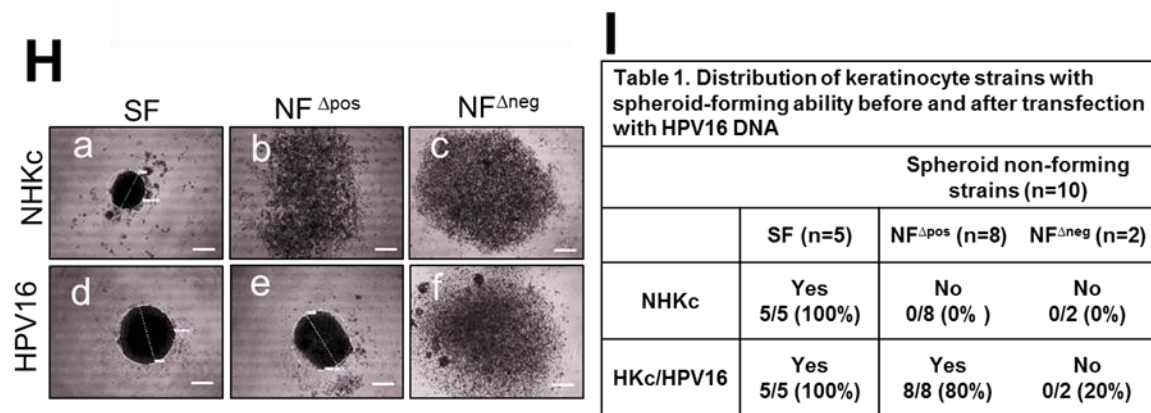
Figure 3.10 Full-length HPV16 DNA abrogates suspension-induced cell death. (H) NHKc suspension cultures from (a) spheroid-forming (SF-NHKc) and (b-c) spheroid non-forming (NF-NHKc) strains before transfection, (d-f) and after transfection with full-length HPV16 DNA. (e) Spheroid-forming ability acquired (Δpos) by a keratinocyte strain that was initially NF. (f) Spheroid-forming ability resisted (Δneg) by a keratinocyte strain that was initially NF despite transfection with full-length HPV16 DNA. (I) Distribution of keratinocyte strains with spheroid-forming ability before and after transfection with full-length HPV16 DNA.
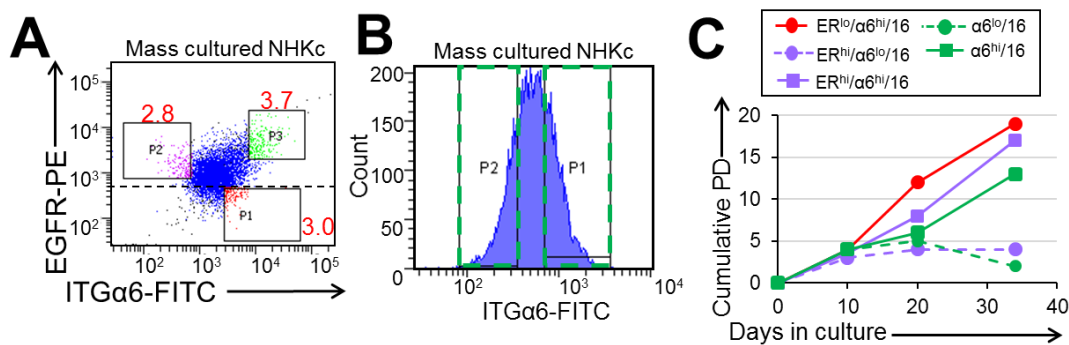
Figure 3.11 Terminally-differentiated cells respond to transfection sluggishly. Stem/progenitor keratinocytes are preferentially immortalized by HPV16 DNA. (A) Florescence activated cell sorting (FACS) of NHKc populations isolated based on cell-surface levels of epidermal cell markers integrin alpha 6 (ITGα6) and EGFR. (B) Gated fractions of ITGα6 ^{hi} and ITGα6 ^{lo}-expressing cells purified by FACS. (C) Cumulative population doublings observed in EGFR^{lo}/ITGα6^{hi}, EGFR^{hi}/ITGα6^{lo}, EGFR^{hi}/ITGα6^{hi}, ITGα6 ^{hi}, and ITGα6 ^{lo} after transfection with full-length HPV16
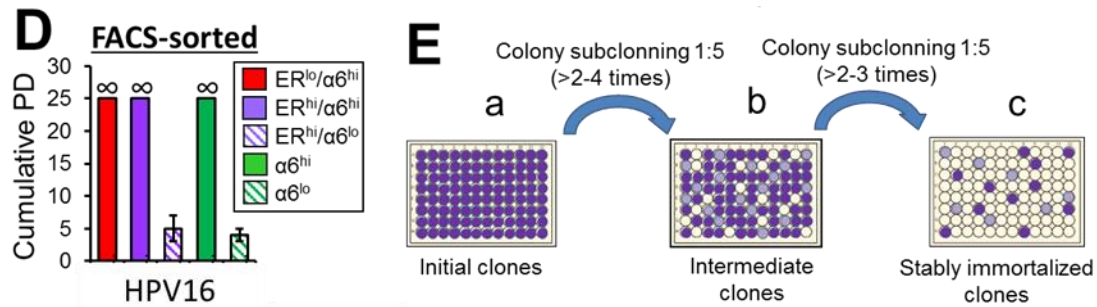
Figure 3.12 Limiting clonal dilution assay. (D) FACS-isolated HPV16-tansfected cells were plated into a 100-mm dish at a density of 5,000 cells/dish until cells reached approximately 80% confluent, then cells were serially passaged 1:500. Colony density was assessed by Giemsa staining. (E) Schematic depicting the immortalization efficiency assay. HPV16-transfected cells are seeded at a critical density of approximately 1-5 cells per well in individual wells of an uncoated 96-well plate. Upon confluence, initial colonies are then serially plated at a 1:5 ratio into new wells of a 96-well plate until clonogenecity potential is exhausted or stably immortalized clones are formed.
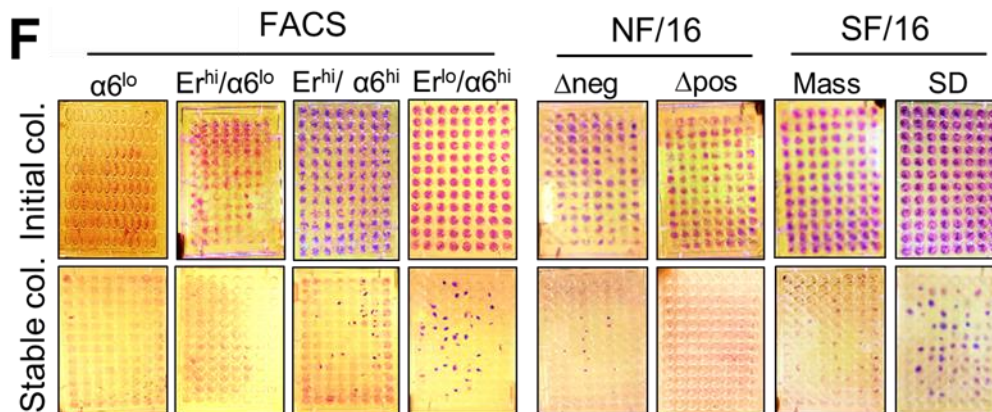
Figure 3.13 Terminally-differentiated cells resist immortalization in culture. (F) Immortalization efficiencies of HKc/HPV16 lines established from various FACS-purified populations, as well as NF, SF, and SD strains.
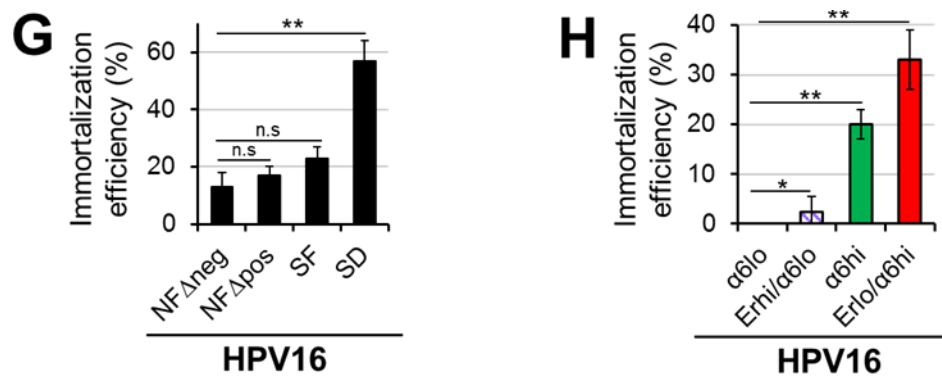
Figure 3.14 Stem/progenitor-like keratinocytes exhibit great immortalization efficiencies. (G-H) Immortalization efficiencies of 8 different lines of HKc/HV16.
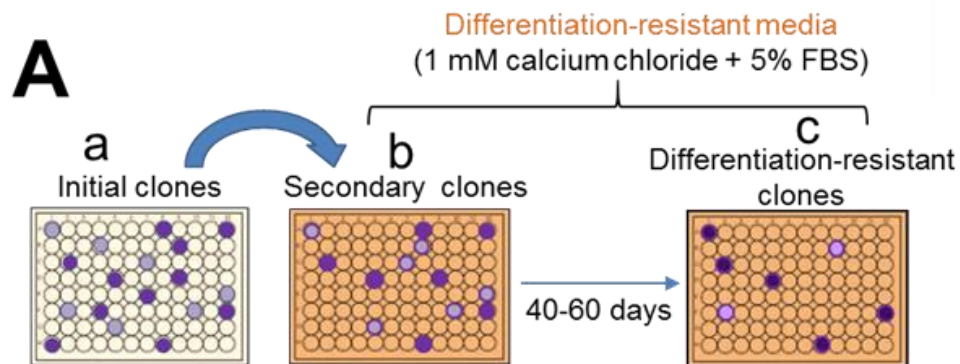
Figure 3.15 Differentiation resistance assay. (A) Schematic depicting the differentiation-resistance assay. In brief, (a) stably immortalized HKc/HPV16 colonies are (b) subcultivated 1:5 in differentiation-resistance (DR) media (1mM calcium chloride and 5% FBS) until lingering clones (c) continually sustain growth in DR media, at which point they are considered successfully transformed (HKc/DR^{tr}).
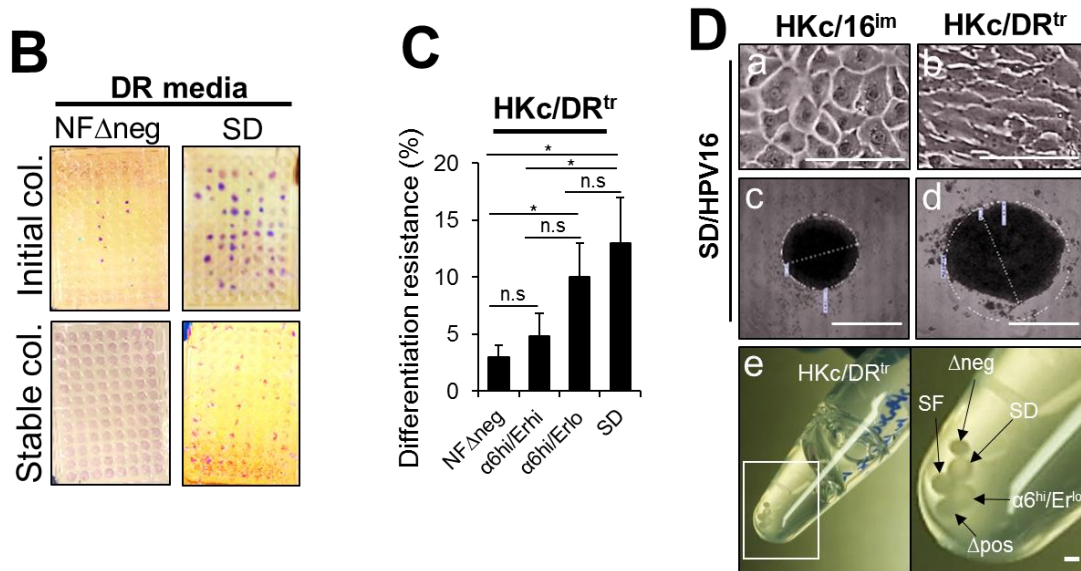
Figure 3.16 Immortalized stem/progenitor-like keratinocytes readily acquire differentiation-resistance. (B) Representative images of stably immortalized (^{im}) colonies subject to several rounds of clonal subcultivation in DR media. (C) Proportion of differentiation-resistant clones in various HKc/HPV16^{im} lines. (D) Phase contrast image of (a) a HKc/HPV16^{im} line established from SF-NHKc and its corresponding (b) HKc/DR^{tr} line, as well as (c-d) respective spheroid cultures. (e)
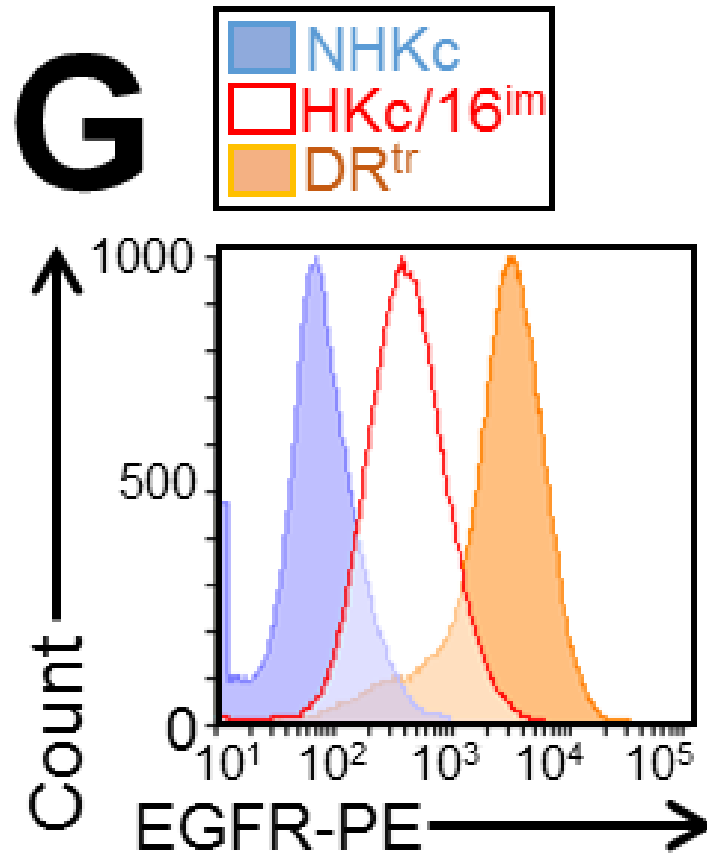
Figure 3.17 HKc/DR^{tr} lines present greatly elevated levels of EGFR. (G) Flow cytometry analysis of cell surface EGFR levels in NHKc, HKc/HPV16^{im}, and HKc/DR^{tr}. (H) Scratch-wound assay depicting the migratory behaviors of HKc/HPV16^{im} and HKc/DR^{tr} after 24 h in culture. Black lines depict original wound boundaries. Yellow lines depict area of new epithelial recovery. (I) Percentage of wound closure achieved 24 h after scratching HKc/HPV16^{im} and HKc/DR^{tr} monolayers.
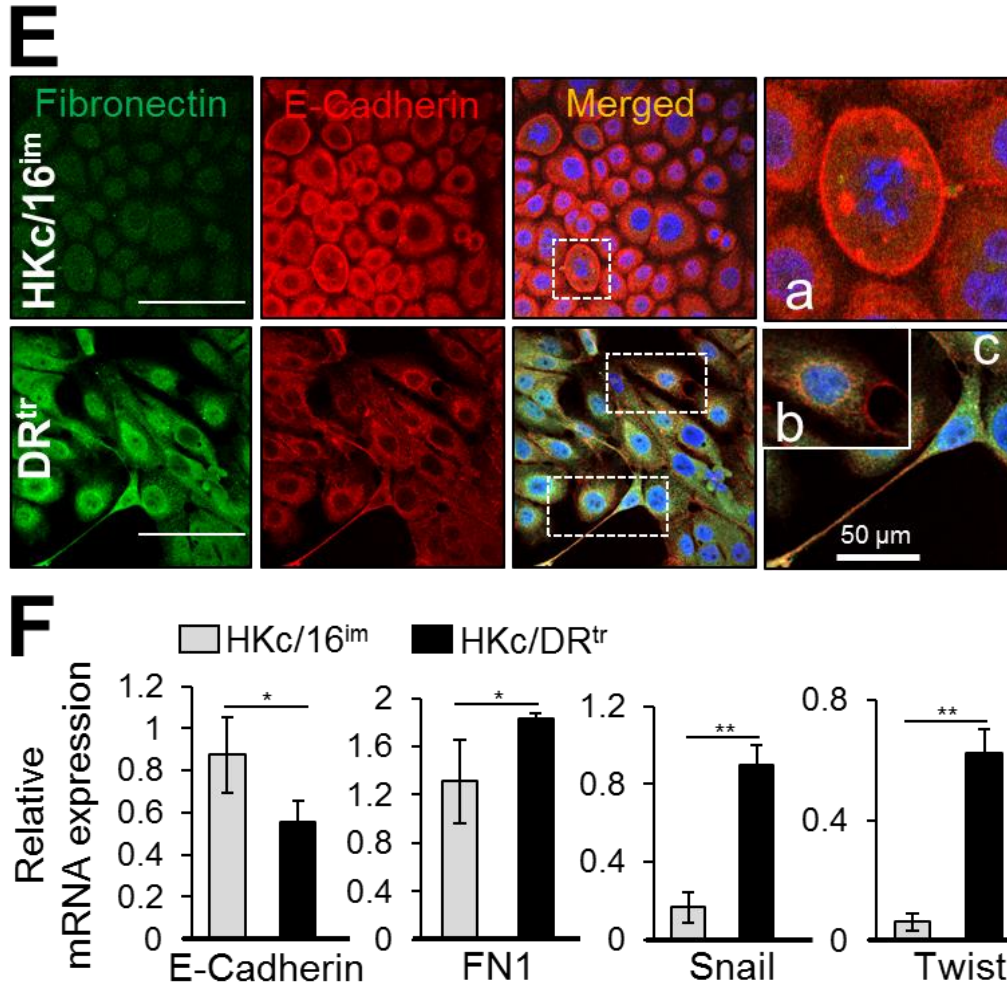
Figure 3.18 HKc/DR^{tr} lines present mesenchymal-like features. (E) Intensity of cell membrane E-Cadherin and cytosolic fibronectin evaluated by Zeiss LSM 710 confocalmicroscope. Magnified image of (a) cells from a HKc/HPV1^{6im} line and (b-c) a corresponding HKc/D^{Rtr} line. (F) Relative mRNA expression of genes involved in epithelial to mesenchymal transition (EMT) as determined by RT-qPCR in HKc/HPV16^{im} and HKc/DR^{tr}, relative to NHKc. Data were normalized to GAPDH expression and reported as mean +/- standard deviation.
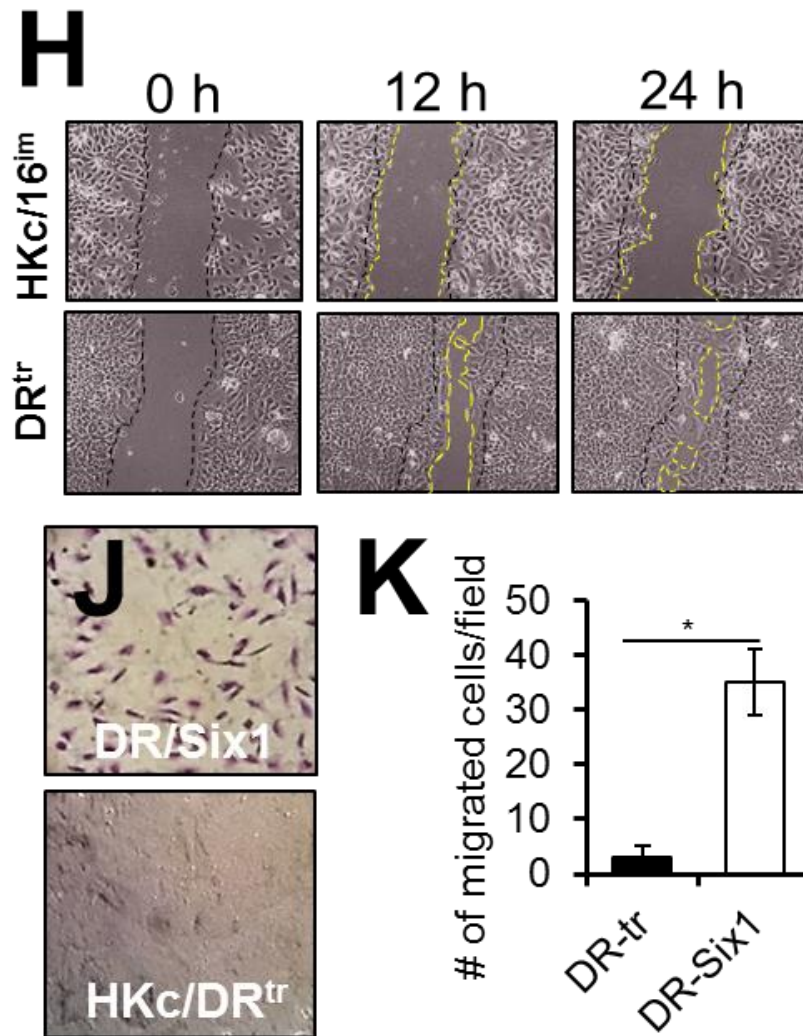
Figure 3.19 HKc/DR^{tr} are migratory noninvasive cell lines. (H) Scratch-wound assay depicting the migratory behaviors of HKc/HPV16^{im} and HKc/DR^{tr} after 24 h in culture. Black lines depict original wound boundaries. Yellow lines depict area of new epithelial recovery. (I) Percentage of wound closure achieved 24 h after scratching HKc/HPV16^{im} and HKc/DR^{tr} monolayers. (J) Matrigel cell invasion in HKc/DR^{tr} and tumorigenic HKc/DR-SIX1 cells as determined by transwell migration. Invading cells were quantified after crystal violet staining. Images are shown at ×100. (K) The number of migrating cells was directly counted. Each column represents the mean of five different fields. Bars indicate standard deviation, and *, **, and *** indicate statistically significant P values ≤ 0.05, 0.01 and 0.001, respectively.
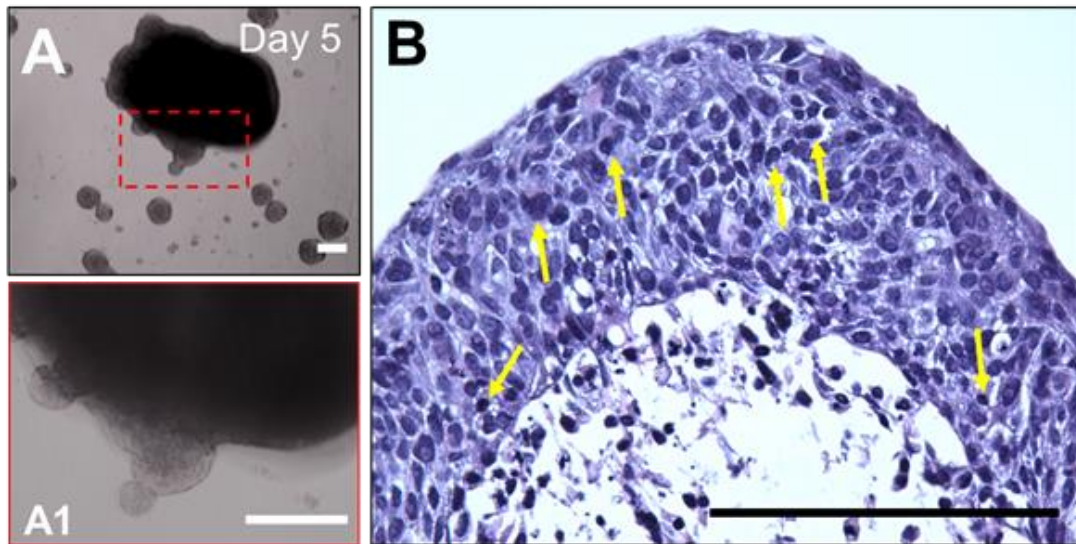
Figure 3.20 HKc/DR^{tr} form tumoroid-like aggregates in bulk suspension culture. (A) Tumoroid-like structures formed 5 days after seeding 1.5×10^6 HKc/DR^{tr} cells in suspension cultures within a 100-mm dish. Scale bar=100 μM. (A1) x200 magnification of tumoroid-like aggregates in suspension culture. Scale bar=100 μM. (B) Hematoxylin and eosin (H&E) staining of tumoroid-like structures at day 5. Dysplastic basal-like cells can be seen throughout the thickness of the section. Arrows
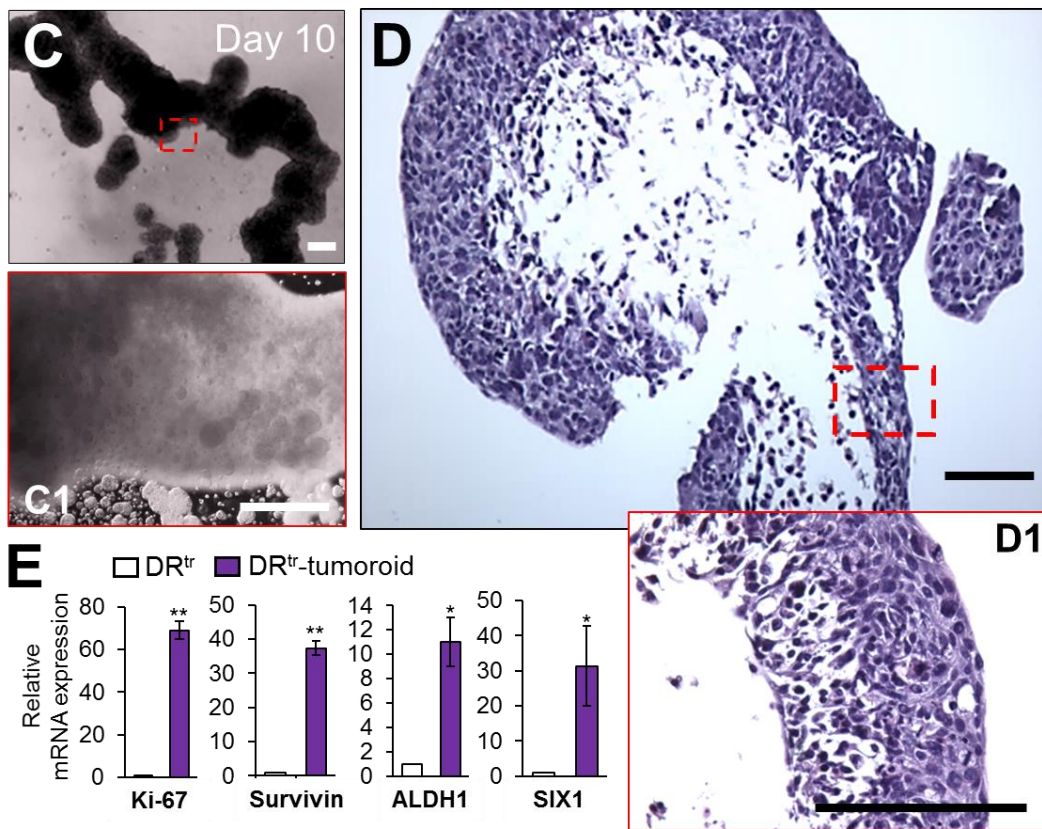
Figure 3.21. HKc/DR^tr tumoroids exhibit cancer stem cell characteristics. (C) Tumoroid-like structures formed after 10 days in suspension culture. (C1) x400 magnification of tumoroid-like structure. (D) Hematoxylin and eosin (H&E) staining of tumoroid-like sections after day 10 at x400 magnification. Scale bar=100 μM. (D1) x200 magnification of tumoroid-like aggregate. Scale bars=50 μM. (E) Relative mRNA expression of genes involved in cancer spheroid formation as determined by RT-qPCR in tumoroid-like structure, relative to NHKc. Data were normalized to GAPDH expression and reported as mean +/- standard deviation. Bars indicate standard deviation, and *, **, and *** indicate statistically significant P values ≤ 0.05, 0.01 and 0.001, respectively.

3.4 DISCUSSION

Basal epithelial stem cells have widely been speculated to be targets of cancer initiation in a variety of tissues, including ovarian, skin, breast, and prostate (Blanpain, 2013; Flesken-Nikitin et al., 2013; Lawson et al., 2015; Peterson et al., 2015; Pignon et al., 2013). In HPV-driven cancers, cells of the basal layer are presumed to be preferentially targeted and transformed by the HPV oncogenes. Since the basal layer is the proliferative compartment of the epidermis, and a stem cell niche of the stratified epidermis, KSC are thought to be key actors in HPV-mediated neoplasia(Bodily & Laimins, 2011; Maglennon et al., 2011; Michael, Lambert, & Strati, 2013b; Schmitt et al., 1996). Epidermal basal stem cells are often distinguished by their intense expression of the transmembrane glycoprotein Integrin alpha 6 (ITGα6) and their reduced expression of the proliferative marker EGFR (Le Roy et al., 2010b; Webb, Li, & Kaur, 2004). Coincidently, the INTα6 receptor, which is exclusively expressed by basal cells, has been postulated as the main receptor of HPV16 cell entry(Evander et al., 1997; Letian & Tianyu, 2010; Yoon, Kim, Park, & Cheong, 2001b), corroborating speculations that the virus preferentially targets basal stem cells. We have previously shown that reduced basal levels of EGFR correspond with increased cell proliferation after infection with HPV16 E6 and E7 oncoproteins, whereas elevated basal levels of EGFR, a characteristic of committed progenitors (CP), correspond with a less proliferative response (Akerman et al., 2001b; Bheda, Creek, & Pirisi, 2008b)·(Wan et al., 2008). We have also shown that HPV16 oncoproteins cooperate to increase EGFR, inducing enhanced clonogenicity by overcoming mechanisms by which excessive EGFR signaling stimulate terminal differentiation (Akerman et al., 2001b; Bheda et al., 2008a). In this study, we explored

the relationship between the stem cell properties of NHKc cultures and their influence on the susceptibility of NHKc to transformation by HPV16 DNA. In our study, HPV16-transfected keratinocyte cultures established from various mass cultured NHKc strains acquired similar numbers of PD in culture (~1PD every 3.3 days). While, SD-NHKc cultures, a population enriched for stem/progenitor-like cells, responded to transfection with exuberant proliferation, achieving approximately 1PD every 1.3 days. Moreover, HPV16-transfected EGFR^{lo}/ ITGα6^{hi} most closely resembled SD/HPV16 in regards to proliferation response and clonogenic potential.

We observed that transfection of NHKc with the full-length HPV16 genome induced basal stem cell characteristics in all keratinocyte strains, and generally induced spheroid-forming abilities in NF/NHKc after their transfection with HPV16 DNA. We also found that P63/K14 double-positive populations were also strongly selected for with each round of HKc/HPV16 clonal selection. HKc/HPV16 cultures appeared increasingly homogeneous by passage 10 and displayed uniformly small-sized cells that were packed in cobblestone-like patterns. Whereas, HKc/neo clones mostly contained loosely packed flattened cells with a low proliferative potential and considerably reduced expression of P63 and K14. It is likely that immortalized cells surviving the clonal selections are derived from a same clonal origin. The question then arises as to whether epidermal stem cells (EpSCs) present within keratinocyte cultures can naturally outcompete their neighboring CP and TD cells during clonal selection, or whether EpSCs were more efficiently immortalized by HPV16 DNA, which in turn enabled them to outcompete their CP and TD counterparts. We expected that if EpSCs were naturally outcompeting neighboring cells, then HKc/neo should have also increasingly been enriched for stem-

92

like basal cells during the clonal selection process, but the opposite occurred. The number of P63/K14-expressing clones dramatically decreased in HKc/neo with each round of passaging, indicating that their EpSCs reserves were continually being depleted during passaging. A similar phenomenon is observed in NHKc cultures during their maintenance on plastic (Fuchs, 2012; Guo & Jahoda, 2009). Therefore, the enrichment of basal stem/progenitor-like cells in HKc/HPV16 after multiple rounds of passaging is likely an indication of better immortalization of EpSCs, which enables them to successfully self-renew and thus outcompete coexisting CP and TD cells within these cultures. Cultures enriched for stem/progenitor-like cells are likely at a clonal advantage than mass-cultured cells, causing them to exhibit better responses when transfected with HPV16 DNA. Therefore. the successful establishment of stable HKc/HPV16 lines in culture is likely the consequence of a few immortalized EpSCs that are continually selected for throughout the passaging clonal pressure. This reasoning corroborates with our limited dilution experiments, where we found that the long-term clonal growth of HKc/HPV16 was better sustained in lines established from SD/NHKc and EGFR^{lo}/ ITGα6^{hi} populations, while lines established from mass cultured cells isolated from the same epidermal strain were significantly more resistant to the immortalization protocol. Moreover, we found that CP and TD cells were completely unable to achieve stable immortalization.

We and others have previously shown that when HKc/HPV16 are transferred to medium containing 1mM CaCl and 5% fetal bovine serum the majority of cells flatten and cease to proliferate (Altomare, Velidandla, Pirisi, & Creek, 2013; Chen, Pirisi, & Creek, 2013; Kowli, Velidandla, Creek, & Pirisi, 2013; Pirisi et al., 1988; Sherman & Schlegel, 1996). Remarkably, successfully immortalized lines established from purified

populations of stem/progenitor-like cells readily achieved differentiation resistance in DR conditions, all without a need to first undergo growth factor independence (Pirisi et al., 1988). However, HKc/HPV16[im] established from mass cultures of matching strains were significantly less efficient at acquiring differentiation resistance. Interestingly, the spheroid-forming abilities of HKc/DR cultures were not merely conserved in culture, but were considerably improved as cells transitioned and progressed through transformation. This was particularly striking in NF/HPV16[Δneg], whose HKc/DR clones displayed a robust spheroid-forming ability in suspension. Spheroid-forming stem-like cells are likely present in all cultures, including NF/HPV16[Δneg], but are selected for during clonal selection, enabling them to achieve greater homogeneity and thus yielding a spheroid forming phenotype during further progression into transformation.

We have previously reported that elevated expression of Six1 mRNA in HKc/DR corresponded with increased tumorigenicity and an enrichment of cancer stem cells (CSC) (H. Xu et al., 2014). We found that HKc/DR[tr] lines established from EpSC-enriched cultures exhibited EMT-like characteristics and formed tumoroid-like aggregates that expressed nearly 25-fold greater Six1 mRNA levels than their monolayer counterparts. HKc/DR[tr] tumoroids also maintained elevated mRNA levels of genes associated with CSC, and exhibited several hallmarks of pre-neoplastic cells. Yet, they were noninvasive in Matrigel, suggesting that their transformation status is not sufficient to induce tumorigenity in mice. Additional events are likely needed to stimulate malignant progression in these cells, reaffirming previous observations from our group (Pirisi et al., 1987; H. Xu et al., 2014; Hanwen Xu, Pirisi, & Creek, 2015). The growth of HKc/DR[tr] cells as tumoroid-like structures that robustly express cancer stem cell markers

may indicate that suspension cultivation of HPV16-transformed cells as multicellular aggregates may further encourage neoplastic transformation, potentially creating a condition in which enough aberrance can be stimulated to improve proclivity to tumorigenicity without the help of exogenous factors. It is interesting to speculate as to what effects further enrichment of EpSC and CSC in primary cultures could have on achieving tumorigenicity. Our data may be linked to recent reports correlating successful tumor graphing and host-cancer progression in mice (Oh et al., 2015). As it is seen in this study that cultures enriched for stem-like cells achieve greater pre-neoplastic-like transformation, it is possible that epithelial tissue dense in stem cells is more prone to transformation when expose to an oncogenic insult, thus yielding successful grafting in a xenograft host compared to tissue that is depleted of progenitor/stem-like cells.

Taken together, our findings reveal that, at least in culture, EpSCs are not only more efficiently immortalized but also readily undergo HPV-driven pre-neoplastic transformation. The proliferative responses seen in SD/HPV16 established from four different SD-NHKc strains excludes the possibility that variations in host cell genetics play a major role in producing these characteristics, indicating that such response is probably a result of dramatic changes at the epigenetic and transcriptome level. More experimentation would be required to determine the status of virus DNA integration in the host genome in SD/HPV16 compared to their mass and TD counterparts. In either case, these data expand upon previous observations from our group, demonstrating that acute expression of HPV16 genome in normal HKc is accompanied by an increase in epidermal stem cell features (Pirisi et al., 1988). These finding support the notion that stem/progenitor-like cells, rather than cells committed to terminal differentiation,

expressing the HPV16 genome are more poised to repopulate in cell culture, consistent

with the cell-competition model proposed by several groups (Hufbauer et al., 2013;

Michael et al., 2013b). Given that SD-NHKc are an actively proliferating population of

keratinocytes, their dynamic status may further predispose them to HPV-driven

transformation as suggested by recent reports (Nanba et al., 2015; Ryser et al., 2015). Our

data depicts epidermal stemness as a foremost phenotypic determinant of susceptibility to

HPV-mediated transformation in primary human keratinocyte cultures, corroborating

with recent findings by Hufbauer et al (Hufbauer et al., 2013). Therefore, depleting

populations of basal stem cells from malignant tissue may be a promising approach to

halt or revert HPV16-driven neoplastic lesions. Assessment of EpSCs density in primary

tissue could be explored as a predictive biomarker of susceptibility to HPV-mediated

transformation. Tissue stem cell density could help identify among the many people who

present with persistent HPV infections, the relatively few that are truly at risk for

developing cancer. Further studies are warranted to define more clearly the role of

epidermal tissue stem cell density and HPV-mediated transformation *in vivo*.

3.5 REFERENCES

Akerman, G. S., Tolleson, W. H., Brown, K. L., Zyzak, L. L., Mourateva, E., Engin, T.
S., … Pirisi, L. (2001). Human papillomavirus type 16 E6 and E7 cooperate to
increase epidermal growth factor receptor (EGFR) mRNA levels, overcoming
mechanisms by which excessive EGFR signaling shortens the life span of normal
human keratinocytes. *Cancer Research*, *61*(9), 3837–3843.

Akerman, G. S., Tolleson, W. H., Brown, K. L., Zyzak, L. L., Mourateva, E., Engin, T. S., … Pirisi, L. (2001). Human papillomavirus type 16 E6 and E7 cooperate to increase epidermal growth factor receptor (EGFR) mRNA levels, overcoming mechanisms by which excessive EGFR signaling shortens the life span of normal human keratinocytes. *Cancer Research*, *61*(9), 3837–3843.

Akerman, G. S., Tolleson, W. H., Brown, K. L., Zyzak, L. L., Mourateva, E., Engin, T. S., … Pirisi, L. (2001). Human papillomavirus type 16 E6 and E7 cooperate to increase epidermal growth factor receptor (EGFR) mRNA levels, overcoming mechanisms by which excessive EGFR signaling shortens the life span of normal human keratinocytes. *Cancer Research*, *61*(9), 3837–3843.

Altomare, D., Velidandla, R., Pirisi, L., & Creek, K. E. (2013). Partial loss of Smad signaling during in vitro progression of HPV16-immortalized human keratinocytes. *BMC Cancer*, *13*(1), 424. https://doi.org/10.1186/1471-2407-13-424

Barrandon, Y., & Green, H. (1987). Three clonal types of keratinocyte with different capacities for multiplication. *Proceedings of the National Academy of Sciences*, *84*(8), 2302–2306.

Bheda, A., Creek, K. E., & Pirisi, L. (2008a). Loss of p53 induces epidermal growth factor receptor promoter activity in normal human keratinocytes. *Oncogene*, *27*(31), 4315–4323. https://doi.org/10.1038/onc.2008.65

Bheda, A., Creek, K. E., & Pirisi, L. (2008b). Loss of p53 induces epidermal growth factor receptor promoter activity in normal human keratinocytes. *Oncogene*, *27*(31), 4315–4323. https://doi.org/10.1038/onc.2008.65

Blanpain, C. (2013). Tracing the cellular origin of cancer. *Nature Cell Biology*, *15*(2), 126–134. https://doi.org/10.1038/ncb2657

Blanpain, C., & Fuchs, E. (2006). Epidermal stem cells of the skin. *Annual Review of Cell and Developmental Biology*, *22*, 339–373. https://doi.org/10.1146/annurev.cellbio.22.010305.104357

Bodily, J., & Laimins, L. A. (2011). Persistence of human papillomavirus infection: keys to malignant progression. *Trends in Microbiology*, *19*(1), 33–39. https://doi.org/10.1016/j.tim.2010.10.002

Borena, B. M., Meyer, E., Chiers, K., Martens, A., Demeyere, K., Broeckx, S. Y., … Spaas, J. H. (2014). Sphere-Forming Capacity as an Enrichment Strategy for Epithelial-Like Stem Cells from Equine Skin. *Cellular Physiology and Biochemistry*, *34*(4), 1291–1303. https://doi.org/10.1159/000366338

Chen, Y., Pirisi, L., & Creek, K. E. (2013). Ski protein levels increase during in vitro progression of HPV16-immortalized human keratinocytes and in cervical cancer. *Virology*, *444*(1–2), 100–108. https://doi.org/10.1016/j.virol.2013.05.039

Chow, L. T., Broker, T. R., & Steinberg, B. M. (2010). The natural history of human papillomavirus infections of the mucosal epithelia: NATURAL HISTORY OF HPV INFECTIONS AND PATHOLOGY. *APMIS*, *118*(6–7), 422–449. https://doi.org/10.1111/j.1600-0463.2010.02625.x

Clayton, E., Doupé, D. P., Klein, A. M., Winton, D. J., Simons, B. D., & Jones, P. H. (2007). A single type of progenitor cell maintains normal epidermis. *Nature*, *446*(7132), 185–189. https://doi.org/10.1038/nature05574

Clifford, G. M., Smith, J. S., Plummer, M., Muñoz, N., & Franceschi, S. (2003). Human

    papillomavirus types in invasive cervical cancer worldwide: a meta-analysis.

    British Journal of Cancer, *88*(1), 63–73. https://doi.org/10.1038/sj.bjc.6600688

Coulombe, P. A., Kopan, R., & Fuchs, E. (1989). Expression of keratin K14 in the

    epidermis and hair follicle: insights into complex programs of differentiation. *The*

    Journal of Cell Biology, *109*(5), 2295–2312.

De Rosa, L., & De Luca, M. (2012). Cell biology: Dormant and restless skin stem cells.

    Nature, *489*(7415), 215–217. https://doi.org/10.1038/489215a

Doupe, D. P., Alcolea, M. P., Roshan, A., Zhang, G., Klein, A. M., Simons, B. D., &

    Jones, P. H. (2012). A Single Progenitor Population Switches Behavior to

    Maintain and Repair Esophageal Epithelium. *Science*, *337*(6098), 1091–1093.

    https://doi.org/10.1126/science.1218835

Doupé, D. P., & Jones, P. H. (2012). Interfollicular epidermal homeostasis: dicing with

    differentiation. *Experimental Dermatology*, *21*(4), 249–253.

    https://doi.org/10.1111/j.1600-0625.2012.01447.x

Evander, M., Frazer, I. H., Payne, E., Qi, Y. M., Hengst, K., & McMillan, N. A. (1997).

    Identification of the alpha6 integrin as a candidate receptor for papillomaviruses.

    Journal of Virology, *71*(3), 2449–2456.

Fakhry, C. (2006). Clinical Implications of Human Papillomavirus in Head and Neck

    Cancers. *Journal of Clinical Oncology*, *24*(17), 2606–2611.

    https://doi.org/10.1200/JCO.2006.06.1291

Fitsialos, G., Chassot, A.-A., Turchi, L., Dayem, M. A., LeBrigand, K., Moreilhon, C., …

    Ponzio, G. (2007). Transcriptional signature of epidermal keratinocytes subjected

to in vitro scratch wounding reveals selective roles for ERK1/2, p38, and

phosphatidylinositol 3-kinase signaling pathways. *The Journal of Biological

Chemistry*, *282*(20), 15090–15102. https://doi.org/10.1074/jbc.M606094200

Flesken-Nikitin, A., Hwang, C.-I., Cheng, C.-Y., Michurina, T. V., Enikolopov, G., &

Nikitin, A. Y. (2013). Ovarian surface epithelium at the junction area contains a

cancer-prone stem cell niche. *Nature*, *495*(7440), 241–245.

https://doi.org/10.1038/nature11979

Fortunel, N. O. (2003). Long-term expansion of human functional epidermal precursor

cells: promotion of extensive amplification by low TGF- 1 concentrations.

Journal of Cell Science, *116*(19), 4043–4052. https://doi.org/10.1242/jcs.00702

Fuchs, E. (2012). The Impact of Cell Culture on Stem Cell Research. *Cell Stem Cell*,

10(6), 640–641. https://doi.org/10.1016/j.stem.2012.03.010

Gago, N., Pérez-López, V., Sanz-Jaka, J. P., Cormenzana, P., Eizaguirre, I., Bernad, A.,

& Izeta, A. (2009). Age-Dependent Depletion of Human Skin-Derived Progenitor

Cells: Age-Dependent Depletion of Human SKPs. *STEM CELLS*, *27*(5), 1164–

1172. https://doi.org/10.1002/stem.27

Green, H. (1977). Terminal differentiation of cultured human epidermal cells. *Cell*, *11*(2),

405–416.

Guo, A., & Jahoda, C. A. B. (2009). An improved method of human keratinocyte culture

from skin explants: cell expansion is linked to markers of activated progenitor

cells. *Experimental Dermatology*, *18*(8), 720–726. https://doi.org/10.1111/j.1600-

0625.2009.00900.x

Henderson, S., Chakravarthy, A., Su, X., Boshoff, C., & Fenton, T. R. (2014). APOBEC-Mediated Cytosine Deamination Links PIK3CA Helical Domain Mutations to Human Papillomavirus-Driven Tumor Development. *Cell Reports*, *7*(6), 1833–1841. https://doi.org/10.1016/j.celrep.2014.05.012

Herfs, M., Yamamoto, Y., Laury, A., Wang, X., Nucci, M. R., McLaughlin-Drubin, M. E., … Crum, C. P. (2012). A discrete population of squamocolumnar junction cells implicated in the pathogenesis of cervical cancer. *Proceedings of the National Academy of Sciences*, *109*(26), 10516–10521. https://doi.org/10.1073/pnas.1202684109

Higgins, C. A., Richardson, G. D., Ferdinando, D., Westgate, G. E., & Jahoda, C. A. B. (2010). Modelling the hair follicle dermal papilla using spheroid cell cultures: Letter to the Editor. *Experimental Dermatology*, *19*(6), 546–548. https://doi.org/10.1111/j.1600-0625.2009.01007.x

Horsley, V., Aliprantis, A. O., Polak, L., Glimcher, L. H., & Fuchs, E. (2008). NFATc1 Balances Quiescence and Proliferation of Skin Stem Cells. *Cell*, *132*(2), 299–310. https://doi.org/10.1016/j.cell.2007.11.047

Hossein Neamatzadeh, Reza Soleimanizad, Masoud Zare-Shehneh, Saba Gharibi, Abolfazl Shekari, & Amir Bahman Rahimzadeh. (1996). Association between p53 Codon 72 (Arg72Pro) Polymorphism and Primary Open-Angle Glaucoma in Iranian Patients. https://doi.org/10.6091/ibj.1379.2014

Hsu, Y.-C., Li, L., & Fuchs, E. (2014). Emerging interactions between skin stem cells and their niches. *Nature Medicine*, *20*(8), 847–856. https://doi.org/10.1038/nm.3643

Hufbauer, M., Biddle, A., Borgogna, C., Gariglio, M., Doorbar, J., Storey, A., … Akgul, B. (2013). Expression of Betapapillomavirus Oncogenes Increases the Number of Keratinocytes with Stem Cell-Like Properties. *Journal of Virology*, *87*(22), 12158–12165. https://doi.org/10.1128/JVI.01510-13

Johnson, J. L., Koetsier, J. L., Sirico, A., Agidi, A. T., Antonini, D., Missero, C., & Green, K. J. (2014). The Desmosomal Protein Desmoglein 1 Aids Recovery of Epidermal Differentiation after Acute UV Light Exposure. *Journal of Investigative Dermatology*, *134*(8), 2154–2162. https://doi.org/10.1038/jid.2014.124

Jones, P. H., & Watt, F. M. (1993). Separation of human epidermal stem cells from transit amplifying cells on the basis of differences in integrin function and expression. *Cell*, *73*(4), 713–724.

Kang, B. M., Kwack, M. H., Kim, M. K., Kim, J. C., & Sung, Y. K. (2012). Sphere Formation Increases the Ability of Cultured Human Dermal Papilla Cells to Induce Hair Follicles from Mouse Epidermal Cells in a Reconstitution Assay. *Journal of Investigative Dermatology*, *132*(1), 237–239. https://doi.org/10.1038/jid.2011.250

Kines, R. C., Thompson, C. D., Lowy, D. R., Schiller, J. T., & Day, P. M. (2009). The initial steps leading to papillomavirus infection occur on the basement membrane prior to cell surface binding. *Proceedings of the National Academy of Sciences*, *106*(48), 20458–20463. https://doi.org/10.1073/pnas.0908502106

Kowli, S., Velidandla, R., Creek, K. E., & Pirisi, L. (2013). TGF-β regulation of gene expression at early and late stages of HPV16-mediated transformation of human

keratinocytes. *Virology*, *447*(1–2), 63–73.

https://doi.org/10.1016/j.virol.2013.08.034

La Fleur, L., Johansson, A.-C., & Roberg, K. (2012a). A CD44high/EGFRlow

Subpopulation within Head and Neck Cancer Cell Lines Shows an Epithelial-

Mesenchymal Transition Phenotype and Resistance to Treatment. *PLoS ONE*,

7(9), e44071. https://doi.org/10.1371/journal.pone.0044071

La Fleur, L., Johansson, A.-C., & Roberg, K. (2012b). A CD44high/EGFRlow

Subpopulation within Head and Neck Cancer Cell Lines Shows an Epithelial-

Mesenchymal Transition Phenotype and Resistance to Treatment. *PLoS ONE*,

7(9), e44071. https://doi.org/10.1371/journal.pone.0044071

Lagadec, C., Vlashi, E., Della Donna, L., Meng, Y., Dekmezian, C., Kim, K., & Pajonk,

F. (2010). Survival and self-renewing capacity of breast cancer initiating cells

during fractionated radiation treatment. *Breast Cancer Research*, *12*(1), R13.

https://doi.org/10.1186/bcr2479

Lawson, D. A., Bhakta, N. R., Kessenbrock, K., Prummel, K. D., Yu, Y., Takai, K., …

Werb, Z. (2015). Single-cell analysis reveals a stem-cell program in human

metastatic breast cancer cells. *Nature*, *526*(7571), 131–135.

https://doi.org/10.1038/nature15260

Le Roy, H., Zuliani, T., Wolowczuk, I., Faivre, N., Jouy, N., Masselot, B., …

Polakowska, R. (2010a). Asymmetric Distribution of Epidermal Growth Factor

Receptor Directs the Fate of Normal and Cancer Keratinocytes In Vitro. *Stem

Cells and Development*, *19*(2), 209–220. https://doi.org/10.1089/scd.2009.0150

Le Roy, H., Zuliani, T., Wolowczuk, I., Faivre, N., Jouy, N., Masselot, B., …

Polakowska, R. (2010b). Asymmetric Distribution of Epidermal Growth Factor

Receptor Directs the Fate of Normal and Cancer Keratinocytes In Vitro. *Stem

Cells and Development*, *19*(2), 209–220. https://doi.org/10.1089/scd.2009.0150

Letian, T., & Tianyu, Z. (2010). Cellular receptor binding and entry of human

papillomavirus. *Virology Journal*, *7*(1), 2. https://doi.org/10.1186/1743-422X-7-2

Liu, Y., Clem, B., Zuba-Surma, E. K., El-Naggar, S., Telang, S., Jenson, A. B., … Dean,

D. C. (2009). Mouse Fibroblasts Lacking RB1 Function Form Spheres and

Undergo Reprogramming to a Cancer Stem Cell Phenotype. *Cell Stem Cell*, *4*(4),

336–347. https://doi.org/10.1016/j.stem.2009.02.015

Longworth, M. S., & Laimins, L. A. (2004). Pathogenesis of Human Papillomaviruses in

Differentiating Epithelia. *Microbiology and Molecular Biology Reviews*, *68*(2),

362–372. https://doi.org/10.1128/MMBR.68.2.362-372.2004

Ma, D., Chua, A. W. C., Yang, E., Teo, P., Ting, Y., Song, C., … Lee, S. T. (2015).

Breast cancer resistance protein identifies clonogenic keratinocytes in human

interfollicular epidermis. *Stem Cell Research & Therapy*, *6*(1).

https://doi.org/10.1186/s13287-015-0032-2

Maglennon, G. A., McIntosh, P., & Doorbar, J. (2011). Persistence of viral DNA in the

epithelial basal layer suggests a model for papillomavirus latency following

immune regression. *Virology*, *414*(2), 153–163.

https://doi.org/10.1016/j.virol.2011.03.019

Michael, S., Lambert, P. F., & Strati, K. (2013a). The HPV16 oncogenes cause aberrant

stem cell mobilization. *Virology*, *443*(2), 218–225.

https://doi.org/10.1016/j.virol.2013.04.008

Michael, S., Lambert, P. F., & Strati, K. (2013b). The HPV16 oncogenes cause aberrant

stem cell mobilization. *Virology*, *443*(2), 218–225.

https://doi.org/10.1016/j.virol.2013.04.008

Miettinen, P. J., Berger, J. E., Meneses, J., Phung, Y., Pedersen, R. A., Werb, Z., &

Derynck, R. (1995). Epithelial immaturity and multiorgan failure in mice lacking

epidermal growth factor receptor. *Nature*, *376*(6538), 337–341.

https://doi.org/10.1038/376337a0

Mo, J., Sun, B., Zhao, X., Gu, Q., Dong, X., Liu, Z., … Sun, R. (2013). The in-vitro

spheroid culture induces a more highly differentiated but tumorigenic population

from melanoma cell lines. *Melanoma Research*, *23*(4), 254–263.

https://doi.org/10.1097/CMR.0b013e32836314e3

Nanba, D., Toki, F., Tate, S., Imai, M., Matsushita, N., Shiraishi, K., … Barrandon, Y.

(2015). Cell motion predicts human epidermal stemness. *The Journal of Cell

Biology*, *209*(2), 305–315. https://doi.org/10.1083/jcb.201409024

Nanney, L. B., Magid, M., Stoscheck, C. M., & King, L. E. (1984). Comparison of

Epidermal Growth Factor Binding and Receptor Distribution in Normal Human

Epidermis and Epidermal Appendages. *Journal of Investigative Dermatology*,

83(5), 385–393. https://doi.org/10.1111/1523-1747.ep12264708

Oh, B. Y., Lee, W. Y., Jung, S., Hong, H. K., Nam, D.-H., Park, Y. A., … Cho, Y. B.

(2015). Correlation between tumor engraftment in patient-derived xenograft

models and clinical outcomes in colorectal cancer patients. *Oncotarget*, *6*(18), 16059–16068. https://doi.org/10.18632/oncotarget.3863

Parsa, R., Yang, A., McKeon, F., & Green, H. (1999). Association of p63 with proliferative potential in normal and neoplastic human keratinocytes. *The Journal of Investigative Dermatology*, *113*(6), 1099–1105. https://doi.org/10.1046/j.1523-1747.1999.00780.x

Pastrana, E., Silva-Vargas, V., & Doetsch, F. (2011). Eyes wide open: a critical review of sphere-formation as an assay for stem cells. *Cell Stem Cell*, *8*(5), 486–498. https://doi.org/10.1016/j.stem.2011.04.007

Patel, G. K., Wilson, C. H., Harding, K. G., Finlay, A. Y., & Bowden, P. E. (2006). Numerous keratinocyte subtypes involved in wound re-epithelialization. *The Journal of Investigative Dermatology*, *126*(2), 497–502. https://doi.org/10.1038/sj.jid.5700101

Pellegrini, G., Dellambra, E., Golisano, O., Martinelli, E., Fantozzi, I., Bondanza, S., … De Luca, M. (2001). p63 identifies keratinocyte stem cells. *Proceedings of the National Academy of Sciences of the United States of America*, *98*(6), 3156–3161. https://doi.org/10.1073/pnas.061032098

Peterson, S. C., Eberl, M., Vagnozzi, A. N., Belkadi, A., Veniaminova, N. A., Verhaegen, M. E., … Wong, S. Y. (2015). Basal Cell Carcinoma Preferentially Arises from Stem Cells within Hair Follicle and Mechanosensory Niches. *Cell Stem Cell*, *16*(4), 400–412. https://doi.org/10.1016/j.stem.2015.02.006

Pignon, J.-C., Grisanzio, C., Geng, Y., Song, J., Shivdasani, R. A., & Signoretti, S. (2013). p63-expressing cells are the stem cells of developing prostate, bladder,

and colorectal epithelia. *Proceedings of the National Academy of Sciences*, *110*(20), 8105–8110. https://doi.org/10.1073/pnas.1221216110

Pinto, A. P., & Crum, C. P. (2000). Natural history of cervical neoplasia: defining progression and its consequence. *Clinical Obstetrics and Gynecology*, *43*(2), 352–362.

Pirisi, L., Creek, K. E., Doniger, J., & DiPaolo, J. A. (1988). Continuous cell lines with altered growth and differentiation properties originate after transfection of human keratinocytes with human papillomavirus type 16 DNA. *Carcinogenesis*, *9*(9), 1573–1579.

Pirisi, L., Yasumoto, S., Feller, M., Doniger, J., & DiPaolo, J. A. (1987). Transformation of human fibroblasts and keratinocytes with human papillomavirus type 16 DNA. *Journal of Virology*, *61*(4), 1061–1066.

Redvers, R. P., Li, A., & Kaur, P. (2006). Side population in adult murine epidermis exhibits phenotypic and functional characteristics of keratinocyte stem cells. *Proceedings of the National Academy of Sciences of the United States of America*, *103*(35), 13168–13173. https://doi.org/10.1073/pnas.0602579103

Rheinwald, J. G., & Green, H. (1975). Serial cultivation of strains of human epidermal keratinocytes: the formation of keratinizing colonies from single cells. *Cell*, *6*(3), 331–343.

Roshan, A., Murai, K., Fowler, J., Simons, B. D., Nikolaidou-Neokosmidou, V., & Jones, P. H. (2016). Human keratinocytes have two interconvertible modes of proliferation. *Nature Cell Biology*, *18*(2), 145–156. https://doi.org/10.1038/ncb3282

Rybak, A. P., He, L., Kapoor, A., Cutz, J.-C., & Tang, D. (2011). Characterization of sphere-propagating cells with stem-like properties from DU145 prostate cancer cells. *Biochimica Et Biophysica Acta*, *1813*(5), 683–694. https://doi.org/10.1016/j.bbamcr.2011.01.018

Ryser, M. D., Myers, E. R., & Durrett, R. (2015). HPV Clearance and the Neglected Role of Stochasticity. *PLOS Computational Biology*, *11*(3), e1004113. https://doi.org/10.1371/journal.pcbi.1004113

Sada, A., Jacob, F., Leung, E., Wang, S., White, B. S., Shalloway, D., & Tumbar, T. (2016). Defining the cellular lineage hierarchy in the interfollicular epidermis of adult skin. *Nature Cell Biology*, *18*(6), 619–631. https://doi.org/10.1038/ncb3359

Schmitt, A., Rochat, A., Zeltner, R., Borenstein, L., Barrandon, Y., Wettstein, F. O., & Iftner, T. (1996). The primary target cells of the high-risk cottontail rabbit papillomavirus colocalize with hair follicle stem cells. *Journal of Virology*, *70*(3), 1912–1922.

Schneider, T. E., Barland, C., Alex, A. M., Mancianti, M. L., Lu, Y., Cleaver, J. E., … Ghadially, R. (2003). Measuring stem cell frequency in epidermis: a quantitative in vivo functional assay for long-term repopulating cells. *Proceedings of the National Academy of Sciences of the United States of America*, *100*(20), 11412–11417. https://doi.org/10.1073/pnas.2034935100

Shamir, E. R., & Ewald, A. J. (2014). Three-dimensional organotypic culture: experimental models of mammalian biology and disease. *Nature Reviews Molecular Cell Biology*, *15*(10), 647–664. https://doi.org/10.1038/nrm3873

Sherman, L., & Schlegel, R. (1996). Serum- and calcium-induced differentiation of human keratinocytes is inhibited by the E6 oncoprotein of human papillomavirus type 16. *Journal of Virology*, *70*(5), 3269–3279.

Sun, Y., Goderie, S. K., & Temple, S. (2005). Asymmetric distribution of EGFR receptor during mitosis generates diverse CNS progenitor cells. *Neuron*, *45*(6), 873–886. https://doi.org/10.1016/j.neuron.2005.01.045

Takeuchi, K., Kato, M., Suzuki, H., Akhand, A. A., Wu, J., Hossain, K., … Nakashima, I. (2001). Acrolein induces activation of the epidermal growth factor receptor of human keratinocytes for cell death. *Journal of Cellular Biochemistry*, *81*(4), 679–688.

Tani, H., Morris, R. J., & Kaur, P. (2000). Enrichment for murine keratinocyte stem cells based on cell surface phenotype. *Proceedings of the National Academy of Sciences of the United States of America*, *97*(20), 10960–10965.

Toma, J. G., McKenzie, I. A., Bagli, D., & Miller, F. D. (2005). Isolation and characterization of multipotent skin-derived precursors from human skin. *Stem Cells (Dayton, Ohio)*, *23*(6), 727–737. https://doi.org/10.1634/stemcells.2004-0134

Tomar, S., Graves, C. A., Altomare, D., Kowli, S., Kassler, S., Sutkowski, N., … Pirisi, L. (2016). Human papillomavirus status and gene expression profiles of oropharyngeal and oral cancers from European American and African American patients: Gene Expression and Racial Disparity in Oropharyngeal/Oral Cancer. *Head & Neck*, *38*(S1), E694–E704. https://doi.org/10.1002/hed.24072

Tumbar, T., Guasch, G., Greco, V., Blanpain, C., Lowry, W. E., Rendl, M., & Fuchs, E.

(2004). Defining the epithelial stem cell niche in skin. *Science (New York, N.Y.)*,

303(5656), 359–363. https://doi.org/10.1126/science.1092436

Van Der Schueren, B., Cassiman, J. J., & Van Den Berghe, H. (1980). Morphological

characteristics of epithelial and fibroblastic cells growing out from biopsies of

human skin. *The Journal of Investigative Dermatology*, *74*(1), 29–35.

Vollmers, A., Wallace, L., Fullard, N., Höher, T., Alexander, M. D., & Reichelt, J.

(2012). Two- and Three-Dimensional Culture of Keratinocyte Stem and Precursor

Cells Derived from Primary Murine Epidermal Cultures. *Stem Cell Reviews and

Reports*, *8*(2), 402–413. https://doi.org/10.1007/s12015-011-9314-y

Wakita, H., & Takigawa, M. (1999). Activation of epidermal growth factor receptor

promotes late terminal differentiation of cell-matrix interaction-disrupted

keratinocytes. *The Journal of Biological Chemistry*, *274*(52), 37285–37291.

Wan, F., Miao, X., Quraishi, I., Kennedy, V., Creek, K. E., & Pirisi, L. (2008). Gene

expression changes during HPV-mediated carcinogenesis: A comparison between

an *in vitro* cell model and cervical cancer. *International Journal of Cancer*,

123(1), 32–40. https://doi.org/10.1002/ijc.23463

Watt, F. M., Jordan, P. W., & O'Neill, C. H. (1988). Cell shape controls terminal

differentiation of human epidermal keratinocytes. *Proceedings of the National

Academy of Sciences of the United States of America*, *85*(15), 5576–5580.

Webb, A., Li, A., & Kaur, P. (2004). Location and phenotype of human adult

keratinocyte stem cells of the skin. *Differentiation; Research in Biological

Diversity*, *72*(8), 387–395. https://doi.org/10.1111/j.1432-0436.2004.07208005.x

Woodworth, C. D., Doniger, J., & DiPaolo, J. A. (1989). Immortalization of human

foreskin keratinocytes by various human papillomavirus DNAs corresponds to

their association with cervical carcinoma. *Journal of Virology*, *63*(1), 159–164.

Xu, H., Pirisi, L., & Creek, K. E. (2015). Six1 overexpression at early stages of HPV16-

mediated transformation of human keratinocytes promotes differentiation

resistance and EMT. *Virology*, *474*, 144–153.

https://doi.org/10.1016/j.virol.2014.10.010

Xu, H., Zhang, Y., Altomare, D., Pena, M. M., Wan, F., Pirisi, L., & Creek, K. E. (2014).

Six1 promotes epithelial-mesenchymal transition and malignant conversion in

human papillomavirus type 16-immortalized human keratinocytes.

Carcinogenesis, *35*(6), 1379–1388. https://doi.org/10.1093/carcin/bgu050

Yoon, C. S., Kim, K. D., Park, S. N., & Cheong, S. W. (2001a). alpha(6) Integrin is the

main receptor of human papillomavirus type 16 VLP. *Biochemical and

Biophysical Research Communications*, *283*(3), 668–673.

https://doi.org/10.1006/bbrc.2001.4838

Yoon, C. S., Kim, K. D., Park, S. N., & Cheong, S. W. (2001b). alpha(6) Integrin is the

main receptor of human papillomavirus type 16 VLP. *Biochemical and

Biophysical Research Communications*, *283*(3), 668–673.

https://doi.org/10.1006/bbrc.2001.4838

Yu, H., Fang, D., Kumar, S. M., Li, L., Nguyen, T. K., Acs, G., … Xu, X. (2006).

Isolation of a Novel Population of Multipotent Adult Stem Cells from Human

Hair Follicles. *The American Journal of Pathology*, *168*(6), 1879–1888.

https://doi.org/10.2353/ajpath.2006.051170

Zyzak, L. L., MacDonald, L. M., Batova, A., Forand, R., Creek, K. E., & Pirisi, L.

    (1994). Increased levels and constitutive tyrosine phosphorylation of the

    epidermal growth factor receptor contribute to autonomous growth of human

    papillomavirus type 16 immortalized human keratinocytes. *Cell Growth &*

    Differentiation: The Molecular Biology Journal of the American Association for

    Cancer Research, 5(5), 537–547.

CHAPTER 4

INVESTIGATION OF GENOMIC DETERMINANTS OF IMMORTALIZATION RESPONSE TO HPV16 AND SUPPLEMENTAL FIGURES:

Cervical cancer is one of the most predominant human cancers, affecting about half a million women yearly, worldwide. Virtually all cervical cancers are caused by human papillomavirus (HPV). HPV infection is quite common, however only a small number of those infections result in cancer. The reasons why certain women develop cancer and others don't are many and primarily involve the immunological response to HPV and a woman's ability to clear the viral infection. In addition to immune responses, host-cell specific factors may also contribute to the individual risk of HPV-mediated cancer. During infection, HPV E6 oncoprotein binds to and degrades p53. This degradation mechanism is influenced by the presence of arginine or proline amino acids encoded by codon 72 on the p53 gene. Hence, polymorphism in codon 72 has been cited as a potential determinant of transformation outcome. Furthermore, the stem cell properties of a woman's basal epithelial cells have been invoked as a risk factor for transformation. In our model system, we utilized normal human keratinocytes (NHKc) in 3-D culture to investigate the roles of p53 Arg/Pro on stem-like multicellular-spheroid development and conducted HPV16-transfections of NHKc to determine the influence of p53 codon 72 on HPV16-mediated transformation. In this study, we aimed at discover the genetic and molecular basis for these different responses.

We observed that while some individual HKc strains are readily transformed by HPV16, some appear to be more resistant, and certain non-transformed HKc easily adapt into multi-cellular spheroids compared to others. We also observed that the transition of NHKc to HKc/DR was associated with marked induction of the Apolipoprotein B mRNA editing enzyme 3B (APOBEC 3B). The identification of determinants of susceptibility to HPV-mediated transformation and carcinogenesis can be used to determine the individual risk of cancer in any woman who presents an HPV infection, greatly improving on current screening, triage and follow-up measures for the prevention of cervical cancer.

4.1 MATERIAL AND METHODS

gDNA preparation and Sanger sequencing

NHKc from isolated from neonatal foreskin as previously (Akerman et al., 2001) and cultured in modified keratinocyte serum-free medium (KSFM). Genomic DNA (gDNA) was isolated from primary mass-cultured keratinocytes or from a set of 63 retrospective head and neck tumor samples (HNSCCs) (Tomar et al., 2016) using TRIzol Reagent (Ambion by Life Technologies, Grand Island, NY). The P53 amplicon products were generated by RT-qPCR in each sample using Phusion High-Fidelity DNA Polymerase (Thermo Scientific, Waltham, MA) and KAPA-SYBR FAR qPCR kit Master Mix. (Wilmington, MA). Amplicons were then purified by Qiagen's PCR Purification Kit (Hilden, Germany). Exon sequencing was done with the M13 primer and the TP53 reverse primer: R-.5'- CCA GGC ATT GAA GTC TCA T-3'. Samples (5 µL of DNA and 1 µM of primers) were used for Sanger sequencing of P53 at exon 4 based upon the quality of the DNA, as judged by the Enginecore staff (Columbia, SC). Codon 72 polymorphisms of

exon 4 of the P53 gene was analyzed by Finch TV 4.1.0 or by PCR-restriction fragment length polymorphism (PCR-RFLP) analysis using the BstU1 restrictive enzyme technique (New England Biolabs, Ipswich, MA) as described by Hoseein et al.(Hossein Neamatzadeh et al., 1996).

Apolipoprotein B mRNA editing enzyme 3B (APOBEC 3B) assessment

Total mRNA was isolated from various HKc/HPV16 lines, their corresponding HKc/DR lines, and NHKc controls. APOBEC mRNA expression levels were assessed by RT-qPCR using the primers: F-5' CGCCAGACCTACTTGTGCTA 3'; R- 5' CATTTGCAGCGCCTCCTTAT 3'

Clonogenicity of Nutlin-treated cells

Various HKc/HPV16 lines established in our lab were treated with increasing concentrations of Nutlin-A (provided by Dr. Phillip Buckhaults) over the curse of 10 days in culture. Colonies density was counted and colony diameter was also assessed by Giemsa staining.

4.2 RESULTS

Spheroid formation ability and P53 codon 72 status differs from donors of various ethnic backgrounds. When assessing the p53 genotyping of tissue from various donors, we found that the spheroid-forming phenotype was significantly greater in NHKc from African Americans (AA) compared to NHKc from European Americans (EA) (n=59, p= 0.0158). Sanger sequencing of DNA samples from African-American and

European American epithelial tissue (n= 66). Sequence analysis of P53 codon 72 revealed the Pro/Pro homozygous genotype to be present at greater levels in AA samples, while the Arg/Arg homozygous genotype was present at greater levels in EA specimens. Pro/Arg heterozygous genotype was approximately evenly distributed among the two ethnic groups.

HPV16-mediated immortalization leads to a marked increase of mRNA editing enzyme APOBEC 3B in HKc/HPV16 and differentiation-resistant HKc/HPV16 (HKc/DR). Next, we isolated total mRNA from HKc/HPV16 lines established from NF-NHKc and SF-NHKc, then assessed Apolipoprotein B mRNA editing enzyme 3B (APOBEC 3B) mRNA expression levels. We've observed significant increases in transcripts encoding APOBEC 3B in HKc/HPV16 relative to corresponding NHKc lines. Except for two strains (M 7.11.13 8BK and M7.28.13 12BK), APOBEC 3B levels were at least 4 folds higher in HKc/HPV16 (passages 6-15) and Hkc/DR lines (passage 20-30) relative to their respective normal lines (passage 2-5). Interestingly, we observed the greatest upregulation of APOBEC mRNA in HKc/HPV16 lines established from SD/NHKc cultures. Among all immortalized strains, HKc/DR lines express significantly greater levels of APOBEC 3B mRNA compared to their respective NHKc lines. These data depict a strong association between HPV-mediated immortalization and APOBEC levels.

HPV16-mediated immortalization leads to a marked increase in mRNA editing enzyme APOBEC 3B in HKc/HPV16 HKc/DR. To determine the effect of Nutlin 3-A on HPV-driven immortlization of HKc by treating adherent HKc/HPV16 cells

116

with increasing concentrations of Nutlin, then staining plates with Giemsa stain. We've observed an inhibitory effect on colony formation in HKc/HPV16 lines after treatment with Nutlin-3a.

Categorization of HKc/HPV16 by growth patterns and cell surface marker expression. Next, we chose to characterize all 15 of our established HKc/HPV16 lines to track their growth patterns and behaviors in culture. We found that the behaviours of several lines could be predicted based on endogenous cell surface EGFR levels and ITα6 levels.

4.3 FIGURES
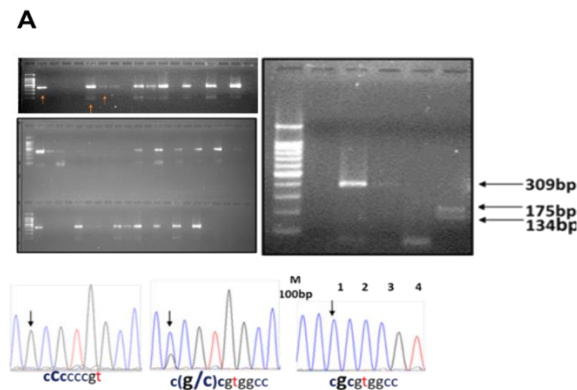
Figure 4.1 Assessment of p53 codon 72 status by PCR-restriction fragment length polymorphism (PCR-RLFP) and Sanger sequence analysis of DNA samples from African American and European American tissue. DNA samples from cells used in the spheroid assays, as well as from a set of 63 head and neck tumor samples (HNSCCs) of known HPV status were sequenced for P53 codon 72 phenotype variance. (A) PCR with PCR-restriction fragment length polymorphism (PCR-RLFP) and (bellow) sequence analysis. The 309-bp target DNA fragment containing cgc/ccc sites of the p53 gene codon 72 located in exon 4 was digested with Bstu1. Arrows depict a single 309-bp band indicative of a loss of Bstu1 restriction site (ARG/ARG phenotype), while the PRO genotype (PRO/PRO) produced two bands (175-bp and 134-bp). Direct sequencing confirmed the PCR-RFLP analysis.

B

	AA	EA
SF	16	8
SNF	11	23

	Arg/Arg	Pro/Pro	Pro/Arg
AA	2	7	9
EA	12	8	14
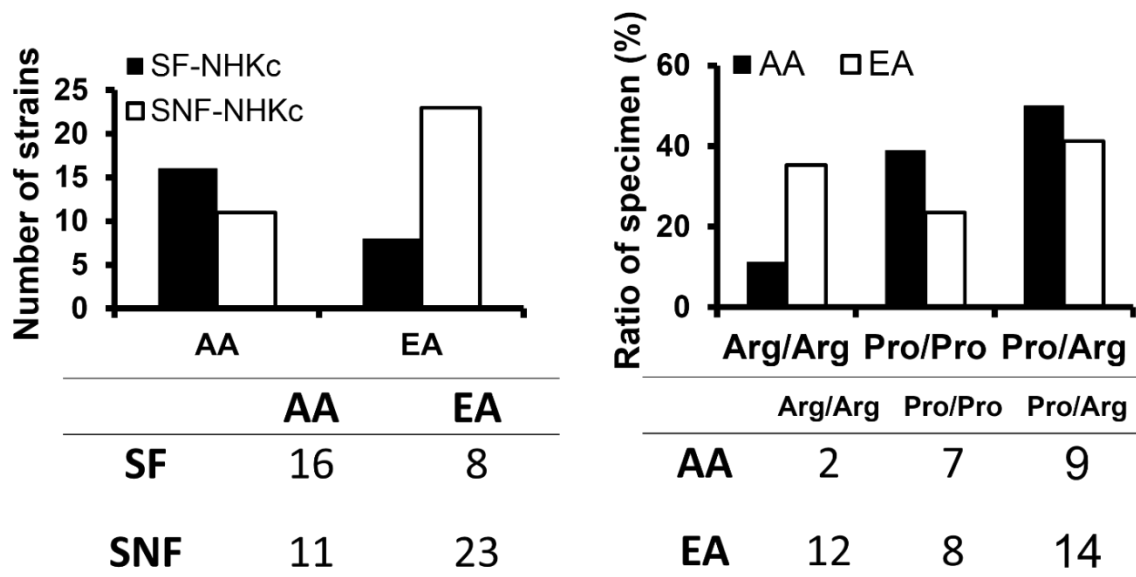
Figure 4.2 Determination of p53 codon 72 status in DNA samples from African American and European American tissue. (B) Spheroid-forming phenotype and P53 codon 72 genotype distribution among African-American and European-American samples.
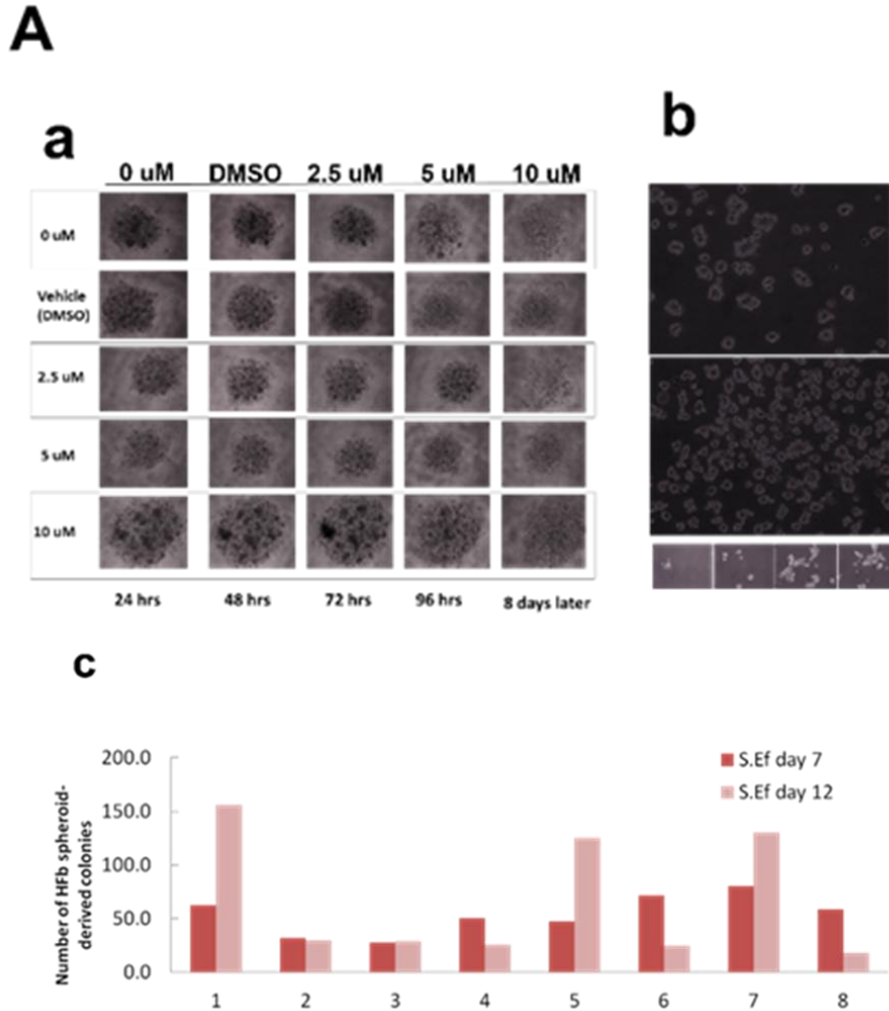
Figure 4.3 Effects of Nutlin 3A on HFb spheroid forming ability. (A) 1 x 10^4 cells/well were seeded in a agar/media-coated 96-well plate and cells were cultured in stem cell-modified KSFM media and treated with increasing concentrations of Nutlin-3a (0uM, DMSO, 2.5 uM, 5uM, 10 uM) over the course of 8 days in suspension culture; (b) Human fibroblasts (HFb) were also cultured in 3-D suspension and Hfb spheroids were transposed into a new adhesive 96-well plate to determine the effect of Nutlin-3a on spheroid seeding efficiency; (c) derived cells were cultured in stem cell-modified/F12 media and the number of colonies were counted at day 7 and day 12 to evaluate cell seeding efficiency. Yellow rows depict spheroids with elevated stemness qualities.

119
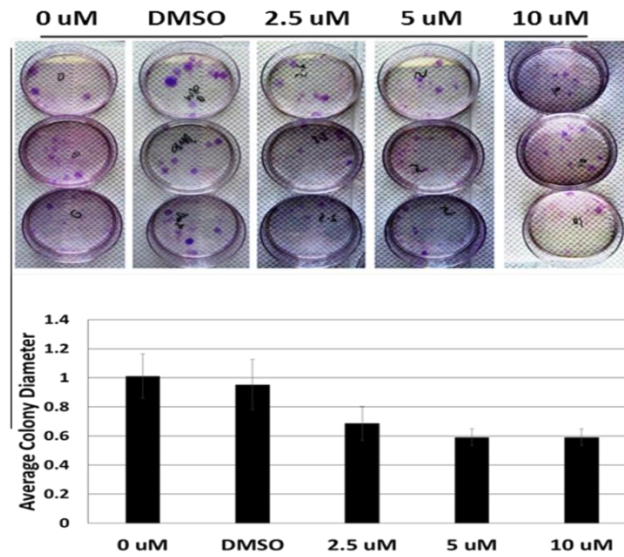
Figure 4.4 Clonogenicity assay on NHKc after Nutlin treatment. (B) 5 x 10^4 keratinocytes were plated in 60 mm dish and treated with varying concentrations of Nutlin-3a; (b) colony size by measure of colony diameter was determined at each treatment concentration.

C

Strain	Sr.D day 7	Sr.D day 12	Race	p53 Genotype	MDM2 Genotype day 7	S.E	S.E day 12
1	85	18	CA	R/R	T/T	62.4	155.6
2	107	34	CA	P/P	G/G	31.8	29.4
3	18	24	CA	R/R	G/G	27.8	29.2
4	6	23	AA	P/P	T/T	50	26.1
5	17	4	CA	P/P	T/T	47.1	125
6	64	56	CA	R/R	T/T	71.9	25
7	20	10	AA	P/P	T/T	80	130
8	51	56	AA	R/R	T/T	58.8	17.9

Figure 4.5 HFb seeding efficiency, as well as MDM2 and P53 genotyping. (C) Seeding efficiency at day 7 and day 12 in 8 different HF strains with varying P53 codon 72 and MDM2 genotype distributions. Yellow rows depict HFb spheroids with low seeding efficiencies after 12 days in culture.
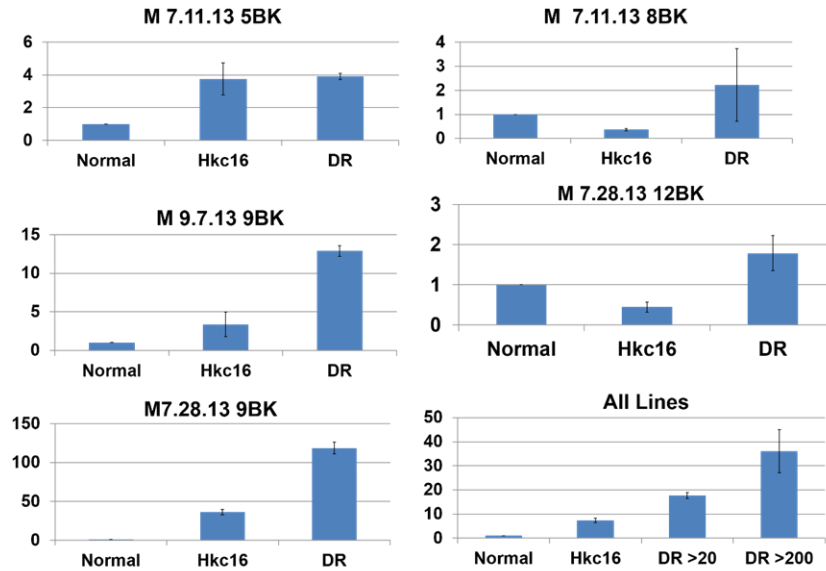
Figure 4.6 APOBEC 3B mRNA expression is dramatically increased in HPV16-immortalized keratinocytes. (A) Relative APOBEC 3B mRNA levels in five different Hkc/HPV16 and differentiation resistant strains (Hkc/DR) at early (P>20) and advanced passages (P>200) after immortalization with HPV16 DNA.

Figure 4.7 P53 genotyping as assessed by PCR-RFLP. (B) Specific amplification of the expected amplicons (342 bp) was confirmed by agarose gel (2%) electrophoresis for all five Hkc/DR lines (lane 2-6), a well-established Hkc/DR line (lane 8), and a no-template control (lane 7).

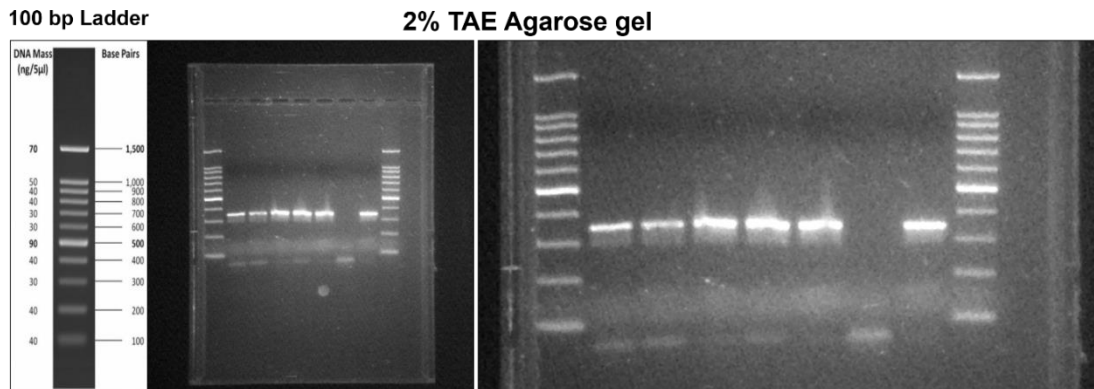| | | | | Before transfection | | | | | | After transfection | | | | | |
	Strain	Spheroid formation	Anoikis resistance	Spheroid-derived line	Cell morphology	Colony morphology	Avg. population doubling per day	Max # of passages	Population of EGFR+/ITGα6+ cells	Cell morphology	Colony morphology	Spheroid-formation	Avg. population doubling per day	Transformation efficiency (%)	Ethnicity
Spheroid non-forming (SNF)															
1	Y1	No	No	None	Cobblestone-shaped	Circumscribed	0.31±0.5	3	9.4	Cobblestone-shaped	Circumscribed	Yes	0.50±0.1	17±0.6	AA
2	Y3B	No	No	None	Cobblestone-shaped	Circumscribed	0.41±0.5	5	14.1	Cobblestone-shaped	Circumscribed	No	0.53±0.3		EA
3	Y5	No	No	None	Cobblestone-shaped	Circumscribed	0.42±0.4	3	5.8	Cobblestone-shaped	Circumscribed	Yes	0.52±0.5		AA
4	Y5B	No	No	None	Cobblestone-shaped	Circumscribed	0.40±0.2	5	21.5	Cobblestone-shaped	Circumscribed	Yes	0.50±0.1		AA
5	Y9D	No	No	None	Cobblestone-shaped	Circumscribed	0.45±0.2	3	6.1	Cobblestone-shaped	Circumscribed	No	0.49±0.4		EA
6	Y6A	No	No	None	Cobblestone-shaped	Circumscribed	0.34±0.4	4	8.7	Cobblestone-shaped	Circumscribed	Yes	0.48±0.1		EA
7	Y9	No	No	None	Cobblestone-shaped	Circumscribed	0.46±0.3	3	9.4	Cobblestone-shaped	Circumscribed	Yes	0.54±0.2		AA
8	Y9B	No	No	None	Cobblestone-shaped	Circumscribed	0.44±0.4	3	2.3	Cobblestone-shaped	Circumscribed	Yes	0.52±0.3		AA
9	Y9C	No	No	None	Cobblestone-shaped	Circumscribed	0.47±0.1	3	4.3	Cobblestone-shaped	Circumscribed	Yes	0.49±0.3		EA
10	Y10B	No	No	None	Cobblestone-shaped	Circumscribed	0.35±0.2	3	1.9	Cobblestone-shaped	Circumscribed	Yes	0.34±0.4		EA
Spheroid-forming (SF)															
11	Y2	Yes	Yes	Yes	Cobblestone-shaped	Wide-spread	0.47±0.1	3	27.8	Cobblestone-like	Widespread	Yes	0.48±0.2		AA
11b	SD-Y2	Yes	Yes	Yes	Cobblestone-shaped	Wide-spread	0.57±0.2	6	40.2	Small cells cobblestone-like	Whole-plate confluent	Yes	1.0±0.2		-
12	Y4B	Yes	Yes	Yes	Cobblestone-like shaped	Wide-spread	0.37±0.2	4	29.4	Cobblestone-like	Widespread	Yes	0.55±0.3		AA
12b	SD-Y4B	Yes	Yes	Yes	Cobblestone-shaped	Wide-spread	0.51±0.1	5	64.1	Cobblestone-like	Whole-plate confluent	Yes	1.0±0.4		-
13	Y6E	Yes	Yes	Yes	Cobblestone-shaped	Wide-spread	0.40±0.2	4	24.9	Cobblestone-like	Widespread	Yes	0.42±0.4	23±0.9	AA
13b	SD-Y6E	Yes	Yes	Yes	Cobblestone-shaped	Wide-spread	0.43±0.1	6	79.0	Small cell cobblestone-like	Whole-plate confluent	Yes	1.3±0.2	63±0.4	-
14	Y6F	Yes	Yes	Yes	Cobblestone-shaped	Wide-spread	0.38±0.2	4	9.4	Cobblestone-like	Widespread	Yes	0.38±0.3		AA
14b	SD-Y6F	Yes	Yes	Yes	Cobblestone-shaped	Wide-spread	0.54±0.3	5	24.4	Cobblestone-like	Whole-plate confluent	Yes	0.56±0.3		-
15	Y6B	Yes	Yes	No	Cobblestone-shaped	Wide-spread	0.43±0.5	4	11.5	Cobblestone-like	Widespread	Yes	0.53±0.3		AA

Figure 4.8 Behavior and phenotypic characteristics of various HKc/HPV16 lines in culture.

Table 4.1. Primers used for Real-Time PCR

Gene	Forward Primer: 5'-3'	Reverse Primer: 5'-3'
ALDH1	GCACGCCAGACTTACCTGTC	CCTCCTCAGTTGCAGGATTAAAG
APOBEC-3B	CGC CAG ACC TAC TTG TGC TAT	CAT TTG CAG CGC CTC CTT AT
BIRC5	AGGACCACCGCATCTCTACAT	AAGTCTGGCTCGTTCTCAGTG
CDH1	CGA GAG CTA CAC GTT CAC GG	GGG TGT CGA GGG AAA AAT AGG
EGFR	AGGCACGAGTAACAAGCTCAC	ATGAGGACATAACCAGCCACC
FLG	TGAAGCCTATGACACCACTGA	TCCCCTACGCTTTCTTGTCCT
FN1	CGGTGGCTGTCAGTCAAAG	AAACCTCGGCTTCCTCCATAA
GAPDH	GGA GCG AGA TCC CTC CAA AAT	GGC TGT TGT CAT ACT TCT CAT GG
IVL	TCCTCCAGTCAATACCCATCAG	CAGCAGTCATGTGCTTTTCCT
K10	ATGTCTGTTCGATACAGCTCAAG	CTCCACCAAGGGAGCCTTTG
K14	TGAGCCGCATTCTGAACGAG	GATGACTGCGATCCAGAGGA
K15	CCAAGGTTGATGCACTGATGG	TGTCAGAGACATGCGTCTGC
K5	CCA AGG TTG ATG CAC TGA TGG	TGT CAG AGA CAT GCG TCT GC
Ki-67	ACGCCTGGTTACTATCAAAAGG	CAGACCCATTTACTTGTGTTGGA
KLF4	CCC ACA TGA AGC GAC TTC CC	CAG GTC CAG GAG ATC GTT GAA
NANOG	TTTGTGGGCCTGAAGAAAACT	AGGGCTGTCCTGAATAAGCAG
OCT4	CTGGGTTGATCCTCGGACCT	CCATCGGAGTTGCTCTCCA
SOX2	GCCGAGTGGAAACTTTTGTCG	GGCAGCGTGTACTTATCCTTCT
SNAIL	TCGGAAGCCTAACTACAGCGA	AGATGAGCATTGGCAGCGAG
SIX1	ATT CTC ACC TCC CCA AAG TC	ACT TAG GAC CCC AAG TCC AC
TP63	GGACCAGCAGATTCAGAACGG	AGGACACGTCGAAACTGTGC
TWIST	GTCCGCAGTCTTACGAGGAG	GCTTGAGGGTCTGAATCTTGCT
β-actin	CATGTACGT TGCTATCCAGGC	CTCCTTAATGTCACGCACGAT
ΔN TP63	ATGTTGTACCTGGAAAACAATGCC	CAGGCATGGCACGGATAAC

4.4 DISCUSSION

Given the behavior of NHKc suspension cultures of different stains, 0ur findings suggest an association between spheroid-forming ability in NHKc purified from AA epidermis compared to EA epidermis. The dramatic induction of APOBEC during HKc/HPV16 transition to HKc/DR also reaveals that this gene is strongly correlated with HPV-mediated immortalization as indicated by some reports (Henderson, Chakravarthy, Su, Boshoff, & Fenton, 2014). Moreover, the fact that increasing amounts of Nutlin 3A considerably reduced HKc/HPV16 clonogenicity in culture could be further explored as a treatment method for HPV-driven pre-neoplastic cells. Further investigation would be required to validate these observations and to determine whether P53 genotyping could be employed as a biomarker of spheroid-forming ability in NHKc, and whether this could be potentially used to determine cells' proclivity to transformation after immortalization by HPV16 DNA.

4.5 REFERENCES

Akerman, G. S., Tolleson, W. H., Brown, K. L., Zyzak, L. L., Mourateva, E., Engin, T. S., … Pirisi, L. (2001). Human papillomavirus type 16 E6 and E7 cooperate to increase epidermal growth factor receptor (EGFR) mRNA levels, overcoming mechanisms by which excessive EGFR signaling shortens the life span of normal human keratinocytes. *Cancer Research*, *61*(9), 3837–3843.

Akerman, G. S., Tolleson, W. H., Brown, K. L., Zyzak, L. L., Mourateva, E., Engin, T. S., … Pirisi, L. (2001). Human papillomavirus type 16 E6 and E7 cooperate to increase epidermal growth factor receptor (EGFR) mRNA levels, overcoming

mechanisms by which excessive EGFR signaling shortens the life span of normal human keratinocytes. *Cancer Research*, *61*(9), 3837–3843.

Akerman, G. S., Tolleson, W. H., Brown, K. L., Zyzak, L. L., Mourateva, E., Engin, T. S., … Pirisi, L. (2001). Human papillomavirus type 16 E6 and E7 cooperate to increase epidermal growth factor receptor (EGFR) mRNA levels, overcoming mechanisms by which excessive EGFR signaling shortens the life span of normal human keratinocytes. *Cancer Research*, *61*(9), 3837–3843.

Altomare, D., Velidandla, R., Pirisi, L., & Creek, K. E. (2013). Partial loss of Smad signaling during in vitro progression of HPV16-immortalized human keratinocytes. *BMC Cancer*, *13*(1), 424. https://doi.org/10.1186/1471-2407-13-424

Barrandon, Y., & Green, H. (1987). Three clonal types of keratinocyte with different capacities for multiplication. *Proceedings of the National Academy of Sciences*, *84*(8), 2302–2306.

Bheda, A., Creek, K. E., & Pirisi, L. (2008a). Loss of p53 induces epidermal growth factor receptor promoter activity in normal human keratinocytes. *Oncogene*, *27*(31), 4315–4323. https://doi.org/10.1038/onc.2008.65

Bheda, A., Creek, K. E., & Pirisi, L. (2008b). Loss of p53 induces epidermal growth factor receptor promoter activity in normal human keratinocytes. *Oncogene*, *27*(31), 4315–4323. https://doi.org/10.1038/onc.2008.65

Blanpain, C. (2013). Tracing the cellular origin of cancer. *Nature Cell Biology*, *15*(2), 126–134. https://doi.org/10.1038/ncb2657

Blanpain, C., & Fuchs, E. (2006). Epidermal stem cells of the skin. *Annual Review of Cell and Developmental Biology*, *22*, 339–373. https://doi.org/10.1146/annurev.cellbio.22.010305.104357

Bodily, J., & Laimins, L. A. (2011). Persistence of human papillomavirus infection: keys to malignant progression. *Trends in Microbiology*, *19*(1), 33–39. https://doi.org/10.1016/j.tim.2010.10.002

Borena, B. M., Meyer, E., Chiers, K., Martens, A., Demeyere, K., Broeckx, S. Y., … Spaas, J. H. (2014). Sphere-Forming Capacity as an Enrichment Strategy for Epithelial-Like Stem Cells from Equine Skin. *Cellular Physiology and Biochemistry*, *34*(4), 1291–1303. https://doi.org/10.1159/000366338

Chen, Y., Pirisi, L., & Creek, K. E. (2013). Ski protein levels increase during in vitro progression of HPV16-immortalized human keratinocytes and in cervical cancer. *Virology*, *444*(1–2), 100–108. https://doi.org/10.1016/j.virol.2013.05.039

Chow, L. T., Broker, T. R., & Steinberg, B. M. (2010). The natural history of human papillomavirus infections of the mucosal epithelia: NATURAL HISTORY OF HPV INFECTIONS AND PATHOLOGY. *APMIS*, *118*(6–7), 422–449. https://doi.org/10.1111/j.1600-0463.2010.02625.x

Clayton, E., Doupé, D. P., Klein, A. M., Winton, D. J., Simons, B. D., & Jones, P. H. (2007). A single type of progenitor cell maintains normal epidermis. *Nature*, *446*(7132), 185–189. https://doi.org/10.1038/nature05574

Clifford, G. M., Smith, J. S., Plummer, M., Muñoz, N., & Franceschi, S. (2003). Human papillomavirus types in invasive cervical cancer worldwide: a meta-analysis. *British Journal of Cancer*, *88*(1), 63–73. https://doi.org/10.1038/sj.bjc.6600688

Coulombe, P. A., Kopan, R., & Fuchs, E. (1989). Expression of keratin K14 in the

epidermis and hair follicle: insights into complex programs of differentiation. *The Journal of Cell Biology*, *109*(5), 2295–2312.

De Rosa, L., & De Luca, M. (2012). Cell biology: Dormant and restless skin stem cells.

Nature, *489*(7415), 215–217. https://doi.org/10.1038/489215a

Doupe, D. P., Alcolea, M. P., Roshan, A., Zhang, G., Klein, A. M., Simons, B. D., &

Jones, P. H. (2012). A Single Progenitor Population Switches Behavior to

Maintain and Repair Esophageal Epithelium. *Science*, *337*(6098), 1091–1093.

https://doi.org/10.1126/science.1218835

Doupé, D. P., & Jones, P. H. (2012). Interfollicular epidermal homeostasis: dicing with

differentiation. *Experimental Dermatology*, *21*(4), 249–253.

https://doi.org/10.1111/j.1600-0625.2012.01447.x

Evander, M., Frazer, I. H., Payne, E., Qi, Y. M., Hengst, K., & McMillan, N. A. (1997).

Identification of the alpha6 integrin as a candidate receptor for papillomaviruses.

Journal of Virology, *71*(3), 2449–2456.

Fakhry, C. (2006). Clinical Implications of Human Papillomavirus in Head and Neck

Cancers. *Journal of Clinical Oncology*, *24*(17), 2606–2611.

https://doi.org/10.1200/JCO.2006.06.1291

Fitsialos, G., Chassot, A.-A., Turchi, L., Dayem, M. A., LeBrigand, K., Moreilhon, C., …

Ponzio, G. (2007). Transcriptional signature of epidermal keratinocytes subjected

to in vitro scratch wounding reveals selective roles for ERK1/2, p38, and

phosphatidylinositol 3-kinase signaling pathways. *The Journal of Biological

Chemistry*, *282*(20), 15090–15102. https://doi.org/10.1074/jbc.M606094200

Flesken-Nikitin, A., Hwang, C.-I., Cheng, C.-Y., Michurina, T. V., Enikolopov, G., &
Nikitin, A. Y. (2013). Ovarian surface epithelium at the junction area contains a
cancer-prone stem cell niche. *Nature*, *495*(7440), 241–245.
https://doi.org/10.1038/nature11979

Fortunel, N. O. (2003). Long-term expansion of human functional epidermal precursor
cells: promotion of extensive amplification by low TGF- 1 concentrations.
Journal of Cell Science, *116*(19), 4043–4052. https://doi.org/10.1242/jcs.00702

Fuchs, E. (2012). The Impact of Cell Culture on Stem Cell Research. *Cell Stem Cell*,
10(6), 640–641. https://doi.org/10.1016/j.stem.2012.03.010

Gago, N., Pérez-López, V., Sanz-Jaka, J. P., Cormenzana, P., Eizaguirre, I., Bernad, A.,
& Izeta, A. (2009). Age-Dependent Depletion of Human Skin-Derived Progenitor
Cells: Age-Dependent Depletion of Human SKPs. *STEM CELLS*, *27*(5), 1164–
1172. https://doi.org/10.1002/stem.27

Green, H. (1977). Terminal differentiation of cultured human epidermal cells. *Cell*, *11*(2),
405–416.

Guo, A., & Jahoda, C. A. B. (2009). An improved method of human keratinocyte culture
from skin explants: cell expansion is linked to markers of activated progenitor
cells. *Experimental Dermatology*, *18*(8), 720–726. https://doi.org/10.1111/j.1600-
0625.2009.00900.x

Henderson, S., Chakravarthy, A., Su, X., Boshoff, C., & Fenton, T. R. (2014). APOBEC-
Mediated Cytosine Deamination Links PIK3CA Helical Domain Mutations to
Human Papillomavirus-Driven Tumor Development. *Cell Reports*, *7*(6), 1833–
1841. https://doi.org/10.1016/j.celrep.2014.05.012

Herfs, M., Yamamoto, Y., Laury, A., Wang, X., Nucci, M. R., McLaughlin-Drubin, M.

    E., … Crum, C. P. (2012). A discrete population of squamocolumnar junction

    cells implicated in the pathogenesis of cervical cancer. *Proceedings of the*

    National Academy of Sciences, *109*(26), 10516–10521.

    https://doi.org/10.1073/pnas.1202684109

Higgins, C. A., Richardson, G. D., Ferdinando, D., Westgate, G. E., & Jahoda, C. A. B.

    (2010). Modelling the hair follicle dermal papilla using spheroid cell cultures:

    Letter to the Editor. *Experimental Dermatology*, *19*(6), 546–548.

    https://doi.org/10.1111/j.1600-0625.2009.01007.x

Horsley, V., Aliprantis, A. O., Polak, L., Glimcher, L. H., & Fuchs, E. (2008). NFATc1

    Balances Quiescence and Proliferation of Skin Stem Cells. *Cell*, *132*(2), 299–310.

    https://doi.org/10.1016/j.cell.2007.11.047

Hossein Neamatzadeh, Reza Soleimanizad, Masoud Zare-Shehneh, Saba Gharibi,

    Abolfazl Shekari, & Amir Bahman Rahimzadeh. (1996). Association between p53

    Codon 72 (Arg72Pro) Polymorphism and Primary Open-Angle Glaucoma in

    Iranian Patients. https://doi.org/10.6091/ibj.1379.2014

Hsu, Y.-C., Li, L., & Fuchs, E. (2014). Emerging interactions between skin stem cells

    and their niches. *Nature Medicine*, *20*(8), 847–856.

    https://doi.org/10.1038/nm.3643

Hufbauer, M., Biddle, A., Borgogna, C., Gariglio, M., Doorbar, J., Storey, A., … Akgul,

    B. (2013). Expression of Betapapillomavirus Oncogenes Increases the Number of

    Keratinocytes with Stem Cell-Like Properties. *Journal of Virology*, *87*(22),

    12158–12165. https://doi.org/10.1128/JVI.01510-13

Johnson, J. L., Koetsier, J. L., Sirico, A., Agidi, A. T., Antonini, D., Missero, C., & Green, K. J. (2014). The Desmosomal Protein Desmoglein 1 Aids Recovery of Epidermal Differentiation after Acute UV Light Exposure. *Journal of Investigative Dermatology*, *134*(8), 2154–2162. https://doi.org/10.1038/jid.2014.124

Jones, P. H., & Watt, F. M. (1993). Separation of human epidermal stem cells from transit amplifying cells on the basis of differences in integrin function and expression. *Cell*, *73*(4), 713–724.

Kang, B. M., Kwack, M. H., Kim, M. K., Kim, J. C., & Sung, Y. K. (2012). Sphere Formation Increases the Ability of Cultured Human Dermal Papilla Cells to Induce Hair Follicles from Mouse Epidermal Cells in a Reconstitution Assay. *Journal of Investigative Dermatology*, *132*(1), 237–239. https://doi.org/10.1038/jid.2011.250

Kines, R. C., Thompson, C. D., Lowy, D. R., Schiller, J. T., & Day, P. M. (2009). The initial steps leading to papillomavirus infection occur on the basement membrane prior to cell surface binding. *Proceedings of the National Academy of Sciences*, *106*(48), 20458–20463. https://doi.org/10.1073/pnas.0908502106

Kowli, S., Velidandla, R., Creek, K. E., & Pirisi, L. (2013). TGF-β regulation of gene expression at early and late stages of HPV16-mediated transformation of human keratinocytes. *Virology*, *447*(1–2), 63–73. https://doi.org/10.1016/j.virol.2013.08.034

La Fleur, L., Johansson, A.-C., & Roberg, K. (2012a). A CD44high/EGFRlow Subpopulation within Head and Neck Cancer Cell Lines Shows an Epithelial-

Mesenchymal Transition Phenotype and Resistance to Treatment. *PLoS ONE*, *7*(9), e44071. https://doi.org/10.1371/journal.pone.0044071

La Fleur, L., Johansson, A.-C., & Roberg, K. (2012b). A CD44high/EGFRlow Subpopulation within Head and Neck Cancer Cell Lines Shows an Epithelial-Mesenchymal Transition Phenotype and Resistance to Treatment. *PLoS ONE*, *7*(9), e44071. https://doi.org/10.1371/journal.pone.0044071

Lagadec, C., Vlashi, E., Della Donna, L., Meng, Y., Dekmezian, C., Kim, K., & Pajonk, F. (2010). Survival and self-renewing capacity of breast cancer initiating cells during fractionated radiation treatment. *Breast Cancer Research*, *12*(1), R13. https://doi.org/10.1186/bcr2479

Lawson, D. A., Bhakta, N. R., Kessenbrock, K., Prummel, K. D., Yu, Y., Takai, K., … Werb, Z. (2015). Single-cell analysis reveals a stem-cell program in human metastatic breast cancer cells. *Nature*, *526*(7571), 131–135. https://doi.org/10.1038/nature15260

Le Roy, H., Zuliani, T., Wolowczuk, I., Faivre, N., Jouy, N., Masselot, B., … Polakowska, R. (2010a). Asymmetric Distribution of Epidermal Growth Factor Receptor Directs the Fate of Normal and Cancer Keratinocytes In Vitro. *Stem Cells and Development*, *19*(2), 209–220. https://doi.org/10.1089/scd.2009.0150

Le Roy, H., Zuliani, T., Wolowczuk, I., Faivre, N., Jouy, N., Masselot, B., … Polakowska, R. (2010b). Asymmetric Distribution of Epidermal Growth Factor Receptor Directs the Fate of Normal and Cancer Keratinocytes In Vitro. *Stem Cells and Development*, *19*(2), 209–220. https://doi.org/10.1089/scd.2009.0150

Letian, T., & Tianyu, Z. (2010). Cellular receptor binding and entry of human

    papillomavirus. *Virology Journal*, *7*(1), 2. https://doi.org/10.1186/1743-422X-7-2

Liu, Y., Clem, B., Zuba-Surma, E. K., El-Naggar, S., Telang, S., Jenson, A. B., … Dean,

    D. C. (2009). Mouse Fibroblasts Lacking RB1 Function Form Spheres and

    Undergo Reprogramming to a Cancer Stem Cell Phenotype. *Cell Stem Cell*, *4*(4),

    336–347. https://doi.org/10.1016/j.stem.2009.02.015

Longworth, M. S., & Laimins, L. A. (2004). Pathogenesis of Human Papillomaviruses in

    Differentiating Epithelia. *Microbiology and Molecular Biology Reviews*, *68*(2),

    362–372. https://doi.org/10.1128/MMBR.68.2.362-372.2004

Ma, D., Chua, A. W. C., Yang, E., Teo, P., Ting, Y., Song, C., … Lee, S. T. (2015).

    Breast cancer resistance protein identifies clonogenic keratinocytes in human

    interfollicular epidermis. *Stem Cell Research & Therapy*, *6*(1).

    https://doi.org/10.1186/s13287-015-0032-2

Maglennon, G. A., McIntosh, P., & Doorbar, J. (2011). Persistence of viral DNA in the

    epithelial basal layer suggests a model for papillomavirus latency following

    immune regression. *Virology*, *414*(2), 153–163.

    https://doi.org/10.1016/j.virol.2011.03.019

Michael, S., Lambert, P. F., & Strati, K. (2013a). The HPV16 oncogenes cause aberrant

    stem cell mobilization. *Virology*, *443*(2), 218–225.

    https://doi.org/10.1016/j.virol.2013.04.008

Michael, S., Lambert, P. F., & Strati, K. (2013b). The HPV16 oncogenes cause aberrant

    stem cell mobilization. *Virology*, *443*(2), 218–225.

    https://doi.org/10.1016/j.virol.2013.04.008

Miettinen, P. J., Berger, J. E., Meneses, J., Phung, Y., Pedersen, R. A., Werb, Z., & Derynck, R. (1995). Epithelial immaturity and multiorgan failure in mice lacking epidermal growth factor receptor. *Nature*, *376*(6538), 337–341. https://doi.org/10.1038/376337a0

Mo, J., Sun, B., Zhao, X., Gu, Q., Dong, X., Liu, Z., … Sun, R. (2013). The in-vitro spheroid culture induces a more highly differentiated but tumorigenic population from melanoma cell lines. *Melanoma Research*, *23*(4), 254–263. https://doi.org/10.1097/CMR.0b013e32836314e3

Nanba, D., Toki, F., Tate, S., Imai, M., Matsushita, N., Shiraishi, K., … Barrandon, Y. (2015). Cell motion predicts human epidermal stemness. *The Journal of Cell Biology*, *209*(2), 305–315. https://doi.org/10.1083/jcb.201409024

Nanney, L. B., Magid, M., Stoscheck, C. M., & King, L. E. (1984). Comparison of Epidermal Growth Factor Binding and Receptor Distribution in Normal Human Epidermis and Epidermal Appendages. *Journal of Investigative Dermatology*, *83*(5), 385–393. https://doi.org/10.1111/1523-1747.ep12264708

Oh, B. Y., Lee, W. Y., Jung, S., Hong, H. K., Nam, D.-H., Park, Y. A., … Cho, Y. B. (2015). Correlation between tumor engraftment in patient-derived xenograft models and clinical outcomes in colorectal cancer patients. *Oncotarget*, *6*(18), 16059–16068. https://doi.org/10.18632/oncotarget.3863

Parsa, R., Yang, A., McKeon, F., & Green, H. (1999). Association of p63 with proliferative potential in normal and neoplastic human keratinocytes. *The Journal of Investigative Dermatology*, *113*(6), 1099–1105. https://doi.org/10.1046/j.1523-1747.1999.00780.x

Pastrana, E., Silva-Vargas, V., & Doetsch, F. (2011). Eyes wide open: a critical review of sphere-formation as an assay for stem cells. *Cell Stem Cell*, *8*(5), 486–498. https://doi.org/10.1016/j.stem.2011.04.007

Patel, G. K., Wilson, C. H., Harding, K. G., Finlay, A. Y., & Bowden, P. E. (2006). Numerous keratinocyte subtypes involved in wound re-epithelialization. *The Journal of Investigative Dermatology*, *126*(2), 497–502. https://doi.org/10.1038/sj.jid.5700101

Pellegrini, G., Dellambra, E., Golisano, O., Martinelli, E., Fantozzi, I., Bondanza, S., … De Luca, M. (2001). p63 identifies keratinocyte stem cells. *Proceedings of the National Academy of Sciences of the United States of America*, *98*(6), 3156–3161. https://doi.org/10.1073/pnas.061032098

Peterson, S. C., Eberl, M., Vagnozzi, A. N., Belkadi, A., Veniaminova, N. A., Verhaegen, M. E., … Wong, S. Y. (2015). Basal Cell Carcinoma Preferentially Arises from Stem Cells within Hair Follicle and Mechanosensory Niches. *Cell Stem Cell*, *16*(4), 400–412. https://doi.org/10.1016/j.stem.2015.02.006

Pignon, J.-C., Grisanzio, C., Geng, Y., Song, J., Shivdasani, R. A., & Signoretti, S. (2013). p63-expressing cells are the stem cells of developing prostate, bladder, and colorectal epithelia. *Proceedings of the National Academy of Sciences*, *110*(20), 8105–8110. https://doi.org/10.1073/pnas.1221216110

Pinto, A. P., & Crum, C. P. (2000). Natural history of cervical neoplasia: defining progression and its consequence. *Clinical Obstetrics and Gynecology*, *43*(2), 352–362.

Pirisi, L., Creek, K. E., Doniger, J., & DiPaolo, J. A. (1988). Continuous cell lines with

 altered growth and differentiation properties originate after transfection of human

 keratinocytes with human papillomavirus type 16 DNA. *Carcinogenesis*, *9*(9),

 1573–1579.

Pirisi, L., Yasumoto, S., Feller, M., Doniger, J., & DiPaolo, J. A. (1987). Transformation

 of human fibroblasts and keratinocytes with human papillomavirus type 16 DNA.

 Journal of Virology, *61*(4), 1061–1066.

Redvers, R. P., Li, A., & Kaur, P. (2006). Side population in adult murine epidermis

 exhibits phenotypic and functional characteristics of keratinocyte stem cells.

 Proceedings of the National Academy of Sciences of the United States of America,

 103(35), 13168–13173. https://doi.org/10.1073/pnas.0602579103

Rheinwald, J. G., & Green, H. (1975). Serial cultivation of strains of human epidermal

 keratinocytes: the formation of keratinizing colonies from single cells. *Cell*, *6*(3),

 331–343.

Roshan, A., Murai, K., Fowler, J., Simons, B. D., Nikolaidou-Neokosmidou, V., & Jones,

 P. H. (2016). Human keratinocytes have two interconvertible modes of

 proliferation. *Nature Cell Biology*, *18*(2), 145–156.

 https://doi.org/10.1038/ncb3282

Rybak, A. P., He, L., Kapoor, A., Cutz, J.-C., & Tang, D. (2011). Characterization of

 sphere-propagating cells with stem-like properties from DU145 prostate cancer

 cells. *Biochimica Et Biophysica Acta*, *1813*(5), 683–694.

 https://doi.org/10.1016/j.bbamcr.2011.01.018

Ryser, M. D., Myers, E. R., & Durrett, R. (2015). HPV Clearance and the Neglected Role of Stochasticity. *PLOS Computational Biology*, *11*(3), e1004113. https://doi.org/10.1371/journal.pcbi.1004113

Sada, A., Jacob, F., Leung, E., Wang, S., White, B. S., Shalloway, D., & Tumbar, T. (2016). Defining the cellular lineage hierarchy in the interfollicular epidermis of adult skin. *Nature Cell Biology*, *18*(6), 619–631. https://doi.org/10.1038/ncb3359

Schmitt, A., Rochat, A., Zeltner, R., Borenstein, L., Barrandon, Y., Wettstein, F. O., & Iftner, T. (1996). The primary target cells of the high-risk cottontail rabbit papillomavirus colocalize with hair follicle stem cells. *Journal of Virology*, *70*(3), 1912–1922.

Schneider, T. E., Barland, C., Alex, A. M., Mancianti, M. L., Lu, Y., Cleaver, J. E., … Ghadially, R. (2003). Measuring stem cell frequency in epidermis: a quantitative in vivo functional assay for long-term repopulating cells. *Proceedings of the National Academy of Sciences of the United States of America*, *100*(20), 11412–11417. https://doi.org/10.1073/pnas.2034935100

Shamir, E. R., & Ewald, A. J. (2014). Three-dimensional organotypic culture: experimental models of mammalian biology and disease. *Nature Reviews Molecular Cell Biology*, *15*(10), 647–664. https://doi.org/10.1038/nrm3873

Sherman, L., & Schlegel, R. (1996). Serum- and calcium-induced differentiation of human keratinocytes is inhibited by the E6 oncoprotein of human papillomavirus type 16. *Journal of Virology*, *70*(5), 3269–3279.

Sun, Y., Goderie, S. K., & Temple, S. (2005). Asymmetric distribution of EGFR receptor during mitosis generates diverse CNS progenitor cells. *Neuron*, *45*(6), 873–886. https://doi.org/10.1016/j.neuron.2005.01.045

Takeuchi, K., Kato, M., Suzuki, H., Akhand, A. A., Wu, J., Hossain, K., … Nakashima, I. (2001). Acrolein induces activation of the epidermal growth factor receptor of human keratinocytes for cell death. *Journal of Cellular Biochemistry*, *81*(4), 679–688.

Tani, H., Morris, R. J., & Kaur, P. (2000). Enrichment for murine keratinocyte stem cells based on cell surface phenotype. *Proceedings of the National Academy of Sciences of the United States of America*, *97*(20), 10960–10965.

Toma, J. G., McKenzie, I. A., Bagli, D., & Miller, F. D. (2005). Isolation and characterization of multipotent skin-derived precursors from human skin. *Stem Cells (Dayton, Ohio)*, *23*(6), 727–737. https://doi.org/10.1634/stemcells.2004-0134

Tomar, S., Graves, C. A., Altomare, D., Kowli, S., Kassler, S., Sutkowski, N., … Pirisi, L. (2016). Human papillomavirus status and gene expression profiles of oropharyngeal and oral cancers from European American and African American patients: Gene Expression and Racial Disparity in Oropharyngeal/Oral Cancer. *Head & Neck*, *38*(S1), E694–E704. https://doi.org/10.1002/hed.24072

Tumbar, T., Guasch, G., Greco, V., Blanpain, C., Lowry, W. E., Rendl, M., & Fuchs, E. (2004). Defining the epithelial stem cell niche in skin. *Science (New York, N.Y.)*, *303*(5656), 359–363. https://doi.org/10.1126/science.1092436

Van Der Schueren, B., Cassiman, J. J., & Van Den Berghe, H. (1980). Morphological
characteristics of epithelial and fibroblastic cells growing out from biopsies of
human skin. *The Journal of Investigative Dermatology*, *74*(1), 29–35.

Vollmers, A., Wallace, L., Fullard, N., Höher, T., Alexander, M. D., & Reichelt, J.
(2012). Two- and Three-Dimensional Culture of Keratinocyte Stem and Precursor
Cells Derived from Primary Murine Epidermal Cultures. *Stem Cell Reviews and
Reports*, *8*(2), 402–413. https://doi.org/10.1007/s12015-011-9314-y

Wakita, H., & Takigawa, M. (1999). Activation of epidermal growth factor receptor
promotes late terminal differentiation of cell-matrix interaction-disrupted
keratinocytes. *The Journal of Biological Chemistry*, *274*(52), 37285–37291.

Wan, F., Miao, X., Quraishi, I., Kennedy, V., Creek, K. E., & Pirisi, L. (2008). Gene
expression changes during HPV-mediated carcinogenesis: A comparison between
an *in vitro* cell model and cervical cancer. *International Journal of Cancer*,
123(1), 32–40. https://doi.org/10.1002/ijc.23463

Watt, F. M., Jordan, P. W., & O'Neill, C. H. (1988). Cell shape controls terminal
differentiation of human epidermal keratinocytes. *Proceedings of the National
Academy of Sciences of the United States of America*, *85*(15), 5576–5580.

Webb, A., Li, A., & Kaur, P. (2004). Location and phenotype of human adult
keratinocyte stem cells of the skin. *Differentiation; Research in Biological
Diversity*, *72*(8), 387–395. https://doi.org/10.1111/j.1432-0436.2004.07208005.x

Woodworth, C. D., Doniger, J., & DiPaolo, J. A. (1989). Immortalization of human
foreskin keratinocytes by various human papillomavirus DNAs corresponds to
their association with cervical carcinoma. *Journal of Virology*, *63*(1), 159–164.

Xu, H., Pirisi, L., & Creek, K. E. (2015). Six1 overexpression at early stages of HPV16-mediated transformation of human keratinocytes promotes differentiation resistance and EMT. *Virology*, *474*, 144–153. https://doi.org/10.1016/j.virol.2014.10.010

Xu, H., Zhang, Y., Altomare, D., Pena, M. M., Wan, F., Pirisi, L., & Creek, K. E. (2014). Six1 promotes epithelial-mesenchymal transition and malignant conversion in human papillomavirus type 16-immortalized human keratinocytes. *Carcinogenesis*, *35*(6), 1379–1388. https://doi.org/10.1093/carcin/bgu050

Yoon, C. S., Kim, K. D., Park, S. N., & Cheong, S. W. (2001a). alpha(6) Integrin is the main receptor of human papillomavirus type 16 VLP. *Biochemical and Biophysical Research Communications*, *283*(3), 668–673. https://doi.org/10.1006/bbrc.2001.4838

Yoon, C. S., Kim, K. D., Park, S. N., & Cheong, S. W. (2001b). alpha(6) Integrin is the main receptor of human papillomavirus type 16 VLP. *Biochemical and Biophysical Research Communications*, *283*(3), 668–673. https://doi.org/10.1006/bbrc.2001.4838

Yu, H., Fang, D., Kumar, S. M., Li, L., Nguyen, T. K., Acs, G., … Xu, X. (2006). Isolation of a Novel Population of Multipotent Adult Stem Cells from Human Hair Follicles. *The American Journal of Pathology*, *168*(6), 1879–1888. https://doi.org/10.2353/ajpath.2006.051170

Zyzak, L. L., MacDonald, L. M., Batova, A., Forand, R., Creek, K. E., & Pirisi, L. (1994). Increased levels and constitutive tyrosine phosphorylation of the epidermal growth factor receptor contribute to autonomous growth of human

papillomavirus type 16 immortalized human keratinocytes. *Cell Growth &*

Differentiation: The Molecular Biology Journal of the American Association for

Cancer Research, 5(5), 537–547.